

Spring 2004

Performance evaluation of communication systems with transmit diversity

Chunjun Gao

New Jersey Institute of Technology

Follow this and additional works at: <https://digitalcommons.njit.edu/dissertations>



Part of the [Electrical and Electronics Commons](#)

Recommended Citation

Gao, Chunjun, "Performance evaluation of communication systems with transmit diversity" (2004). *Dissertations*. 627.
<https://digitalcommons.njit.edu/dissertations/627>

This Dissertation is brought to you for free and open access by the Theses and Dissertations at Digital Commons @ NJIT. It has been accepted for inclusion in Dissertations by an authorized administrator of Digital Commons @ NJIT. For more information, please contact digitalcommons@njit.edu.

Copyright Warning & Restrictions

The copyright law of the United States (Title 17, United States Code) governs the making of photocopies or other reproductions of copyrighted material.

Under certain conditions specified in the law, libraries and archives are authorized to furnish a photocopy or other reproduction. One of these specified conditions is that the photocopy or reproduction is not to be “used for any purpose other than private study, scholarship, or research.” If a user makes a request for, or later uses, a photocopy or reproduction for purposes in excess of “fair use” that user may be liable for copyright infringement,

This institution reserves the right to refuse to accept a copying order if, in its judgment, fulfillment of the order would involve violation of copyright law.

Please Note: The author retains the copyright while the New Jersey Institute of Technology reserves the right to distribute this thesis or dissertation

Printing note: If you do not wish to print this page, then select “Pages from: first page # to: last page #” on the print dialog screen



The Van Houten library has removed some of the personal information and all signatures from the approval page and biographical sketches of theses and dissertations in order to protect the identity of NJIT graduates and faculty.

ABSTRACT

PERFORMANCE EVALUATION OF COMMUNICATION SYSTEMS WITH TRANSMIT DIVERSITY

**by
Chunjun Gao**

Transmit diversity is a key technique to combat fading with multiple transmit antennae for next-generation wireless communication systems. Space-time block code (STBC) is a main component of this technique. This dissertation consists of four parts: the first three discuss performance evaluation of STBCs in various circumstances, the fourth outlines a novel differential scheme with full transmit diversity.

In the first part, closed-form expressions for the bit error rate (BER) are derived for STBC based on Alamouti's scheme and utilizing M-ary phase shift keying (MPSK) modulation. The analysis is carried out for a slow, flat Rayleigh fading channel with coherent detection and with non-coherent differential encoding/decoding. The BER expression for coherent detection is exact. But for differential detection it is an approximation appropriate for a high signal-to-noise ratio. Numerical results are provided for analysis and simulations for BPSK and QPSK modulations.

A signal-to-noise ratio loss of approximately 3 dB always occurs with conventional differential detection for STBC compared to coherent detection. In the second part of this dissertation, a multiple-symbol differential detection (MSDD) technique is proposed for MPSK STBCs, which greatly reduces this performance loss by extending the observation interval for decoding. The technique uses maximum likelihood block sequence detection instead of traditional block-by-block detection and is carried out on the slow, flat Rayleigh fading channel. A generalized decision metric for an observation interval of N blocks is derived. It is shown that for a moderate number of blocks, MSDD provides more than 1.0 dB performance

improvement corresponding to conventional differential detection. In addition, a closed-form pairwise error probability for differential BPSK STBC is derived for an observation interval of N blocks, and an approximate BER is obtained to evaluate the performance.

In the third part, the BER performance of STBC over a spatio-temporal correlated channel with coherent and noncoherent detection is illustrated, where a general space-time correlation model is utilized. The simulation results demonstrate that spatial correlation negatively effects the performance of the STBC scheme with differential detection but temporal correlation positively impacts it. However, with coherent detection, spatial correlation still has negative effect on the performance but temporal correlation has no impact on it.

In the final part of this dissertation, a differential detection scheme for DS/CDMA MIMO link is presented. The transmission provides for full transmit and receive diversity gain using a simple detection scheme, which is a natural extension of differential detection combined with an orthogonal transmit diversity (OTD) approach. A capacity analysis for this scheme is illustrated.

**PERFORMANCE EVALUATION OF COMMUNICATION SYSTEMS
WITH TRANSMIT DIVERSITY**

**by
Chunjun Gao**

**A Dissertation
Submitted to the Faculty of
New Jersey Institute of Technology
in Partial Fulfillment of the Requirements for the Degree of
Doctor of Philosophy in Electrical Engineering**

Department of Electrical and Computer Engineering

May 2004

Copyright © 2004 by Chunjun Gao
ALL RIGHTS RESERVED

APPROVAL PAGE

PERFORMANCE EVALUATION OF COMMUNICATION SYSTEMS WITH TRANSMIT DIVERSITY

Chunjun Gao

Dr. Alexander M. Haimovich, Dissertation Advisor
Professor, NJIT

Date

Dr. Ali Abdi, Committee Member
Assistant Professor, NJIT

Date

Dr. Yeheskel Bar-Ness, Committee Member
Distinguished Professor, NJIT

Date

~~Dr.~~ Jack H. Winters, Committee Member
IEEE Fellow, Jack Winters Communications, LLC

Date

Dr. Roy You/~~Comm~~tee Member
Assistant Professor, NJIT

Date

BIOGRAPHICAL SKETCH

Author: Chunjun Gao
Degree: Doctor of Philosophy
Date: May 2004

Undergraduate and Graduate Education:

- Doctor of Philosophy in Electrical Engineering,
New Jersey Institute of Technology, Newark, NJ, 2004
- Master of Science in Electrical Engineering,
Shanghai University, Shanghai, China, 1994
- Bachelor of Science in Electrical Engineering,
China Institute of Metrology, Hangzhou, China, 1989

Major: Electrical Engineering

Presentations and Publications:

Chunjun Gao and Alexander M. Haimovich and Debang Lao, "Multiple-Symbol Differential Detection for Space-Time Block Codes: Decision Metric and Performance Analysis," *Submitted To IEEE Trans. on Commun.*, Jan., 2004.

Chunjun Gao and Alexander M. Haimovich, "BER Analysis of MPSK Space-Time Block Codes with Differential Detection," *IEEE Commun. Lett.*, vol. 7, pp 314-317, 2003.

Ali Abdi and Chunjun Gao and Alexander M. Haimovich, "Level Crossing Rate and Average Fade Duration in MIMO Mobile Fading Channels," *VTC FALL '03*, Orlando, Florida, Sep., 2003.

Chunjun Gao and Alexander M. Haimovich, "A More Powerful Space-Time Trellis-Coded Modulation Scheme," *MILICOM'02*, Anaheim, California, Oct., 2002.

Chunjun Gao and Alexander M. Haimovich, "Performance Comparison of Two Space-Time Trellis-Coded Modulation," *VTC Fall'02*, Vancouver, Canada, vol. 1, pp. 52-56, Sep., 2002.

- Chunjun Gao and Alexander M. Haimovich, "Bit Error Probability for Space-Time Block Code with Coherent and Differential Detection," *VTG Fall'02*, Vancouver, Canada, vol. 1, pp. 24-28, Sep. 2002.
- Chunjun Gao and Alexander M. Haimovich, "A Differential Detection Scheme for DS/CDMA Spatial Diversity," *ICC'02*, New York City, USA, pp. 465-469, May, 2002.
- Chunjun Gao and Alexander M. Haimovich, "Multiple-Symbol Differential Detection for Space-Time Block Codes," *CISS'02*, Princeton University, USA, WP-1, No.2, May, 2002.
- Chunjun Gao and Alexander M. Haimovich, "Performance Analysis of Rayleigh Fading and Cochannel Interference in Wireless Communication," *Technical Report*, New Jersey Inst. of Tech., March, 2002.

*Oh, I have slipped the surly bonds of earth and danced the
skies on laughter-silvered wings; Sunward I've climbed,
and joined the tumbling mirth of sun-split clouds-and
done a hundred things you have not dreamed of – wheeled
and soared and swung high in the sunlit silence. Hov'ring
there, I've chased the shouting wind along, and flung
my eager craft through footless halls of air. Up, up the
long, delirious burning blue I've topped the windswept
heights with easy grace where never lark, or even eagle
flew. And, while with silent, lifting mind I've trod the
high untrespassed sanctity of space, put out my hand, and
touched the face of God.*

“High Flight”, By John Gillespie Magee, Jr.
from www.skygod.com

ACKNOWLEDGMENT

I would like to express my deepest gratitude to my advisor, Professor Alexander M. Haimovich in electrical engineering, for his guidance and support during my Ph.D. study and research. His working style, combining seriousness, creativity, and wisdom, has often helped me cut a long exploration journey short, and has been a great benefit to my research. It has been very rewarding to have him as my advisor.

My deep gratitude also goes to Professor Ali Abdi, one of my committee members, who has instructed and counseled me throughout the course of my Ph.D. research. I would also like to thank Dr. Bar-Ness and Dr. You for serving on my dissertation committee and making keen suggestions for my dissertation proposal. I would especially like to thank Dr. Jack Winters, who spent his precious time on my dissertation report and gave me some constructive ideas to improve my dissertation. I would like to express my deep gratitude to Professor Joe Pifer of Rutgers University, who spent much time reviewing my dissertation and helped me improve my technical English.

My appreciation also extends to Dr. Ronald Kane and Clarisa Gonzalez-Lenahan in the Office of Graduate Studies for their generous help and encouragement during the hard times in the course of my research. I would also like to thank all my colleagues at the Center of Communications and Signal Processing Research (CCSPR) of NJIT for their friendship, their countless hours of conversation, and their enlightening ideas.

Finally, I would like to deeply thank my family: First, my father, who was my first mentor and gave me encouragement, full support and earnest guidance during my childhood, but who unfortunately passed away a long time ago. Also my mother, who has always dedicated her unique love to me, and finally my three sisters, brother-

in-laws and my nephews and nieces, who always give me happy times whenever the whole family can get together.

TABLE OF CONTENTS

Chapter	Page
1 INTRODUCTION	1
1.1 Motivation	1
1.1.1 Both the Transmitter and the Receiver Know the CSI	1
1.1.2 Only the Receiver Knows the CSI	1
1.1.3 Neither the Transmitter Nor the Receiver Knows the CSI	3
1.2 System Model	4
2 BER ANALYSIS OF MPSK SPACE-TIME BLOCK CODE	6
2.1 Introduction	6
2.2 Coherent Detection	7
2.2.1 Receiver Model	7
2.2.2 BER Analysis	9
2.3 Differential Detection	13
2.3.1 Differential Encoding/Decoding	13
2.3.2 Receiver Model	14
2.3.3 BER Analysis	15
2.4 Numerical Results	19
2.5 Conclusions	20
3 MSDD FOR MPSK SPACE-TIME BLOCK CODES	21
3.1 Introduction	21
3.2 Receiver Model	22
3.3 Decision Metric for MSDD	23
3.3.1 Coherent Detection	23
3.3.2 Non-coherent Detection	24
3.4 Performance Analysis	30
3.4.1 Closed-Form Pairwise Error Probability	32

TABLE OF CONTENTS

(Continued)

Chapter	Page
3.4.2 Approximate Bit Error Rate	35
3.5 Numerical Results	38
3.6 Conclusions	40
4 BER PERFORMANCE OF STBC OVER A SPATIO-TEMPORAL CORRELATED CHANNEL	42
4.1 Introduction	42
4.2 The Spatial and Temporal Correlated MIMO Channel Model	43
4.3 A 2×1 Spatial and Temporal Correlated Rayleigh Fading Channel	48
4.4 Simulation Results	49
4.4.1 Spatial Correlation	50
4.4.2 Temporal Correlation	52
4.5 Conclusions	54
5 A DIFFERENTIAL SCHEME FOR DS/CDMA MIMO SYSTEM	55
5.1 Introduction	55
5.2 Coherent Detection for Known CSI	56
5.2.1 Orthogonal Transmit Diversity	56
5.2.2 MIMO OTD	58
5.3 Differential Detection	59
5.3.1 Single-Antenna System	59
5.3.2 MIMO System	60
5.3.3 Capacity Analysis	61
5.4 Numerical Results	62
5.5 Conclusions	63
6 SUMMARY AND COMMENTS	67
APPENDIX A EVALUATION OF THE VARIANCE OF $\text{Re tr}(\Lambda)$	69
A.1 Evaluation of $\text{Var} [\text{Re tr}(\Lambda_1)]$, $\text{Var} [\text{Re tr}(\Lambda_2)]$	69

TABLE OF CONTENTS

(Continued)

Chapter	Page
A.1.1 Evaluation of V_1 and V_2	71
A.1.2 Evaluation of cross-correlation Θ and Ω	71
A.2 Evaluation of $\text{cov}(\text{Re tr}(\Lambda_1), \text{Re tr}(\Lambda_2))$	76
APPENDIX B THE MINIMUM MSDD DISTANCE OF ρ FOR N BLOCKS	81
B.1 Two Blocks	81
B.2 Three Blocks	82
B.3 N Blocks	82
B.3.1 One-symbol error	82
B.3.2 Two-symbol error	83
B.3.3 Three-symbol error or more errors	85
APPENDIX C PROPERTIES OF THE MSDD DISTANCE ρ	86
APPENDIX D APPROXIMATE BER FOR DIFFERENTIAL STBC WITH COHERENT DETECTION	88
APPENDIX E LCR AND AFD IN MIMO MOBILE FADING CHANNELS .	90
E.1 Introduction	90
E.2 Scalar Crossing in MIMO Systems	90
E.2.1 Mathematical Formulation	90
E.2.2 Numerical Example	93
E.2.3 Applications of Scalar ASD	97
E.3 Vector Crossing in MIMO Systems	98
E.3.1 Mathematical Formulation	98
E.3.2 Special Case of Isotropic Scattering and No Spatial Correlation	99
E.3.3 Application: Analysis of the Block Fading Model	100
E.3.4 Application: Vector AFD in MIMO Channels	103
E.4 Conclusion	103
REFERENCES	105

LIST OF FIGURES

Figure	Page
2.1 Comparison of analysis and simulation with coherent and differential detection in BPSK case (1 bit/s/Hz).	19
2.2 Comparison of analysis and simulation with coherent and non-coherent detection in QPSK case (2 bits/s/Hz).	20
3.1 Multiple symbol differential detection for space-time block code with BPSK signal. Bit Error Rate versus SNR for different length of observation interval, 2 transmit antennas, 1 receive antenna.	29
3.2 Multiple symbol differential detection for space-time block code with QPSK signal. Bit Error Rate versus SNR for different length of observation interval, 2 transmit antennas, 1 receive antenna.	30
3.3 Asymptotic characteristics of MSDD for STBCs over two transmit antennas(14 dB SNR, BPSK, 1 bit/s/Hz).	39
3.4 Theory and simulation result for MSDD of STBC.	40
4.1 Geometrical configuration of a 2×2 channel with local scatterers around the mobile user (two-element arrays at the BS and the user).	44
4.2 Non-isotropic scattering in a narrow street.	44
4.3 Isotropic scattering in an open area (circles are scatterers).	45
4.4 BER performance of Alamouti's STBCs for two channels with different spatial correlation but fixed temporal correlation.	51
4.5 The effect of spatial correlation on BER performance of Alamouti's STBCs for a fast fading channel and a slow fading channel at 15 dB SNR. . .	52
4.6 BER performance of Alamouti's STBCs for two channels with fixed spatial correlation but different temporal correlation.	53
4.7 The effect of temporal correlation on BER performance of Alamouti's STBCs for two channels with a fixed spatial correlation at 15 dB SNR. . .	54
5.1 Performance of Differential Detection (DD) and Coherent Detection (CD) for one user in multiple-input and one-output case.	64
5.2 Performance of Differential Detection (DD) and Coherent Detection (CD) for one user in one-input and multiple-output case.	64
5.3 Performance of Differential Detection (DD) for one user in multiple-input and multiple-output case.	65

LIST OF FIGURES (Continued)

Figure	Page
5.4 Capacity of one user for coherent detection.	65
5.5 Capacity of one user for differential detection.	66
E.1 Downcrossing rate of total instantaneous SNR in a 2×1 channel, with and without spatial correlation (th: theory, sim: simulation).	101
E.2 Average fade duration of total instantaneous SNR in a 2×1 channel, with and without spatial correlation (th: theory, sim: simulation).	102
E.3 Graphical representation of the concept of the stay duration of a single complex process, a SISO channel, within a square region.	102
E.4 Normalized average stay duration in a MIMO channel with the same number of transmit and receive antennas (th: theory, sim: simulation).	103

CHAPTER 1

INTRODUCTION

1.1 Motivation

Transmit diversity has emerged in the last decade as an effective means for achieving spatial diversity in fading channels with an antenna array at the transmitter. Depending on whether the channel state information (CSI) is known or not, systems employing transmit diversity fall into three general categories as follows:

1.1.1 Both the Transmitter and the Receiver Know the CSI

The first category uses implicit or explicit feedback of information from the receiver to the transmitter to configure the transmitter. It has been observed that significant performance gains, at lower complexity, can be achieved if the CSI is available at both the transmitter and the receiver. Telatar [1] analyzed the capacity of a multiple transmitter system with perfectly known channels at both the transmitters and the receiver. This capacity achieving scheme involves spatial water-filling in the direction of the eigenvectors of the channel, in proportion to the eigenvalues, along with independent and identically distributed (i.i.d) Gaussian codes. Narula et al. [2], [3] have considered the problem of multiple transmitters and a single receiver system with imperfect feedback of CSI at the transmitter. The issues in this category are not within the scope of the work, and will not be further addressed.

1.1.2 Only the Receiver Knows the CSI

The second category uses linear processing at the transmitter to spread the information across the antennas. At the receiver, information is obtained by either linear processing or maximum-likelihood decoding techniques. Feedforward information is required to estimate the CSI from the transmitter to the receiver.

These estimates are used to compensate for the channel response at the receiver. Various transmit diversity techniques in this category have been proposed in the open literature. For example, a delay transmit scheme was proposed by Wittneben [4], while a variation of the delay scheme was suggested by Seshadri and Winters [5], where the replicas of the signal are transmitted through multiple antennas at different times. Space-time coding schemes also fall within this category.

Space-time coding has been a topic of intensive research in recent years. Tarokh [6] first proposed a space-time trellis coding scheme on a Rayleigh fading channel. The scheme was shown to provide a good trade-off between constellation size, data rate, diversity advantage and trellis complexity. A much simpler space-time block code (STBC) scheme, which provides full diversity advantage, but is not optimized for coding gain, was proposed by Alamouti [7]. Alamouti's scheme for two transmit antennas supports a maximum likelihood detection scheme based only on linear processing at the receiver. Tarokh et al. [8] generalized the scheme to multiple transmit antennas (three, four or eight), to obtain full diversity for real-valued constellations. For complex constellations, full diversity can be obtained only at the cost of reduced coding rate. Due to its relative simplicity of implementation, Alamouti's scheme [7] has been adopted by 3G standards, such as W-CDMA and CDMA2000. All these designs are based on the assumption that the CSI is perfectly known at the receiver, but unknown at the transmitter.

Since a closed-form bit error rate (BER) expression would serve as an attractive alternative to previously derived bounds for evaluating the performance of STBC [9] [10], a BER analysis for Alamouti's STBC with known CSI is presented in Chapter 2.

1.1.3 Neither the Transmitter Nor the Receiver Knows the CSI

The third category does not require feedback or feedforward information. Instead, multiple transmit antennas are used combined with channel coding to provide diversity. An example of this approach is to combine phase sweeping transmitter diversity [11] with channel coding [12]. Other examples of this approach are space-time differential schemes.

The design of the space-time codes mentioned above is based on the assumption that perfect estimation of CSI is available at the receiver. This is reasonable when channels change slowly compared with the symbol rates, since the transmitters can send training symbols, which enable the receiver to estimate the channel accurately. For cases when accurate channel estimation is not possible or the effort associated with channel estimation is to be avoided, it is of interest to develop techniques, which do not require CSI. This makes differential schemes an attractive alternative. With differential encoding/decoding, CSI is not required either at the transmitter or at the receiver.

Several schemes for dealing with this issue have been proposed in past two years. Tarokh and Jafarkhani [13] first suggested a differential STBC scheme for a slow Rayleigh fading channel with two transmit antennas. In this scheme, neither the transmitters nor the receiver know the CSI. This scheme can achieve a full diversity gain but its non-coherent receiver performs 3 dB poorer than a coherent receiver would. The same authors generalized the differential detection for STBC to more than two transmit antennas [14]. As is the case for single antenna channels, a loss of approximately 3 dB is always paid for this differential scheme compared to the related coherent scheme. Hochwald and Sweldoms [15] proposed a new class of differential modulation schemes for multiple transmit antennas based on unitary space-time modulation. At the same time, a related differential modulation scheme using group codes was proposed by Hughes [16]. These schemes utilize constellations of unitary

matrices or group codes to achieve full transmit diversity without a knowledge of CSI, but with a loss of about 3 dB in performance. While Tarokh's scheme has properties similar to the 2×2 unitary matrixes in the paper [15] or the 2×2 group codes in the paper [16], it outperforms both.

A BER analysis for Alamouti's STBC with differential detection is presented in Chapter 2. Next, in order to narrow the 3 dB performance gap between differential detection and coherent detection, a multiple-symbol differential detection (MSDD) technique for Alamouti's STBC is proposed in Chapter 3. The BER performance of Alamouti's STBCs over a spatial and temporal correlated channel with coherent and noncoherent detection is illustrated in Chapter 4. Then to overcome the implementation complexity of existing differential multiple-input multiple-output (MIMO) systems, a new and simple differential detection scheme for DS/CDMA MIMO links is presented in Chapter 5.

1.2 System Model

Since both Chapter 2 and Chapter 3 deal with issues about Alamouti's STBC scheme, the system model for this scheme is introduced here:

Consider a wireless communication system operating over a slow, flat Rayleigh fading channel in which STBC codewords are sent from two transmit antennas to Q receive antennas following the procedure outlined in Alamouti's paper [7]. Each STBC codeword consists of two symbols transmitted over two time epochs. Let the codeword index be k and the time epoch index within the codeword be t ($t = 1, 2$). Then, the received signal at time index k , time slot t and receive antenna q is given as

$$r_{t,k}^{(q)} = \sqrt{E_s} \sum_{i=1}^2 h_i^{(q)} d_{i,k}^{(t)} + n_{t,k}^{(q)}, \quad 1 \leq q \leq Q, \quad (1.1)$$

where $h_i^{(q)}$ is the path gain from transmit antenna i to the receive antenna q . Path gains are modeled as quasi-static over some frame of arbitrary length, i.i.d. complex-valued Gaussian random variables with zero-mean and variance $1/2$ per dimension. Path gains are assumed to vary independently frame to frame. The quasi-static assumption is to ensure that no time diversity masks the effects of spatial diversity, the main topic of this dissertation. In practical terms, it means that BER is evaluated based on instantaneous SNR values. Noise samples $n_k^{(q)}$ are modeled as i.i.d, zero-mean, complex-valued Gaussian random variables with variance $N_0/2$ per dimension; $d_{i,k}^{(t)}$ is the k -th transmitted symbol from antenna i at time slot t ($t = 1, 2$); E_s is the total symbol energy from the two transmit antennas.

Following Alamouti's scheme [7] with coherent detection, STBC codewords \mathbf{S}_k can be expressed as follows

$$\mathbf{S}_k = \begin{bmatrix} d_{1,k}^{(1)} & d_{1,k}^{(2)} \\ d_{2,k}^{(1)} & d_{2,k}^{(2)} \end{bmatrix} = \begin{bmatrix} s_{1,k} & s_{2,k} \\ -s_{2,k}^* & s_{1,k}^* \end{bmatrix}, \quad (1.2)$$

where the symbol ' $*$ ' denotes complex conjugation, and the symbols $s_{i,k} \in A$, where A is the MPSK constellation

$$A = \left\{ \frac{e^{j2\pi(m-1)/M}}{\sqrt{2}} \mid m = 1, 2, \dots, M \right\}, \quad (1.3)$$

where the factor $1/\sqrt{2}$ is introduced to normalize the total transmit power per symbol epoch to E_s .

With differential detection, STBC codewords \mathbf{C}_k can be expressed

$$\mathbf{C}_k = \begin{bmatrix} d_{1,k}^{(1)} & d_{1,k}^{(2)} \\ d_{2,k}^{(1)} & d_{2,k}^{(2)} \end{bmatrix} = \begin{bmatrix} c_{1,k} & c_{2,k} \\ -c_{2,k}^* & c_{1,k}^* \end{bmatrix}, \quad (1.4)$$

where $c_{i,k}$ ($i = 1, 2$) is differentially encoded [13].

CHAPTER 2

BER ANALYSIS OF MPSK SPACE-TIME BLOCK CODE

2.1 Introduction

Analysis of trellis space-time codes and space-time block codes has been traditionally based on the union or other bounds. The union bound can be found from the pairwise error probability. In Tarokh's paper [6], an upper bound was derived for the pairwise error probability of space-time trellis codes. The bound is used to analyze the diversity and coding gains of such codes. Simon improved these results by obtaining an exact pairwise error probability over the flat Rayleigh fading channel expressed in terms of the Gaussian tail function $Q(\cdot)$ [17]. A union bound on the symbol error probability for STBC was obtained in Li's work [9]. For *receive* diversity over the Rayleigh fading channel with coherent detection, a closed-form expression of the BER was derived in Proakis' book [18] based on the probability density function (PDF) of the instantaneous signal-to-noise ratio (SNR). In Lo's paper [19], an *approximate* expression of the BER was developed for maximum ratio transmission under the assumption of CSI known *both* at the transmitter and at the receiver. By approximating a MIMO Rayleigh channel as a single-input single-output (SISO) Gaussian channel, an *approximate* expression for the BER of certain STBC was obtained in Bauch's work [10].

The work presented in this chapter is motivated by the observation that for the special case of STBC based on Alamouti's scheme, it is possible to obtain closed-form expression for the BER. An closed-form BER expression would serve as an attractive alternative to previously derived bounds for evaluating performance. The expressions are derived from the PDF of the phase of the received signal. While the procedure for deriving the BER applies to any M-ary phase shift keying (MPSK) modulation,

binary PSK (BPSK) and quaternary PSK (QPSK) examples are worked out in detail. BER expressions are derived below for both coherent modulation (only the receiver knows the CSI) and differential modulation (neither the transmitters nor the receiver knows the CSI).

2.2 Coherent Detection

2.2.1 Receiver Model

Based on Equation (1.1) and Equation (1.2), the received signal model is given by

$$\begin{bmatrix} r_{1,k}^{(q)} \\ r_{2,k}^{(q)} \end{bmatrix} = \sqrt{E_s} \begin{bmatrix} s_{1,k} & s_{2,k} \\ -s_{2,k}^* & s_{1,k}^* \end{bmatrix} \begin{bmatrix} h_1^{(q)} \\ h_2^{(q)} \end{bmatrix} + \begin{bmatrix} n_{1,k}^{(q)} \\ n_{2,k}^{(q)} \end{bmatrix}, \quad (2.1)$$

where $r_{1,k}^{(q)}$ and $r_{2,k}^{(q)}$ represent the received signals of antenna q at time slots 1 and 2, respectively. Converting Equation (2.1) to a more convenient form,

$$\begin{bmatrix} r_{1,k}^{(q)} & -r_{2,k}^{*(q)} \end{bmatrix} = \sqrt{E_s} \begin{bmatrix} s_{1,k} & s_{2,k} \end{bmatrix} \begin{bmatrix} h_1^{(q)} & -h_2^{*(q)} \\ h_2^{(q)} & h_1^{*(q)} \end{bmatrix} + \begin{bmatrix} n_{1,k}^{(q)} & -n_{2,k}^{*(q)} \end{bmatrix}, \quad (2.2)$$

Starting with Equation (2.2), the following convenient form can be obtained

$$\begin{bmatrix} r_{1,k}^{(q)} & -r_{2,k}^{*(q)} \\ r_{2,k}^{(q)} & r_{1,k}^{*(q)} \end{bmatrix} = \sqrt{E_s} \begin{bmatrix} s_{1,k} & s_{2,k} \\ -s_{2,k}^* & s_{1,k}^* \end{bmatrix} \begin{bmatrix} h_1^{(q)} & -h_2^{*(q)} \\ h_2^{(q)} & h_1^{*(q)} \end{bmatrix} + \begin{bmatrix} n_{1,k}^{(q)} & -n_{2,k}^{*(q)} \\ n_{2,k}^{(q)} & n_{1,k}^{*(q)} \end{bmatrix}. \quad (2.3)$$

Expressing Equation (2.3) into vector form,

$$\mathbf{R}_k^{(q)} = \sqrt{E_s} \mathbf{S}_k \mathbf{H}^{(q)} + \mathbf{N}_k^{(q)}, \quad (2.4)$$

where the following definitions apply

$$\begin{aligned} \mathbf{R}_k^{(q)} &= \begin{bmatrix} r_{1,k}^{(q)} & -r_{2,k}^{*(q)} \\ r_{2,k}^{(q)} & r_{1,k}^{*(q)} \end{bmatrix}, & \mathbf{S}_k &= \begin{bmatrix} s_{1,k} & s_{2,k} \\ -s_{2,k}^* & s_{1,k}^* \end{bmatrix}, \\ \mathbf{H}^{(q)} &= \begin{bmatrix} h_1^{(q)} & -h_2^{*(q)} \\ h_2^{(q)} & h_1^{*(q)} \end{bmatrix}, & \mathbf{N}_k^{(q)} &= \begin{bmatrix} n_{1,k}^{(q)} & -n_{2,k}^{*(q)} \\ n_{2,k}^{(q)} & n_{1,k}^{*(q)} \end{bmatrix}. \end{aligned} \quad (2.5)$$

For Q receive antennas, the signal model is

$$\mathbf{R}_k = \mathbf{D}_k \mathbf{H} + \mathbf{N}_k, \quad (2.6)$$

where

$$\begin{aligned} \mathbf{R}_k &= [\mathbf{R}_k^{(1)} \mathbf{R}_k^{(2)} \dots \mathbf{R}_k^{(Q)}], \\ \mathbf{N}_k &= [\mathbf{N}_k^{(1)} \mathbf{N}_k^{(2)} \dots \mathbf{N}_k^{(Q)}], \\ \mathbf{D}_k &= \mathbf{S}_k \otimes \mathbf{1}_Q, \\ \mathbf{H} &= \text{diag} [\mathbf{H}^{(1)} \mathbf{H}^{(2)} \dots \mathbf{H}^{(Q)}], \end{aligned} \quad (2.7)$$

the symbol \otimes denotes the Kronecker product and $\mathbf{1}_Q$ is a vector of ones of dimension indicated by the subscript.

Finally the channel model incorporating all K transmitted blocks can be put in the following matrix form

$$\mathbf{R} = \mathbf{D} \mathbf{H} + \mathbf{N}, \quad (2.8)$$

where $\mathbf{R} = [\mathbf{R}_1 \mathbf{R}_2 \dots \mathbf{R}_K]^T$ is a $2K \times 2Q$ matrix, the superscript denotes transposition, and both \mathbf{D} and \mathbf{N} are defined analogous to \mathbf{R} .

2.2.2 BER Analysis

It is known that the optimal maximum likelihood (ML) receiver with known CSI is given by Hughes [16]

$$\hat{\ell} = \arg \min_{\ell} \text{tr} \left\{ (\mathbf{R} - \mathbf{D}_{\ell} \mathbf{H}) (\mathbf{R} - \mathbf{D}_{\ell} \mathbf{H})^{\dagger} \right\}, \quad (2.9)$$

where "tr" denotes the trace function; ' \dagger ' is defined as the Hermitian operation; and \mathbf{D}_{ℓ} represents a specific sequence of transmitted messages. The optimal receiver is based on the entire received sequence (2.8) and since its complexity is exponential in the sequence length K , a simpler suboptimal receiver is suggested based on only one received block. In this case, the quadratic detector reduces to:

$$\begin{aligned} \hat{\ell} &= \arg \min_{\ell} \text{tr} \left\{ (\mathbf{R}_k - \mathbf{D}_{\ell} \mathbf{H}) (\mathbf{R}_k - \mathbf{D}_{\ell} \mathbf{H})^{\dagger} \right\} \\ &= \arg \max_{\ell} \text{Re tr} \left\{ \mathbf{R}_k (\mathbf{D}_{\ell} \mathbf{H})^{\dagger} \right\} \\ &= \arg \max_{\ell} \text{Re tr} \left\{ \mathbf{R}_k \mathbf{H}^{\dagger} \mathbf{1}_Q \mathbf{S}^{(\ell)\dagger} \right\}, \end{aligned} \quad (2.10)$$

where $\mathbf{S}^{(\ell)}$ is a message matrix. The suboptimal receiver in Equation (2.10) can be interpreted as a optimum combiner that generates the matrices $\Upsilon = \mathbf{R}_k \mathbf{H}^{\dagger} \mathbf{1}_Q$ followed by a decision mechanism. Consider now the properties of the combiner output Υ , where $\Upsilon \Upsilon^{\dagger}$ is a 2×2 diagonal matrix with equal entries. Exploiting previous definitions, the (1, 1) element of this matrix can be expressed

$$\begin{aligned} \Upsilon_1 &= \sum_{q=1}^Q h_1^{*(q)} \left(\sqrt{E_s} h_1^{(q)} s_{1,k} + n_{1,k}^{(q)} \right) \\ &\quad + h_2^{(q)} \left(\sqrt{E_s} h_2^{*(q)} s_{1,k} + n_{2,k}^{*(q)} \right). \end{aligned} \quad (2.11)$$

Due to symmetry considerations, the symbols $s_{1,k}$, $s_{2,k}$ have the same error probability, hence just one of the combiner outputs, say Υ_1 , can be analyzed. The BER of $s_{1,k}$ can be obtained from the probability density function (PDF) of Υ_1 .

Define the random variables

$$\begin{aligned}
X_1^{(q)} &= h_1^{*(q)}, \\
X_2^{(q)} &= h_2^{(q)}, \\
Y_1^{(q)} &= \left(\sqrt{E_s} h_1^{(q)} s_{1,k} + n_{1,k}^{(q)} \right)^*, \\
Y_2^{(q)} &= \left(\sqrt{E_s} h_2^{*(q)} s_{1,k} + n_{2,k}^{*(q)} \right)^*;
\end{aligned} \tag{2.12}$$

then Υ_1 can be expressed

$$\Upsilon_1 = \sum_{q=1}^Q \left(X_1^{(q)} Y_1^{(q)*} + X_2^{(q)} Y_2^{(q)*} \right). \tag{2.13}$$

Conditional on the symbol $s_{1,k}$, the sets $(X_i^{(q)}, Y_i^{(q)})$, $i = 1, 2$, are two pairs of correlated, complex-valued, zero-mean, Gaussian random variables. The two pairs are however, mutually statistically independent and identically distributed.

Define $Z_r = \text{Re}(\Upsilon_1)$ and $Z_i = \text{Im}(\Upsilon_1)$. The joint characteristic function $\Psi(jv_1, jv_2)$ of the random variables Z_r and Z_i can be obtained using Proakis' book [18]. An alternative interpretation to Equation (2.10) is that the phase of Υ_1 is the decision variable for the detection of $s_{1,k}$. Define $R = \sqrt{Z_r^2 + Z_i^2}$, and $\Theta = \tan^{-1}(Z_i/Z_r)$.

The goal is to obtain the PDF $p(\theta)$, where lower case notation is for realizations of the corresponding upper case denoted random variables. This is achieved as follows: compute the joint PDF of Z_r and Z_i , $p(z_r, z_i)$, from the Fourier transform of the joint characteristic function $\Psi(jv_1, jv_2)$, and from $p(z_r, z_i)$ obtain $p(r, \theta)$, the joint PDF of the envelope R and the phase Θ . By integrating $p(r, \theta)$ over the variable r , the PDF $p(\theta)$ can be obtained. The result can be found in Proakis' book [18, p. 891]. The error probability of the received signal can be obtained by integrating $p(\theta)$ over the angle interval complementary to the correct decision.

According to Proakis' book [18], the probability of θ in an interval is expressed as

$$\begin{aligned} \Pr(\theta_1 \leq \theta \leq \theta_2) &= -\frac{(-1)^{2Q-1} (1 - \mu^2)^{2Q}}{2\pi (2Q - 1)!} \\ &\times \frac{\partial^{2Q-1}}{\partial b^{2Q-1}} [f(b, \alpha_2) - f(b, \alpha_1)]|_{b=1}, \end{aligned} \quad (2.14)$$

where the function $f(b, \alpha)$ is defined as follows:

$$\begin{aligned} f(b, \alpha_i) &= \frac{1}{b - \mu^2} \left[\frac{\mu \sqrt{1 - (b/\mu^2 - 1) \alpha_i^2}}{b^{1/2}} \cot^{-1} \alpha_i \right. \\ &\quad \left. - \cot^{-1} \left(\frac{\alpha_i b^{1/2}}{\mu \sqrt{1 - (b/\mu^2 - 1) \alpha_i^2}} \right) \right], \end{aligned} \quad (2.15)$$

and

$$\alpha_i = \frac{-\mu \cos \theta_i}{\sqrt{b - \mu^2 \cos^2 \theta_i}}, \quad i = 1, 2. \quad (2.16)$$

The term μ represents the normalized cross-correlation between $X_i^{(q)}$ and $Y_i^{(q)}$, for $i = 1, 2$. To proceed with the BER computation, and with all symbols equally likely, assume symbol $s_{1,k}$ has zero phase, i.e., $s_{1,k} = 1/\sqrt{2}$. Now, the normalized cross-correlation is defined

$$\mu = \frac{m_{xy}}{\sqrt{m_{xx} m_{yy}}}, \quad (2.17)$$

where from Equation (2.12)

$$m_{xx} = E \left(\left| X_i^{(q)} \right|^2 \right) = 1, \quad (2.18)$$

since by assumption $E \left(\left| h_i^{(q)} \right|^2 \right) = 1$,

$$\begin{aligned} m_{yy} &= E \left(\left| Y_i^{(q)} \right|^2 \right) \\ &= E_s/2 + N_0, \end{aligned} \quad (2.19)$$

since $|s_{1,k}|^2 = 1/2$, and

$$\begin{aligned} m_{xy} &= E \left(X_i^{(q)} Y_i^{*(q)} \right) \\ &= \sqrt{E_s/2}. \end{aligned} \quad (2.20)$$

It follows that the normalized cross-correlation is given by where $\rho = E_s/N_0$ is the SNR per symbol.

BPSK For BPSK signals, the BER can be obtained by integrating the density function of θ , $p(\theta)$ over the ranges $0.5\pi \leq \theta \leq \pi$ and $1.5\pi \leq \theta \leq 2\pi$. Since from Proakis' book [18, p. 891], the density $p(\theta)$ is an even function of θ (for any MPSK constellation), it follows that the BER is given by

$$P_2 = 2 \Pr(\pi/2 \leq \theta \leq \pi). \quad (2.21)$$

Using Equation (2.14) in Equation (2.21) and after some algebraic manipulations, the closed-form BER for the non-coherent Alamouti scheme with BPSK is obtained.

$$P_{2b} = \frac{1}{2} \left[1 - \sqrt{\frac{\rho}{\rho+2}} \sum_{q=0}^{2Q-1} \binom{2q}{q} \left(\frac{1}{2(\rho+2)} \right)^q \right]. \quad (2.22)$$

When ρ is large enough, $\sqrt{\frac{\rho}{\rho+2}} \simeq 1$, and $\frac{1}{2(\rho+2)} \simeq \frac{1}{2\rho}$, then

$$P_{2b} \simeq 1 - \sqrt{\frac{\rho}{\rho+2}} - \sum_{q=1}^{2Q-1} C_q^{2q} \left(\frac{1}{2\rho} \right)^q. \quad (2.23)$$

By Mathematica, the asymptotic expression (2.23) can be approximated as

$$P_{2b} \simeq \frac{2^{2Q} \Gamma(0.5 + 2Q)}{\sqrt{\pi} \Gamma(1 + 2Q)} \left(\frac{1}{\rho} \right)^{2Q}, \quad (2.24)$$

where $\Gamma(\cdot)$ is the Euler gamma function. Obviously, the BER varies as $1/\rho$ raised to the $2Q$ th power, and $\left(\frac{1}{\rho} \right)^{2Q}$ is diversity gain. Thus, with $2Q$ fold diversity, the BER decreases inversely with $2Q$ th power of SNR.

QPSK In the QPSK case, a Gray code is used to map pairs of bits into phases. For a transmitted symbol $s_{1,k}$, it is clear that a single bit error is committed when the received phase is $\frac{1}{4}\pi \leq \theta \leq \frac{3}{4}\pi$, and a double bit error is committed when the received phase is $\frac{3}{4}\pi \leq \theta \leq \pi$. Thus, the BER is expressed as

$$P_{4b} = P_r (\pi/4 \leq \theta \leq 3\pi/4) + 2P_r (\pi \leq \theta \leq 3\pi/4). \quad (2.25)$$

Similarly to Equation (2.22), the BER for the non-coherent Alamouti schemes with QPSK modulation for Q receive antennas is obtained

$$P_{4b} = \frac{1}{2} \left[1 - \sqrt{\frac{\rho}{\rho+4}} \sum_{q=0}^{2Q-1} \binom{2q}{q} \left(\frac{1}{\rho+4} \right)^q \right]. \quad (2.26)$$

and the conclusion for diversity is same as that for BPSK case.

2.3 Differential Detection

2.3.1 Differential Encoding/Decoding

The differential STBC scheme analyzed in this dissertation is the one recently proposed by Tarokh and Jafarkhani [13] based on the Alamouti transmit diversity scheme [7]. Follows a brief description of the method.

The STBC codeword \mathbf{S}_k defined in Expression (1.2), consists of two vectors $[s_{1,k}, s_{2,k}]$ and $[-s_{2,k}^*, s_{1,k}^*]$, which have unit length and are orthogonal to each other. Indeed, $\mathbf{S}_k \mathbf{S}_k^\dagger = \mathbf{I}_2$, where \mathbf{I}_2 is the 2×2 identity matrix. The message matrix \mathbf{S}_k is differentially encoded by a procedure resembling standard single-antenna DPSK [18]. To initialize transmission, the transmitter sends a code unitary matrix \mathbf{C}_0 , for example

$$\mathbf{C}_0 = \begin{bmatrix} 1/\sqrt{2} & 1/\sqrt{2} \\ -1/\sqrt{2} & 1/\sqrt{2} \end{bmatrix}. \quad (2.27)$$

The differentially encoded message \mathbf{C}_k at time k , $k \geq 1$, is obtained by multiplying the codeword at time $k - 1$, \mathbf{C}_{k-1} by the current message \mathbf{S}_k , namely

$$\mathbf{C}_k = \mathbf{S}_k \mathbf{C}_{k-1}. \quad (2.28)$$

This process is initialized with $\mathbf{C}_1 = \mathbf{S}_1 \mathbf{C}_0$. These relations are similar to single-antenna DPSK. The only difference is that the variables here are matrices rather than scalars.

The description in Equation (2.28) is consistent with the encoding algorithm in Tarokh's paper [13]:

$$\begin{bmatrix} c_{1,k} \\ c_{2,k} \end{bmatrix} = s_{1,k} \begin{bmatrix} c_{1,k-1} \\ c_{2,k-1} \end{bmatrix} + s_{2,k} \begin{bmatrix} -c_{2,k-1}^* \\ c_{1,k-1}^* \end{bmatrix}. \quad (2.29)$$

Note that the codeword \mathbf{C}_k has the same unitary property as the message matrix \mathbf{S}_k . Indeed, from the definition (1.4) it is easily verified that $\mathbf{C}_k \mathbf{C}_k^\dagger = \mathbf{I}_2$. Obviously, if the codewords \mathbf{C}_k are observable at the receiver, the messages \mathbf{S}_k can be decoded from

$$\mathbf{C}_k \mathbf{C}_{k-1}^\dagger = \mathbf{S}_k \mathbf{C}_{k-1} \mathbf{C}_{k-1}^\dagger = \mathbf{S}_k. \quad (2.30)$$

2.3.2 Receiver Model

Based on Equation (1.1) and Equation (1.4), the signal model at the receiver for the two time slots associated with each codeword is given by

$$\begin{bmatrix} r_{1,k}^{(q)} \\ r_{2,k}^{(q)} \end{bmatrix} = \sqrt{E_s} \begin{bmatrix} c_{1,k} & c_{2,k} \\ -c_{2,k}^* & c_{1,k}^* \end{bmatrix} \begin{bmatrix} h_1^{(q)} \\ h_2^{(q)} \end{bmatrix} + \begin{bmatrix} n_{1,k}^{(q)} \\ n_{2,k}^{(q)} \end{bmatrix}, \quad (2.31)$$

where earlier definitions apply. Starting with Equation (2.31), at the output of each receive antenna, the matrices are formed as $\mathbf{R}_k^{(q)}$, $1 \leq q \leq Q$,

$$\mathbf{R}_k^{(q)} = \mathbf{C}_k \mathbf{H}^{(q)} + \mathbf{N}_k^{(q)}, \quad (2.32)$$

where

$$\mathbf{R}_k^{(q)} = \begin{bmatrix} r_{1,k}^{(q)} & -r_{2,k}^{*(q)} \\ r_{2,k}^{(q)} & r_{1,k}^{*(q)} \end{bmatrix}, \quad \mathbf{C}_k = \begin{bmatrix} c_k^{(1)} & c_k^{(2)} \\ -c_k^{(2)*} & c_k^{(1)*} \end{bmatrix},$$

$$\mathbf{H}^{(q)} = \begin{bmatrix} h_1^{(q)} & -h_2^{(q)*} \\ h_2^{(q)} & h_1^{(q)*} \end{bmatrix}, \quad \mathbf{N}_k^{(q)} = \begin{bmatrix} n_{1,k}^{(q)} & -n_{2,k}^{(q)*} \\ n_{2,k}^{(q)} & n_{1,k}^{(q)*} \end{bmatrix}.$$

Note that this construction ensures the unitary property of $\mathbf{R}_k^{(q)}$ independent of the values of $r_{1,k}^{(q)}$ and $r_{2,k}^{(q)}$. For Q receive antennas, the signal model is

$$\mathbf{R}_k = \mathbf{D}_k \mathbf{H} + \mathbf{N}_k, \quad (2.33)$$

where

$$\mathbf{R}_k = \begin{bmatrix} \mathbf{R}_k^{(1)} & \mathbf{R}_k^{(2)} & \dots & \mathbf{R}_k^{(Q)} \end{bmatrix}, \quad \mathbf{N}_k = \begin{bmatrix} \mathbf{N}_k^{(1)} & \mathbf{N}_k^{(2)} & \dots & \mathbf{N}_k^{(Q)} \end{bmatrix},$$

$$\mathbf{D}_k = \mathbf{C}_k \otimes \mathbf{1}_Q, \quad \mathbf{H} = \text{diag} \left[\mathbf{H}^{(1)} \quad \mathbf{H}^{(2)} \quad \dots \quad \mathbf{H}^{(Q)} \right], \quad (2.34)$$

Stemming from the unitary property of \mathbf{C}_k , the matrices \mathbf{D}_k have the property $\mathbf{D}_k \mathbf{D}_k^\dagger = Q \mathbf{I}_2$, where \mathbf{I} denotes the identity matrix of dimension indicated by the subscript. Likewise, $\mathbf{D}_k = \mathbf{S}_k \mathbf{D}_{k-1}$. Finally the channel model incorporating all K transmitted blocks can be put in the following matrix form

$$\mathbf{R} = \mathbf{D} \mathbf{H} + \mathbf{N}, \quad (2.35)$$

where $\mathbf{R} = [\mathbf{R}_1 \quad \mathbf{R}_2 \quad \dots \quad \mathbf{R}_K]^T$ is a $2K \times 2Q$ matrix, and both \mathbf{D} and \mathbf{N} are defined analogous to \mathbf{R} .

2.3.3 BER Analysis

It is known that the optimal maximum likelihood (ML) receiver with unknown CSI is given by Hughes [16]

$$\hat{\ell} = \arg \max_{\ell} \text{tr} \left\{ \mathbf{R}^\dagger \mathbf{D}_\ell \mathbf{D}_\ell^\dagger \mathbf{R} \right\}, \quad (2.36)$$

where \mathbf{D}_ℓ represents a specific sequence of transmitted messages. The optimal receiver is based on the entire received sequence (2.35) and since its complexity is exponential in the sequence length K , a simpler suboptimal receiver is suggested based on only the last two received blocks. In this case, the quadratic detector reduces to:

$$\begin{aligned}
\hat{\ell} &= \arg \max_{\ell} \text{tr} \left\{ \begin{bmatrix} \mathbf{R}_{k-1}^\dagger & \mathbf{R}_k^\dagger \end{bmatrix} \begin{bmatrix} Q\mathbf{I}_2 & Q\mathbf{S}^{(\ell)\dagger} \\ Q\mathbf{S}^{(\ell)} & Q\mathbf{I}_2 \end{bmatrix} \begin{bmatrix} \mathbf{R}_{k-1} \\ \mathbf{R}_k \end{bmatrix} \right\} \\
&= \arg \max_{\ell} \text{tr} \left\{ \mathbf{R}_{k-1}^\dagger \mathbf{R}_{k-1} + \mathbf{R}_{k-1}^\dagger \mathbf{S}^{(\ell)\dagger} \mathbf{R}_k + \mathbf{R}_k^\dagger \mathbf{S}^{(\ell)} \mathbf{R}_{k-1} + \mathbf{R}_k^\dagger \mathbf{R}_k \right\} \\
&= \arg \max_{\ell} \text{Re tr} \left\{ \mathbf{R}_{k-1}^\dagger \mathbf{S}^{(\ell)\dagger} \mathbf{R}_k \right\} \\
&= \arg \max_{\ell} \text{Re tr} \left\{ \mathbf{S}^{(\ell)\dagger} \mathbf{R}_k \mathbf{R}_{k-1}^\dagger \right\}, \tag{2.37}
\end{aligned}$$

where $\mathbf{S}^{(\ell)}$ is a message matrix, and the identity $\text{tr}\{\mathbf{AB}\} = \text{tr}\{\mathbf{BA}\}$ is used. The suboptimal receiver in Equation (2.37) can be interpreted as a demodulator that generates the matrices $\mathbf{G}_k = \mathbf{R}_k \mathbf{R}_{k-1}^\dagger$ followed by a decision mechanism. Consider now the properties of the demodulator output \mathbf{G}_k . Exploiting previous definitions, the (1,1) element of this matrix can be expressed

$$\begin{aligned}
g &= \sum_{q=1}^Q \left\{ \left(|h_1^{(q)}|^2 + |h_2^{(q)}|^2 \right) s_k^{(1)} \right. \\
&\quad + h_1^{(q)} \left(c_k^{(1)} n_{1,k-1}^{(q)*} - c_{k-1}^{(2)*} n_{2,k}^{(q)*} + c_{k-1}^{(1)*} \nu_1^{(q)} n_{1,k}^{(q)} - c_k^{(2)} \nu_1^{(q)*} n_{2,k-1}^{(q)} \right) \\
&\quad \left. + h_2^{(q)} \left(c_k^{(2)} n_{1,k-1}^{(q)*} + c_{k-1}^{(1)*} n_{2,k}^{(q)*} + c_{k-1}^{(2)*} \nu_2^{(q)} n_{1,k}^{(q)} + c_k^{(1)} \nu_2^{(q)*} n_{2,k-1}^{(q)} \right) \right\}, \tag{2.38}
\end{aligned}$$

where $\nu_i^{(q)} = h_i^{(q)*}/h_i^{(q)}$, $i = 1, 2$, is a random variable and second order noise terms were neglected. It follows that the complex scalar g can serve as a decision statistic for the detection of the message symbol $s_k^{(1)}$. In Equation (2.38), let

$$\begin{aligned}
X_1^{(q)} &= h_1^{(q)}, \\
X_2^{(q)} &= h_2^{(q)}, \\
Y_1^{(q)} &= h_1^{(q)*} s_k^{(1)} + c_k^{(1)} n_{1,k-1}^{(q)*} - c_{k-1}^{(2)*} n_{2,k}^{(q)*} + c_{k-1}^{(1)*} \nu_1^{(q)} n_{1,k}^{(q)} - c_k^{(2)} \nu_1^{(q)*} n_{2,k-1}^{(q)}, \\
Y_2^{(q)} &= h_2^{(q)*} s_k^{(1)} + c_k^{(2)} n_{1,k-1}^{(q)*} + c_{k-1}^{(1)*} n_{2,k}^{(q)*} + c_{k-1}^{(2)*} \nu_2^{(q)} n_{1,k}^{(q)} + c_k^{(1)} \nu_2^{(q)*} n_{2,k-1}^{(q)}. \tag{2.39}
\end{aligned}$$

Then g can be expressed

$$g = \sum_{q=1}^Q \left(X_1^{(q)} Y_1^{(q)} + X_2^{(q)} Y_2^{(q)} \right). \quad (2.40)$$

Consider the properties of the random variables defined in Equation (2.39). Under the assumptions delineated in the Section 1.2, all these random variables have zero-mean. Clearly, $X_1^{(q)}, X_2^{(q)}$ are independent and identically distributed (i.i.d.) complex-valued Gaussian with unity variance. The variates $Y_1^{(q)}, Y_2^{(q)}$ require a bit more careful consideration due to their dependence on $\nu_1^{(q)}$ and $\nu_2^{(q)}$, respectively. It is not difficult to show that $\nu_i^{(q)}$ are of the form $\nu_i^{(q)} = \exp(-j2\phi)$, where ϕ is a uniformly distributed phase in the interval $(-\pi/2, \pi/2)$. It follows that multiplication by $\nu_i^{(q)}$ does not affect the distribution of complex Gaussian variates in Equation (2.39).

It is easy to see that pairs $(X_i^{(q)}, Y_i^{(q)})$, $i = 1, 2$, $q = 1, \dots, Q$, are correlated, complex-valued, zero-mean Gaussian. Moreover, it can be shown that $E[Y_1^{(q)} Y_2^{(q)*}] = 0$, but details are omitted here due to space considerations. Based on these observations, it is concluded that the pairs $(X_i^{(q)}, Y_i^{(q)})$ are i.i.d. This conclusion facilitates the application of known results for the development of BER analysis.

Repeating the procedure carried out for the coherent case, define $Z_r = \text{Re}(g)$, $Z_i = \text{Im}(g)$ and $R = \sqrt{Z_r^2 + Z_i^2}$, $\Theta = \tan^{-1}(Z_i/Z_r)$, and obtain the PDF $p(\theta)$ in the form Proakis' book [18, p. 891]. This PDF is a function of the cross-correlation μ_d defined in Expression (2.17). The following quantities are required for the computation of μ_d :

$$m_{xx} = E\left(|X_i^{(q)}|^2\right) = 1, \quad (2.41)$$

and

$$\begin{aligned}
m_{yy} &= E \left(\left| Y_i^{(q)} \right|^2 \right) \\
&= \frac{E_s}{2} + \frac{N_0}{2} \left(\left| c_k^{(1)} \right|^2 + \left| c_k^{(2)} \right|^2 + \left| c_{k-1}^{(1)*} \right|^2 + \left| c_{k-1}^{(2)*} \right|^2 \right) \\
&= \frac{E_s}{2} + 2N_0,
\end{aligned} \tag{2.42}$$

where the unitary property of the matrices \mathbf{C}_k is exploited.

Finally, assume that the transmitted symbol has zero phase, i.e., $s_{1,k} = 1/\sqrt{2}$ and compute

$$\begin{aligned}
m_{xy} &= E \left(X_i^{(q)} Y_i^{*(q)} \right) \\
&= \sqrt{E_s/2}.
\end{aligned} \tag{2.43}$$

It follows that the normalized cross-correlation for differential STBC is given by

$$\mu_d = \sqrt{\frac{\rho_d}{\rho_d + 2}}, \tag{2.44}$$

where the subscript is used to distinguish between the coherent and differential cases and the SNR per symbol $\rho_d = E_s/2N_0$ is half of that in the coherent case.

Repeating the argument and steps used for coherent case, the BER for BPSK differential STBC is given by

$$P_{2b,\text{diff}} = \frac{1}{2} \left[1 - \sqrt{\frac{\rho_d}{\rho_d + 2}} \sum_{q=0}^{2Q-1} \binom{2q}{q} \left(\frac{1}{2(\rho_d + 2)} \right)^q \right]. \tag{2.45}$$

For QPSK differential STBC, the BER is

$$P_{4b,\text{diff}} = \frac{1}{2} \left[1 - \sqrt{\frac{\rho_d}{\rho_d + 4}} \sum_{q=0}^{2Q-1} \binom{2q}{q} \left(\frac{1}{\rho_d + 4} \right)^q \right]. \tag{2.46}$$

Note that $P_{2b,\text{diff}}$, $P_{4b,\text{diff}}$, have the same expressions as P_{2b} , and P_{4b} respectively, but the definitions of ρ_d and ρ are different.

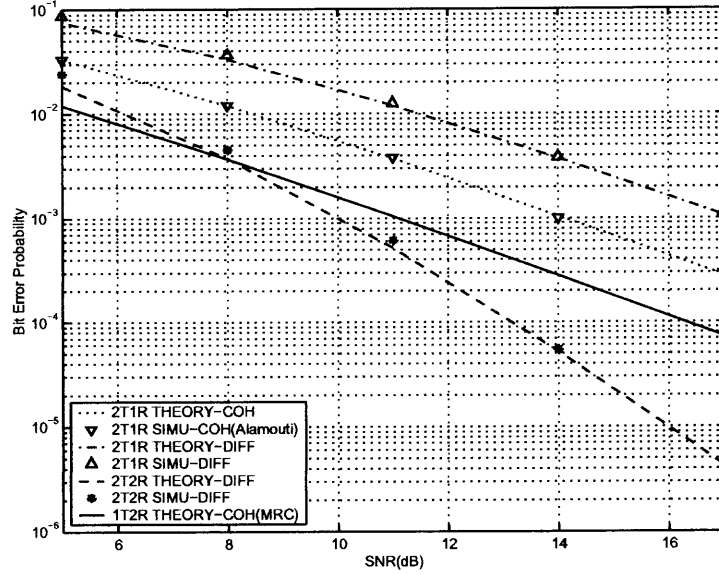


Figure 2.1 Comparison of analysis and simulation with coherent and differential detection in BPSK case (1 bit/s/Hz).

2.4 Numerical Results

Numerical results are provided to demonstrate the analysis developed in this dissertation and to compare it with simulation results.

Figure 2.1 shows the BER versus the SNR for binary coherent and differential Alamouti's STBC. Curves were obtained both by analysis and simulations as indicated by the figure annotations. A very good match is observed between the analysis and simulation. The slight bias at low SNR for the differential case can be attributed to the second order noise terms, which were neglected in the analysis. Figure 2.2 presents the case of coherent and differential STBC with QPSK modulation. The figures confirm that an approximately 3 dB performance gap exists between the coherent and differential schemes. Note that the performance for differential STBC with QPSK is a little better than Tarokh's results [13] since bits are mapped to QPSK symbols using the Gray code.

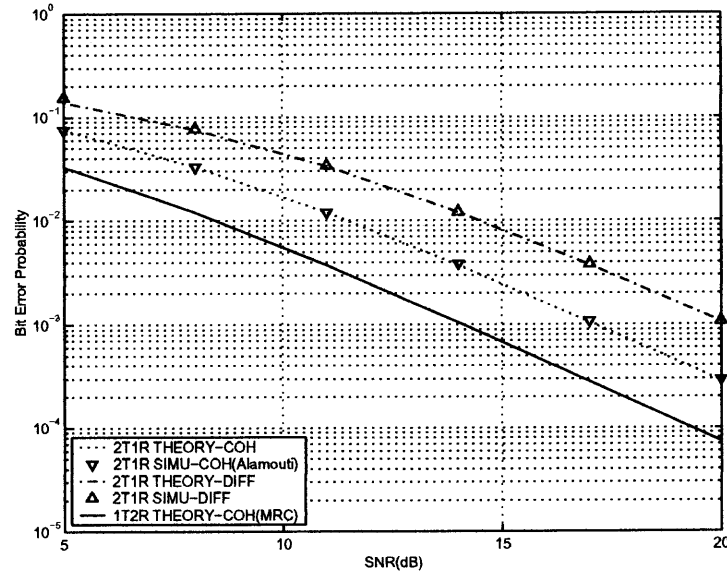


Figure 2.2 Comparison of analysis and simulation with coherent and non-coherent detection in QPSK case (2 bits/s/Hz).

2.5 Conclusions

Closed-form expressions of the BER for coherent and differential schemes based on Alamouti's STBC were derived. The channel model assumed was slow, flat fading Rayleigh. While the procedure outlined is applicable to any MPSK modulation, explicit BER expressions were obtained for BPSK and QPSK. Comparison of analytical and simulation results validates the new expressions. The closed-form expressions show that approximately 3 dB SNR loss is incurred by the differential scheme compared to the coherent case. The method presented is extendable to other MIMO channels.

CHAPTER 3

MSDD FOR MPSK SPACE-TIME BLOCK CODES

3.1 Introduction

Multiple-symbol differential detection (MSDD) was first presented for one transmit antenna over the additive white Gaussian noise (AWGN) channel by Divsalar and Simon [20]. By extending the observation interval to more than two symbols, the technique makes use of maximum likelihood sequence detection instead of symbol-by-symbol detection as in conventional differential detection. The performance of MSDD depends on the number of observation symbols. For a moderate number of symbols, MSDD bridges the performance gap between non-coherent and coherent communications. In Divsalar's and Ho's papers [21] [22], MSDD was applied to the flat Rayleigh fading channel.

Motivated by MSDD, Fan [23] extended the observation interval of differential Alamouti STBC [13] to 3 blocks. As a result, a performance improvement of about 0.5 dB for BPSK messages was demonstrated. In addition, Bhukania et al. [24] expanded MSDD idea to the STBC scheme in Hochwald's paper [15] for 3 blocks and incorporate knowledge of fading correlation, assuming that the channel changes once per block.

In this chapter, differential Alamouti's STBC for larger observation intervals is generalized. The decision metric for N blocks of observation interval is derived. It is shown that for an observation interval of $N = 8$ blocks there is a gain of about 1.5 dB over differential Alamouti's STBC with two blocks. Moreover, based on the generalized decision metric for an observation interval of N blocks, a closed-form pairwise error probability for BPSK STBC is derived, and an approximate bit error rate is obtained to evaluate its performance.

3.2 Receiver Model

Based on the system model in the Section 1.2, to simplify notation and with no loss of generality, assume that there is only one receive antenna. Note that the differential Alamouti's STBC scheme consists of sending the code matrix \mathbf{C}_k rather than message matrix \mathbf{S}_k directly, where \mathbf{C}_k is differentially encoded by Expression (2.28). Now, observe the received signals when the differential code matrix \mathbf{C}_k is transmitted. From Equation (1.1) and Equation (1.4), the corresponding received signals can be written

$$\begin{bmatrix} r_{1,k} \\ r_{2,k} \end{bmatrix} = \sqrt{E_s} \begin{bmatrix} c_{1,k} & c_{2,k} \\ -c_{2,k}^* & c_{1,k}^* \end{bmatrix} \begin{bmatrix} h_1 \\ h_2 \end{bmatrix} + \begin{bmatrix} n_{1,k} \\ n_{2,k} \end{bmatrix}, \quad (3.1)$$

where $r_{1,k}$ and $r_{2,k}$ represent two received signals at time slots 1 and 2, respectively.

Paralleling Equation (3.1) and using matrix notation, the signal model at the receiver for the two time slots associated with each codeword is expressed

$$\mathbf{R}_k = \sqrt{E_s} \mathbf{C}_k \mathbf{H}_k + \Psi_k, \quad (3.2)$$

where

$$\begin{aligned} \mathbf{R}_k &= \begin{bmatrix} r_{1,k} & -r_{2,k}^* \\ r_{2,k} & r_{1,k}^* \end{bmatrix}, \quad \mathbf{C}_k = \begin{bmatrix} c_{1,k} & c_{2,k} \\ -c_{2,k}^* & c_{1,k}^* \end{bmatrix}, \\ \mathbf{H}_k &= \begin{bmatrix} h_1 & -h_2^* \\ h_2 & h_1^* \end{bmatrix}, \quad \Psi_k = \begin{bmatrix} n_{1,k} & -n_{2,k}^* \\ n_{2,k} & n_{1,k}^* \end{bmatrix}. \end{aligned} \quad (3.3)$$

For the MSDD signal model, consider an observation interval consisting of N blocks of symbols, where, consistent with differential decoding, each block is defined as two symbols at two time slots. A frame consists of L symbol blocks. The channel is assumed constant during a frame, which implies that the channel is fixed during the observation interval. Starting from the k th block \mathbf{R}_k , the received sequence can

be expressed as

$$\mathbf{R} = \sqrt{E_s} \mathbf{C} \mathbf{H} + \Psi, \quad (3.4)$$

where

$$\begin{aligned} \mathbf{R} &= [\mathbf{R}_k \ \mathbf{R}_{k-1} \ \dots \ \mathbf{R}_{k-N+1}]^T \\ \mathbf{C} &= \text{diag} \{ \mathbf{C}_k, \mathbf{C}_{k-1}, \dots, \mathbf{C}_{k-N+1} \} \\ \mathbf{H} &= [\mathbf{H}_k \ \mathbf{H}_{k-1} \ \dots \ \mathbf{H}_{k-N+1}]^T \\ \Psi &= [\Psi_k \ \Psi_{k-1} \ \dots \ \Psi_{k-N+1}]^T. \end{aligned} \quad (3.5)$$

The matrices \mathbf{R} , \mathbf{H} , and Ψ are $2N \times 2$ and \mathbf{C} is $2N \times 2N$. For convenience, the $2N \times 2N$ matrix $\mathbf{S} = \text{diag} \{ \mathbf{S}_k, \mathbf{S}_{k-1}, \dots, \mathbf{S}_{k-N+1} \}$ is also defined.

3.3 Decision Metric for MSDD

3.3.1 Coherent Detection

Assume that the observation interval consists of N blocks. If the CSI is known, from Expression (3.4), conditioned on the transmitted symbols \mathbf{C} and the channel \mathbf{H} , the matrix \mathbf{R} is a complex-valued, zero-mean Gaussian random matrix. Its probability density function (PDF) is given by Hughes [16]

$$p(\mathbf{R}|\mathbf{H}, \mathbf{C}) = \frac{1}{(\pi)^{4N}} \exp \left\{ -\text{tr} \left[\left(\mathbf{R} - \sqrt{E_s} \mathbf{C} \mathbf{H} \right)^H \left(\mathbf{R} - \sqrt{E_s} \mathbf{C} \mathbf{H} \right) \right] \right\}. \quad (3.6)$$

If the code matrices are equally likely, the optimal receiver is the maximum-likelihood detector [25] and can be simplified so that \mathbf{C} can be detected by

$$\begin{aligned} \hat{\mathbf{C}} &= \arg \max_{\tilde{\mathbf{C}}_{1,k-i}, \tilde{\mathbf{C}}_{2,k-i} \in F} p(\mathbf{R}|\mathbf{H}, \tilde{\mathbf{C}}) \\ &= \arg \max_{\tilde{\mathbf{C}}_{1,k-i}, \tilde{\mathbf{C}}_{2,k-i} \in F} \text{Re tr} \left[\mathbf{H}^H \tilde{\mathbf{C}}^H \mathbf{R} \right]. \end{aligned} \quad (3.7)$$

The optimal receiver utilizes the entire receive sequence (3.4). Since its complexity is exponential in the sequence length N , a simpler suboptimal receiver can be constructed utilizing only the last two received blocks. Simplifying Equation (3.7),

$$\begin{bmatrix} \hat{\mathbf{C}}_{k-1} & \hat{\mathbf{C}}_k \end{bmatrix} = \arg \max_{\tilde{\mathbf{C}}_{1,k-i}, \tilde{\mathbf{C}}_{2,k-i} \in F} \text{Re tr} \left[\mathbf{H}_k^H \tilde{\mathbf{C}}_k^H \mathbf{R}_k + \mathbf{H}_{k-1}^H \tilde{\mathbf{C}}_{k-1}^H \mathbf{R}_{k-1} \right]. \quad (3.8)$$

If \mathbf{C}_k is differential encoded by Equation (2.28), then the detector is equivalent to

$$\begin{bmatrix} \hat{\mathbf{C}}_{k-1} & \hat{\mathbf{S}}_k \end{bmatrix} = \arg \max_{\tilde{\mathbf{C}}_{1,k-i}, \tilde{\mathbf{C}}_{2,k-i} \in F} \text{Re tr} \left[\mathbf{H}_k^H \tilde{\mathbf{C}}_{k-1}^H \hat{\mathbf{S}}_k \mathbf{R}_k + \mathbf{H}_{k-1}^H \tilde{\mathbf{C}}_{k-1}^H \mathbf{R}_{k-1} \right]. \quad (3.9)$$

Expression (3.7) and (3.9) are the decision metric for the case that channel is known, but the author is concerned with the decision metric for situations when the channel is unknown.

3.3.2 Non-coherent Detection

Assume that the observation interval consists of N blocks. If the CSI is known, from Expression (3.4), conditioned on the transmitted symbols \mathbf{C} and the channel \mathbf{H} , the matrix \mathbf{R} is a complex-valued, zero-mean Gaussian random matrix. Its probability density function (PDF) is given by Hughes [16]

$$p(\mathbf{R}|\mathbf{H}, \mathbf{C}) = \frac{1}{(\pi)^{4N}} \exp \left\{ -\text{tr} \left[\left(\mathbf{R} - \sqrt{E_s} \mathbf{C} \mathbf{H} \right)^\dagger \left(\mathbf{R} - \sqrt{E_s} \mathbf{C} \mathbf{H} \right) \right] \right\}. \quad (3.10)$$

If the code matrices are equally likely, the optimal receiver is the maximum-likelihood detector [25], so \mathbf{C} can be detected by

$$\begin{aligned} \hat{\mathbf{C}} &= \arg \max_{\tilde{\mathbf{C}}_{1,k-i}, \tilde{\mathbf{C}}_{2,k-i} \in A} p(\mathbf{R}|\mathbf{H}, \tilde{\mathbf{C}}) \\ &= \arg \min_{\tilde{\mathbf{C}}_{1,k-i}, \tilde{\mathbf{C}}_{2,k-i} \in A} \text{tr} \left[\left(\mathbf{R} - \sqrt{E_s} \tilde{\mathbf{C}} \mathbf{H} \right)^\dagger \left(\mathbf{R} - \sqrt{E_s} \tilde{\mathbf{C}} \mathbf{H} \right) \right]. \end{aligned} \quad (3.11)$$

Expression (3.11) is the decision metric for the case that channel is known, but the author is concerned with decision metric for situations when the channel is unknown.

Differential encoding can be applied when the channel \mathbf{H} is unknown, but fixed over some time intervals. In this case, the transmitter sends the code matrix \mathbf{C}_k instead of sending messages \mathbf{S}_k directly. For a block of N observations, the received matrix \mathbf{R} given that message matrix \mathbf{S} is transmitted (through code matrix \mathbf{C}) has a multivariate Gaussian conditional PDF

$$p(\mathbf{R}|\mathbf{S}) = \frac{1}{(\pi)^{4N} \det \Lambda} \exp\{-\text{tr}(\mathbf{R}^\dagger \Lambda^{-1} \mathbf{R})\}, \quad (3.12)$$

where Λ is the covariance matrix of \mathbf{R} , $\Lambda = E\{\mathbf{R}\mathbf{R}^\dagger|\mathbf{S}\}$. Since path gains are assumed constant during a frame, $\mathbf{H}_i = \mathbf{H}_j$, $i \neq j$, hence,

$$\begin{aligned} \Lambda &= E \left[\left(\sqrt{E_s} \mathbf{C} \mathbf{H} + \Psi \right) \left(\sqrt{E_s} \mathbf{C} \mathbf{H} + \Psi \right)^\dagger \right] \\ &= E \left[E_s \mathbf{C} \mathbf{H} \mathbf{H}^\dagger \mathbf{C}^\dagger + \Psi \Psi^\dagger \right] \\ &= E_s \mathbf{C} (\mathbf{I}_2 \otimes \mathbf{1}_N) \mathbf{C}^\dagger + N_0 \mathbf{I}_{2N}, \end{aligned} \quad (3.13)$$

where $\mathbf{1}_N$ represents an $N \times N$ matrix with all elements equal 1.

Using the unitary property of the matrix \mathbf{C} , it can be shown that $\det \Lambda$ is independent of the messages $\mathbf{S}_k, \mathbf{S}_{k-1}, \dots, \mathbf{S}_{k-N+1}$.

Define the matrices \mathbf{A} , \mathbf{F} , \mathbf{B} , and \mathbf{D} :

$$\mathbf{A} = N_0 \mathbf{I}_{2N}, \quad (3.14)$$

$$\mathbf{F} = E_s \mathbf{I}_{2N}, \quad (3.15)$$

$$\mathbf{B} = \mathbf{C} (\mathbf{I}_2 \otimes \mathbf{1}_{N \times 1}), \quad (3.16)$$

$$\mathbf{D} = (\mathbf{I}_2 \otimes \mathbf{1}_{N \times 1})^\dagger \mathbf{C}^\dagger, \quad (3.17)$$

where $\mathbf{1}_{N \times 1}$ is a vector of ones. Then Equation (3.13) can be expressed as $\Lambda = \mathbf{B} \mathbf{F} \mathbf{D} + \mathbf{A}$. Using the matrix inversion lemma [26]

$$(\mathbf{A} + \mathbf{B} \mathbf{F} \mathbf{D})^{-1} = \mathbf{A}^{-1} - \mathbf{A}^{-1} \mathbf{B} (\mathbf{F}^{-1} + \mathbf{D} \mathbf{A}^{-1} \mathbf{B})^{-1} \mathbf{D} \mathbf{A}^{-1}, \quad (3.18)$$

and Equation (3.13),

$$\Lambda^{-1} = \frac{1}{N_0} \mathbf{I}_{2N} - \frac{E_s}{N_0 (E_s + N_0)} \mathbf{C} (\mathbf{I}_2 \otimes \mathbf{1}_N) \mathbf{C}^\dagger. \quad (3.19)$$

Since the natural logarithm is a monotonically increasing function of its argument, maximizing $p(\mathbf{R}|\mathbf{S})$ over \mathbf{S} in Equation (3.12) is equivalent to maximizing $\ln(p(\mathbf{R}|\mathbf{S}))$ over \mathbf{S} . Choosing the sequence \mathbf{S} to maximize logarithm of Equation (3.12), results in the decision metric

$$\begin{aligned} \hat{\eta} &= \text{tr} \left[-\ln(\det \Lambda) - (\mathbf{R}^\dagger \Lambda^{-1} \mathbf{R}) \right] \\ &= \text{tr} \left[-\ln(\det \Lambda) - \frac{1}{N_0} \mathbf{R}^\dagger \mathbf{R} + \frac{E_s}{N_0 (E_s + N_0)} \mathbf{R}^\dagger (\mathbf{C} (\mathbf{I}_2 \otimes \mathbf{1}_N) \mathbf{C}^\dagger) \mathbf{R} \right]. \end{aligned} \quad (3.20)$$

As $\det \Lambda$, $\mathbf{R}^\dagger \mathbf{R}$, N_0 , and E_s are independent of transmitted messages, they can be ignored. Then the decision metric becomes:

$$\tilde{\eta} = \text{tr} \left[\mathbf{R}^\dagger \mathbf{C} (\mathbf{I}_2 \otimes \mathbf{1}_N) \mathbf{C}^\dagger \mathbf{R} \right]. \quad (3.21)$$

Expanding Expression (3.21), the metric can be expressed

$$\begin{aligned} \tilde{\eta} &= \text{tr} \left[\sum_{i=0}^{N-1} \sum_{j=0}^{N-1} \mathbf{R}_{k-i}^\dagger \mathbf{C}_{k-i} \mathbf{C}_{k-j}^\dagger \mathbf{R}_{k-j} \right] \\ &= \text{tr} \left[\sum_{i=0}^{N-1} \mathbf{R}_{k-i}^\dagger \mathbf{C}_{k-i} \mathbf{C}_{k-i}^\dagger \mathbf{R}_{k-i} \right] + \text{tr} \left[\sum_{i=0}^{N-1} \sum_{j=0}^{N-1} \mathbf{R}_{k-i}^\dagger \mathbf{C}_{k-i} \mathbf{C}_{k-j}^\dagger \mathbf{R}_{k-j} \right]_{i \neq j} \\ &= T + 2 \text{Re} \text{tr} \left[\sum_{i=1}^{N-1} \sum_{j=0}^{i-1} \mathbf{R}_{k-i}^\dagger \mathbf{C}_{k-i} \mathbf{C}_{k-j}^\dagger \mathbf{R}_{k-j} \right], \end{aligned} \quad (3.22)$$

where

$$T = \text{tr} \left[\sum_{i=0}^N \mathbf{R}_{k-i}^\dagger \mathbf{C}_{k-i} \mathbf{C}_{k-i}^\dagger \mathbf{R}_{k-i} \right], \quad (3.23)$$

and "Re" denotes the real part. Due to the unitary property of \mathbf{C}_{k-i} , T is independent of the transmitted symbol sequence. Thus the decision metric becomes

$$\eta = \text{Re tr} \left[\sum_{i=1}^{N-1} \sum_{j=0}^{i-1} \mathbf{R}_{k-i}^\dagger \mathbf{C}_{k-i} \mathbf{C}_{k-j}^\dagger \mathbf{R}_{k-j} \right]. \quad (3.24)$$

Using the identity for the trace function [26],

$$\text{Re tr} \left[\mathbf{R}_{k-i}^\dagger \mathbf{C}_{k-i} \mathbf{C}_{k-j}^\dagger \mathbf{R}_{k-j} \right] = \text{Re tr} \left[\mathbf{R}_{k-j} \mathbf{R}_{k-i}^\dagger \mathbf{C}_{k-i} \mathbf{C}_{k-j}^\dagger \right], \quad (3.25)$$

from Equation (3.24), (3.25), and (2.30),

$$\eta = \text{Re tr} \left[\sum_{i=1}^{N-1} \sum_{j=0}^{i-1} \mathbf{R}_{k-j} \mathbf{R}_{k-i}^\dagger \mathbf{C}_{k-i} \mathbf{C}_{k-j}^\dagger \right] \quad (3.26)$$

$$= \text{Re tr} \left[\sum_{i=1}^{N-1} \sum_{j=0}^{i-1} \mathbf{R}_{k-j} \mathbf{R}_{k-i}^\dagger (\mathbf{S}_{k-j} \dots \mathbf{S}_{k-i+1})^\dagger \right]. \quad (3.27)$$

The differentially encoded message $\hat{\mathbf{S}}$ can then be detected from

$$\hat{\mathbf{S}} = \arg \max_{\tilde{s}_{1,k-i}, \tilde{s}_{2,k-i} \in A} \text{Re tr} \left[\sum_{i=1}^{N-1} \sum_{j=0}^{i-1} \mathbf{R}_{k-j} \mathbf{R}_{k-i}^\dagger \left(\tilde{\mathbf{S}}_{k-j} \tilde{\mathbf{S}}_{k-j-1} \dots \tilde{\mathbf{S}}_{k-i+1} \right)^\dagger \right]. \quad (3.28)$$

This is the MSDD decision metric for an observation interval of N blocks. Notice that no channel information is required for the signal detection. For an observation interval of N blocks, there are $N - 1$ message blocks (the first block \mathbf{C}_0 does not contain information). Each block contains two unknown symbols. Hence, for M -PSK symbols, there are $M^{2(N-1)}$ possible message block sequences $\tilde{\mathbf{S}}_k, \tilde{\mathbf{S}}_{k-1}, \dots, \tilde{\mathbf{S}}_{k-N+2}$. As in single antenna MSDD, the complexity of the receiver increases exponentially with the length of the observation interval.

Next, the special cases of $N = 2$ and $N = 3$ is discussed.

Two-Block Observation Interval When $N = 2$, Equation (3.28) becomes

$$\hat{\mathbf{S}}_k = \arg \max_{\tilde{s}_{1,k}, \tilde{s}_{2,k} \in A} \text{Re tr} \left\{ \mathbf{R}_k \mathbf{R}_{k-1}^\dagger \tilde{\mathbf{S}}_k^\dagger \right\}. \quad (3.29)$$

Let \mathbf{S}_k be the message matrix that is differentially encoded and transmitted. Then

$$\begin{aligned} \mathbf{R}_k \mathbf{R}_{k-1}^\dagger &= (|h_{1,1}|^2 + |h_{2,1}|^2) E_s \mathbf{S}_k + \sqrt{E_s} \mathbf{C}_k \mathbf{H}_k \Psi_{k-1}^\dagger \\ &\quad + \sqrt{E_s} \Psi_k \mathbf{H}_{k-1}^\dagger \mathbf{C}_{k-1}^\dagger + \Psi_k \Psi_{k-1}^\dagger. \end{aligned} \quad (3.30)$$

Equation (3.30) is similar to the expression (26) in Tarokh's paper [13]. MSDD is a generalization of the differential space-time codes in Tarokh's paper [13]. The notation not only enables to express the MSDD decision statistic, but also provides a simpler way to express known results for two blocks observation interval.

Three-Block Observation Interval Another special case of interest is an observation interval of $N = 3$. A receiver scheme with significant notational complexity was suggested in the paper [23]. Once again, the notation provides a simple decision statistic expressed as a special case of Equation (3.28). $\mathbf{S}_k, \mathbf{S}_{k-1}$ can be detected by

$$\begin{aligned} [\hat{\mathbf{S}}_k \hat{\mathbf{S}}_{k-1}] &= \arg \max_{\tilde{\mathbf{s}}_{1,k}, \tilde{\mathbf{s}}_{2,k} \in A} \text{Re tr} \left\{ \mathbf{R}_k \mathbf{R}_{k-1}^\dagger \tilde{\mathbf{S}}_k^\dagger + \right. \\ &\quad \left. \mathbf{R}_{k-1} \mathbf{R}_{k-2}^\dagger \tilde{\mathbf{S}}_{k-1}^\dagger + \mathbf{R}_k \mathbf{R}_{k-2}^\dagger (\tilde{\mathbf{S}}_k \tilde{\mathbf{S}}_{k-1})^\dagger \right\}. \end{aligned} \quad (3.31)$$

Using decision metric in Equation (3.28), blocks of differentially encoded signals can be detected by observing intervals of different lengths. Figure 3.1 and Figure 3.2 consist of curves for various observation intervals and for BPSK and QPSK modulations, respectively. The curves for $N = 2$ correspond to the scheme suggested in Tarokh's paper [13]. Indeed these curves match those in the reference. The curve for $N = 3$ in Figure 3.1 matches well the results in Fan's paper [23]. Note that there is an almost 0.5 dB improvement by increasing the observation interval from $N = 2$ to $N = 3$.

Since the computation complexity of the decision statistic in Equation (3.28) increases exponentially with N , results for observation intervals of only 8 blocks (16

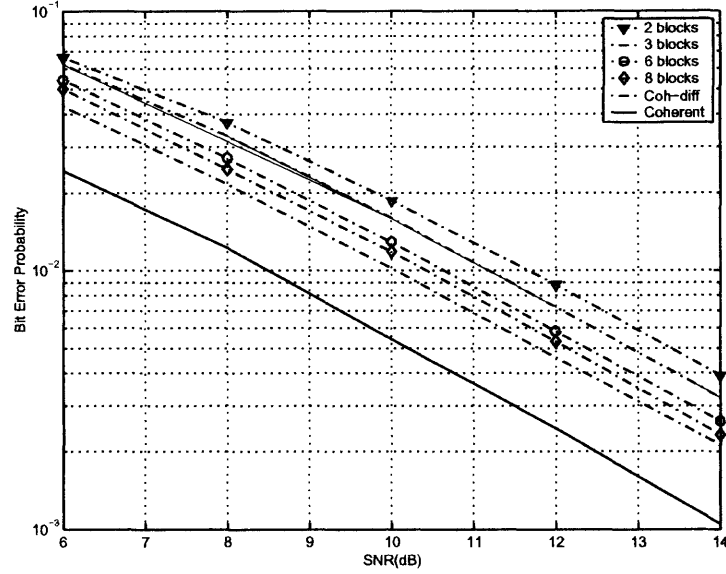


Figure 3.1 Multiple symbol differential detection for space-time block code with BPSK signal. Bit Error Rate versus SNR for different length of observation interval, 2 transmit antennas, 1 receive antenna.

symbols) are presented. For BPSK and $N = 8$, there is about 1.5 dB performance improvement compared to the conventional differential detection. This implies a 1.5 dB and 1 dB gain, respectively, over previously published results for 2 and 3 block observation intervals.

For comparison, by utilizing decision metric (3.9), the simulation results for differential Alamouti STBC and regular Alamouti STBC with coherent detection (for regular STBC, only an observation interval of one block is needed) have also been obtained, which are represented by "Coh-Diff" and "Coherent" in Figure 3.1 and Figure 3.2 respectively. It appears that those curves will converge to the one for differential STBC with coherent detection for both BPSK and QPSK modulation. Through theoretical analysis, this observation result will be verified later.

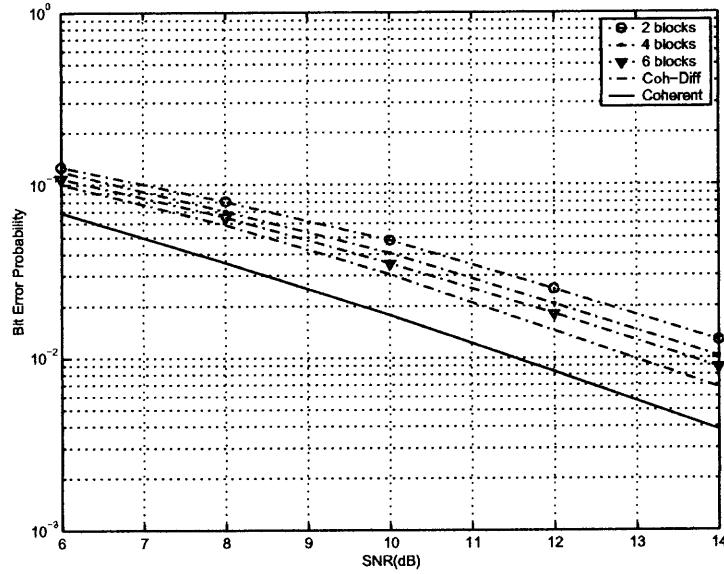


Figure 3.2 Multiple symbol differential detection for space-time block code with QPSK signal. Bit Error Rate versus SNR for different length of observation interval, 2 transmit antennas, 1 receive antenna.

3.4 Performance Analysis

Before addressing performance analysis, some theorems are provided (without proof due to space constraints) :

Theorem 1: If \mathbf{A}, \mathbf{B} are two 2×2 orthogonal real matrices, then $\mathbf{AB} = \mathbf{BA}$.

Theorem 2: If \mathbf{A}, \mathbf{B} are two 2×2 orthogonal complex matrices, then $\text{Re tr}(\mathbf{AB}) = \text{Re tr}(\mathbf{BA})$.

Theorem 3: Assume that \mathbf{A}, \mathbf{B} are two 2×2 orthogonal complex matrices, if $\mathbf{C} = \mathbf{AB}$, and $\mathbf{D} = \mathbf{A} + \mathbf{B}$, then \mathbf{C} is an orthogonal matrix, and \mathbf{D} is a unitary matrix.

Theorem 4: If \mathbf{A} is a 2×2 unitary complex matrix, then $\text{Re tr}(\mathbf{A}) = \text{Re tr}(\mathbf{A}^\dagger)$.

Theorem 5: Assume that Φ is a 2×2 unitary random complex matrix, each element of which has zero mean and variance $N_0/2$ per dimension, \mathbf{H}_k is a 2×2 unitary constant complex matrix defined in (3.3), and \mathbf{A} is a 2×2 orthogonal real constant

matrix, then the mean $E[\text{Re tr}(\mathbf{A}\mathbf{H}_k\Phi)] = 0$, and the variance $\text{Var}[\text{Re tr}(\mathbf{A}\mathbf{H}_k\Phi)] = 2(|h_1|^2 + |h_2|^2)N_0$.

Theorem 6: Assume that Φ is a 2×2 unitary random complex matrix, each element of which has zero mean and variance $N_0/2$ per dimension, \mathbf{H}_k is a 2×2 unitary constant complex matrix defined in (3.3), and \mathbf{A}, \mathbf{B} are two 2×2 constant unitary real matrices, then

$$\begin{aligned} & \text{cov}\{\text{Re tr}(\mathbf{A}\mathbf{H}_k\Phi), \text{Re tr}(\mathbf{B}\mathbf{H}_k\Phi)\} \\ &= N_0(|h_1|^2 + |h_2|^2) \text{Re tr}(\mathbf{A}\mathbf{B}^\dagger). \end{aligned} \quad (3.32)$$

Theorem 7: Assume that Φ, Ψ are two 2×2 unitary random complex matrices, each element of which has zero mean and variance $N_0/2$ per dimension and \mathbf{A}, \mathbf{B} are two 2×2 unitary constant complex matrices, then the mean $E\{\text{Re tr}(\Phi\mathbf{A}) \text{Re tr}(\Psi\mathbf{B})\} = 0$.

Suppose that the messages sent at each block are the same BPSK messages, namely, $\mathbf{S}_k = \mathbf{S}_\zeta$. Since errors occur during transmission of code matrix \mathbf{C}_k due to channel fading and noise, after differential decoding, assume that the message \mathbf{E}_k in each block is detected, where

$$\mathbf{S}_\zeta = \begin{bmatrix} s_{1,\zeta} & s_{2,\zeta} \\ -s_{2,\zeta} & s_{1,\zeta} \end{bmatrix}, \quad \mathbf{E}_k = \begin{bmatrix} e_{1,k} & e_{2,k} \\ -e_{2,k} & e_{1,k} \end{bmatrix}, \quad (3.33)$$

and $e_{1,k}, e_{2,k} \in A$, which is defined in Expression (1.3). Obviously $\mathbf{E}_k \mathbf{E}_k^\dagger = \mathbf{I}_2$. In order to measure the difference between \mathbf{S}_k and \mathbf{E}_k , define $\mathbf{D}_k = \mathbf{E}_k \mathbf{S}_k^\dagger$. So the matrix distance between \mathbf{S}_k and \mathbf{E}_k can be expressed to $\text{Re tr}(\mathbf{I}_2 - \mathbf{D}_k)$. When no error occurs, $\mathbf{D}_k = \mathbf{I}_2$, so $\text{Re tr}(\mathbf{I}_2 - \mathbf{D}_k) = 0$. Meanwhile, $\mathbf{D}_k \mathbf{D}_k^\dagger = \mathbf{I}_2$, so matrix \mathbf{D}_k has the same orthogonal property as the message matrix \mathbf{S}_k and code matrix \mathbf{C}_k . Since

$\mathbf{D}_k, \mathbf{D}_{k-1}, \dots, \mathbf{D}_{k-N+2}$ are orthogonal matrices, from Theorem 3,

$$\text{Re tr} (\mathbf{I}_2 - \mathbf{D}_k \mathbf{D}_{k-1} \dots \mathbf{D}_{k-N+2}) \geq 0. \quad (3.34)$$

Now, the code matrix is observed. Recall that code matrices $\mathbf{C}_k, \mathbf{C}_{k-1}, \dots, \mathbf{C}_{k-N+1}$ are transmitted instead of transmitting message matrices $\mathbf{S}_k, \mathbf{S}_{k-1}, \dots, \mathbf{S}_{k-N+2}$ directly. Due to the influence of fading and noise, suppose that while $\mathbf{C}_k, \mathbf{C}_{k-1}, \dots, \mathbf{C}_{k-N+1}$ are transmitted, $\mathbf{Q}_k, \mathbf{Q}_{k-1}, \dots, \mathbf{Q}_{k-N+1}$ are actually received which causes that the differentially decoded message matrices $\mathbf{S}_k, \mathbf{S}_{k-1}, \dots, \mathbf{S}_{k-N+2}$ to be transformed to the error message matrices $\mathbf{E}_k, \mathbf{E}_{k-1}, \dots, \mathbf{E}_{k-N+2}$. Obviously

$$\mathbf{Q}_k = \mathbf{E}_k \mathbf{Q}_{k-1} = \mathbf{E}_k \mathbf{E}_{k-1} \mathbf{E}_{k-2} \dots \mathbf{E}_{k-N+2} \mathbf{C}_{k-N+1}, \quad (3.35)$$

and $\mathbf{Q}_k \mathbf{Q}_{k-1}^\dagger = \mathbf{E}_k$. Since \mathbf{C}_{k-i} and \mathbf{Q}_{k-i} , ($i = 0, \dots, N-1$) are orthogonal real matrices when BPSK messages are employed, from Theorem 1, the difference between \mathbf{C}_{k-i} and \mathbf{Q}_{k-i} , ($i = 0, \dots, N-1$) can be expressed as

$$\text{Re tr} \left\{ \mathbf{Q}_{k-i} \mathbf{C}_{k-i}^\dagger \right\} = \text{Re tr} \left\{ \mathbf{D}_{k-i} \mathbf{D}_{k-i-1} \dots \mathbf{D}_{k-N+2} \right\}. \quad (3.36)$$

From Equation (3.26), the decision value for a correct decision can be expressed as

$$\eta_c = \text{Re tr} \left\{ \sum_{i=1}^{N-1} \sum_{j=0}^{i-1} \left(\mathbf{R}_{k-j} \mathbf{R}_{k-i}^\dagger \mathbf{C}_{k-i} \mathbf{C}_{k-j}^\dagger \right) \right\}, \quad (3.37)$$

and the decision value for an erroneous decision can be obtained by

$$\eta_e = \text{Re tr} \left\{ \sum_{i=1}^{N-1} \sum_{j=0}^{i-1} \left(\mathbf{R}_{k-j} \mathbf{R}_{k-i}^\dagger \mathbf{Q}_{k-i} \mathbf{Q}_{k-j}^\dagger \right) \right\}. \quad (3.38)$$

3.4.1 Closed-Form Pairwise Error Probability

If the receiver decodes to \mathbf{E} when \mathbf{S} is actually sent, the error decision value η_e for \mathbf{E} should be greater than the correct decision value η_c for \mathbf{S} , the error probability

$P(\mathbf{S} \rightarrow \mathbf{E}|\mathbf{S})$ given \mathbf{S} is usually defined as pairwise error probability. Here, it can be expressed as

$$\begin{aligned} P(\mathbf{S} \rightarrow \mathbf{E}|\mathbf{S}) &= P(\eta_e - \eta_c > 0|\mathbf{S}) \\ &= P\left(\sum_{i=1}^{N-1} \sum_{j=0}^{i-1} \text{Re tr}(\Phi_{k-i,k-j}) > 0\right). \end{aligned} \quad (3.39)$$

Substituting Expression (2.32) into Equation (3.37) and (3.38), utilizing Theorem 1 and 2,

$$\begin{aligned} &\text{Re tr} \{\Phi_{k-i,k-j}\} \\ &\simeq E_s \text{Re tr} \left\{ \mathbf{H}_{k-i} \mathbf{H}_{k-j}^\dagger (\mathbf{D}_{k-j} \mathbf{D}_{k-j-1} \dots \mathbf{D}_{k-i+1} - \mathbf{I}_2) \right\} \\ &\quad + \sqrt{E_s} \text{Re tr} \left\{ \mathbf{C}_{k-j} \mathbf{H}_{k-j} \Psi_{k-i}^\dagger \mathbf{Q}_{k-i} \mathbf{Q}_{k-j}^\dagger + \Psi_{k-j} \mathbf{H}_{k-i}^\dagger \mathbf{C}_{k-i}^\dagger \mathbf{Q}_{k-i} \mathbf{Q}_{k-j}^\dagger \right. \\ &\quad \left. - \mathbf{C}_{k-j} \mathbf{H}_{k-j} \Psi_{k-i}^\dagger \mathbf{C}_{k-i} \mathbf{C}_{k-j}^\dagger - \Psi_{k-j} \mathbf{H}_{k-i}^\dagger \mathbf{C}_{k-i}^\dagger \mathbf{C}_{k-i} \mathbf{C}_{k-j}^\dagger \right\}. \end{aligned} \quad (3.40)$$

Note that the second-order noise terms in Expression (3.40) are ignored since they are quite small compared to other noise terms when SNR is large enough. Meanwhile, path gains \mathbf{H}_{k-j} , \mathbf{H}_{k-i} are assumed to be unchanged during a frame.

Let

$$\begin{aligned} \Delta &= \sum_{i=1}^{N-1} \sum_{j=0}^{i-1} \text{Re tr} \{\Phi_{k-i,k-j}\} \\ &= -E_s (|h_1|^2 + |h_2|^2) \rho + \sqrt{E_s} \text{Re tr}(\Lambda), \end{aligned} \quad (3.41)$$

where the MSDD distance is defined as

$$\rho = \text{Re tr} \left\{ \sum_{i=1}^{N-1} \sum_{j=0}^{i-1} (\mathbf{I}_2 - \mathbf{D}_{k-j} \mathbf{D}_{k-j-1} \dots \mathbf{D}_{k-i+1}) \right\}, \quad (3.42)$$

and

$$\begin{aligned} \Lambda &= \sum_{i=1}^{N-1} \sum_{j=0}^{i-1} \left\{ \mathbf{C}_{k-j} \mathbf{H}_{k-j} \Psi_{k-i}^\dagger \mathbf{Q}_{k-i} \mathbf{Q}_{k-j}^\dagger + \Psi_{k-j} \mathbf{H}_{k-i}^\dagger \mathbf{C}_{k-i}^\dagger \mathbf{Q}_{k-i} \mathbf{Q}_{k-j}^\dagger \right. \\ &\quad \left. - \mathbf{C}_{k-j} \mathbf{H}_{k-j} \Psi_{k-i}^\dagger \mathbf{C}_{k-i} \mathbf{C}_{k-j}^\dagger - \Psi_{k-j} \mathbf{H}_{k-i}^\dagger \mathbf{C}_{k-i}^\dagger \mathbf{C}_{k-i} \mathbf{C}_{k-j}^\dagger \right\}. \end{aligned} \quad (3.43)$$

Since \mathbf{Q}_{k-i} , \mathbf{Q}_{k-j} , \mathbf{C}_{k-i} and \mathbf{C}_{k-j} can be regarded as constant orthogonal matrices when \mathbf{S} and \mathbf{E} are given, Expression (3.41) can be regarded as the sum of a constant Ω and some Gaussian random variables. Note that the elements of the unitary noise matrices Ψ_{k-i} , Ψ_{k-j} are zero-mean. By Theorem 5, $E[\text{Re tr}(\Lambda)] = 0$, where $E[\cdot]$ denotes the mathematical expectation. Since ρ is assumed to be a constant when \mathbf{S} is given, the mean of Δ is only related to $\text{Re tr}(\Lambda)$. Finally,

$$E\{\Delta\} = -E_s(|h_1|^2 + |h_2|^2)\rho. \quad (3.44)$$

However, the variance of Δ is more complicated, because some terms in Expression (3.43) are correlated, although most of the terms are assumed to be mutually independent. Through Theorems 1 to 7, it is proved in Appendix A that the variance of Δ can be expressed as

$$\begin{aligned} \text{Var}\{\Delta\} &= E_s \text{Var}[\text{Re tr}(\Lambda)] \\ &= 4N(N-1)(|h_1|^2 + |h_2|^2)E_s N_0 \\ &\quad + 2(N-2)E_s N_0(|h_1|^2 + |h_2|^2) \text{Re tr} \left\{ \sum_{i=1}^{N-1} \sum_{j=0}^{i-1} (\mathbf{D}_{k-j} \mathbf{D}_{k-j-1} \dots \mathbf{D}_{k-i+1} + \mathbf{I}_2) \right\} \\ &\quad - 4(N-1)E_s N_0(|h_1|^2 + |h_2|^2) \text{Re tr} \left\{ \sum_{i=1}^{N-1} \sum_{j=0}^{i-1} (\mathbf{D}_{k-j} \mathbf{D}_{k-j-1} \dots \mathbf{D}_{k-i+1}) \right\}, \end{aligned} \quad (3.45)$$

where $\text{Var}[\cdot]$ denotes mathematical variance.

Note that

$$\sum_{i=1}^{N-1} \sum_{j=0}^{i-1} \mathbf{I}_2 = N(N-1). \quad (3.46)$$

Then Expression (3.45) can be simplified to

$$\text{Var}\{\Delta\} = 2N\rho(|h_1|^2 + |h_2|^2)E_s N_0. \quad (3.47)$$

From Expression (3.39), (3.41), (3.44) and (3.47),

$$\begin{aligned}
 P_r(\mathbf{S} \longrightarrow \mathbf{E}|\mathbf{S}) &= P_r(\eta_e > \eta_c|\mathbf{S}) \\
 &= P_r(\Delta > 0|\mathbf{S}) \\
 &= Q\left(\sqrt{\gamma\rho(|h_1|^2 + |h_2|^2)/2N}\right), \tag{3.48}
 \end{aligned}$$

where ‘ Q ’ denotes Q function and γ is defined as E_s/N_0 , SNR per symbol.

Define the instantaneous SNR as

$$\gamma_b = \gamma \sum_{l=1}^2 |h_l|^2, \tag{3.49}$$

using the alternative form of the Gaussian Q-function [17], then

$$\begin{aligned}
 P_r(\mathbf{S} \longrightarrow \mathbf{E}|\mathbf{S}) &= Q\left(\sqrt{(\rho/2N)\gamma_b}\right) \\
 &= \frac{1}{\pi} \int_0^{\pi/2} \exp\left(-\frac{(\rho/2N)\gamma_b}{2\sin^2\theta}\right) d\theta. \tag{3.50}
 \end{aligned}$$

Since the PDF of γ_b can be obtained in Proakis’ book [18], then

$$P_r(\mathbf{S} \longrightarrow \mathbf{E}|\mathbf{S}) = \int_0^\infty Q\left(\sqrt{(\rho/2N)\gamma_b}\right) p(\gamma_b) d\gamma_b. \tag{3.51}$$

Using the integration tool in Win’s paper [27] for Equation (3.51),

$$P_r(\mathbf{S} \longrightarrow \mathbf{E}|\mathbf{S}) = \frac{1}{2} \left[1 - \mu - \frac{1}{2}\mu(1 - \mu^2) \right], \tag{3.52}$$

where

$$\mu = \sqrt{\frac{(\rho/2N)\gamma}{(\rho/2N)\gamma + 2}}. \tag{3.53}$$

3.4.2 Approximate Bit Error Rate

The error probability (3.52) of the pairwise message matrix error event $\{\mathbf{S} \longrightarrow \mathbf{E}\}$ as the event, at which the receiver decodes into message

matrix E when S is actually transmitted, has been obtained. Let $\mathbf{u} = (s_{1,k-i}, s_{2,k-i}, \dots, s_{1,k-N+2}, s_{2,k-N+2})$ represent a sequence with $2(N-1)\log_2 M$ information bits, and $\hat{\mathbf{u}} = (e_{1,k-i}, e_{2,k-i}, \dots, e_{1,k-N+2}, e_{2,k-N+2})$ denote an error sequence with the same number of information bits. The BER P_b given S is union-bounded by Divsalar's and Liu's papers [20][28]

$$P_b \leq \frac{1}{2(N-1)\log_2 M} \sum_{\mathbf{S} \neq \mathbf{E}} \Theta(\mathbf{u}, \hat{\mathbf{u}}) P_r(\mathbf{S} \rightarrow \mathbf{E}|\mathbf{S}), \quad (3.54)$$

where $\Theta(\mathbf{u}, \hat{\mathbf{u}})$ represents the Hamming distance between sequence \mathbf{u} and $\hat{\mathbf{u}}$. The pairwise message matrix error rate $P_r(\mathbf{S} \rightarrow \mathbf{E}|\mathbf{S})$ is given by Equation (3.52). M represents the modulation level ($M = 2$ for BPSK) and $2(N-1)\log_2 M$ denotes the total number of transmitted message bits.

From Equation (3.52) and (3.53), it is evident that if γ and N are fixed and $\rho \rightarrow \infty$, then $\mu \rightarrow 1$ and $P_r(\mathbf{S} \rightarrow \mathbf{E}|\mathbf{S}) \rightarrow 0$. Since $dP_r(\mathbf{S} \rightarrow \mathbf{E}|\mathbf{S})/d\rho < 0$, $P_r(\mathbf{S} \rightarrow \mathbf{E}|\mathbf{S})$ is a monotonically decreasing function of the MSDD distance ρ . Moreover, it is shown in Appendix C that, when γ and N are large enough, $P(\mathbf{S} \rightarrow \mathbf{E}|\mathbf{S}) \sim 1/\rho^2$. Hence, at a given SNR (γ is constant), it is expected that the minimum ρ will dominate the union bound (3.54), and this BER analysis approach was adapted in Divsalar's and Lao's papers [20][29] as well. The expectation can be verified by some special cases illustrated as follows.

To simplify the analysis, assume that all the BPSK message symbols are $1/\sqrt{2}$ s. There are three cases to describe the error event for one block by the matrix distance: (i) If no symbol error occurs, then $\text{Re tr}(\mathbf{I}_2 - \mathbf{D}_k) = 0$. (ii) If one-symbol error happens, then $\text{Re tr}(\mathbf{I}_2 - \mathbf{D}_k) = 2$. (iii) If two-symbol error occurs, then $\text{Re tr}(\mathbf{I}_2 - \mathbf{D}_k) = 4$.

Case 1 $N=2$ From Expression (3.52), when $N = 2$, there is only one-block message \mathbf{S}_k . One-symbol error and two-symbol error probably occur for this case.

For one-symbol error, $\text{Re tr}(\mathbf{D}_k) = 0$, then $\rho_1 = 2$, $\Theta_1(\mathbf{u}, \hat{\mathbf{u}}) = 1$. For two-symbol error, $\text{Re tr}(\mathbf{D}_k) = -2$, then $\rho_2 = 4$, $\Theta_2(\mathbf{u}, \hat{\mathbf{u}}) = 2$. Apparently, the minimum ρ ($\rho_{\min} = 2$) is only caused by one-symbol error. If only the minimum ρ is considered, from Expression (3.54)

$$P_b \simeq \frac{1}{2} \left[1 - \mu - \frac{1}{2} \mu (1 - \mu^2) \right]. \quad (3.55)$$

where $\mu = \sqrt{\frac{\gamma}{\gamma+4}}$. The expression (3.55) is exactly the closed-form error bit rate for differential detection with an observation interval of two blocks derived in the paper [30], which verifies that one-bit error dominates the performance in this case.

Case 2 $N=3$ When $N = 3$, there are two blocks of messages \mathbf{S}_k and \mathbf{S}_{k-1} , so the number of total information bits is 4. Since there are too many cases when errors occur, only some dominant terms in Expression (3.54) are considered. By calculating ρ for any case, it is evident that the minimum ρ ($\rho_{\min} = 4$) is only caused by one-symbol error and two-symbol error. If only the minimum ρ is considered, from Equation (3.54), the approximate BER is

$$P_b \simeq \frac{1}{2} \left[1 - \mu - \frac{1}{2} \mu (1 - \mu^2) \right] + \frac{1}{2} * \frac{1}{2} \left[1 - \mu - \frac{1}{2} \mu (1 - \mu^2) \right] \quad (3.56)$$

where $\mu = \sqrt{\frac{\gamma}{\gamma+3}}$.

Case 3 $N \rightarrow \infty$ In the general case for arbitrary N , the dominant terms in the union bound (3.54) occur for the sequence that results in the minimum value of ρ . By analysis, it is found to be a general rule for this scheme that only one-symbol error and two-symbol error can generate the minimum value of ρ , and $\rho_{\min} = 2(N - 1)$, which is shown in Appendix B. Since there are $2(N - 1)$ solutions for one-symbol error and $(N - 2)$ solutions for two-symbol error when ρ_{\min} occurs, and a total of $2(N -$

1) information bits are transmitted, then the approximate BER is

$$\begin{aligned}
 P_b &\simeq \frac{1 * 2(N-1)}{2(N-1)} P_b^{(1)} + \frac{2 * (N-2)}{2(N-1)} P_b^{(2)}, \\
 &= \frac{1}{2} \left[1 - \mu - \frac{1}{2} \mu (1 - \mu^2) \right] \\
 &\quad + \frac{(N-2)}{(N-1)} * \frac{1}{2} \left[1 - \mu - \frac{1}{2} \mu (1 - \mu^2) \right], \tag{3.57}
 \end{aligned}$$

where

$$\mu = \sqrt{\frac{[(N-1)/N] \gamma}{[(N-1)/N] \gamma + 2}}. \tag{3.58}$$

Obviously, Equation (3.57) can be used in the special cases for $N = 2, 3$. If $N \rightarrow \infty$, then $\mu \rightarrow \sqrt{\frac{\gamma}{\gamma+2}}$, so

$$P_b \simeq 2 * \left\{ \frac{1}{2} \left[1 - \mu - \frac{1}{2} \mu (1 - \mu^2) \right] \right\}. \tag{3.59}$$

Note that the pairwise error probability

$$P_b^{(1)} = P_b^{(2)} = \frac{1}{2} \left[1 - \mu - \frac{1}{2} \mu (1 - \mu^2) \right]. \tag{3.60}$$

When $N \rightarrow \infty$, $\mu \rightarrow \sqrt{\frac{\gamma}{\gamma+2}}$, so Expression (3.59) is exactly the closed-form BER for differential STBC with coherent detection (D.11) derived in Appendix D. Hence, the approximate BER of this scheme (3.59) approximately converges to the performance of differential STBC with coherent detection for a given SNR, which is identical with the MSDD results for receive diversity [29].

3.5 Numerical Results

Numerical results are provided to compare the analysis and simulation result. The simulation is carried out over a quasi-static, flat Rayleigh fading channel, for which the channel gains are assumed to be constant during a frame, but changes from frame to frame.

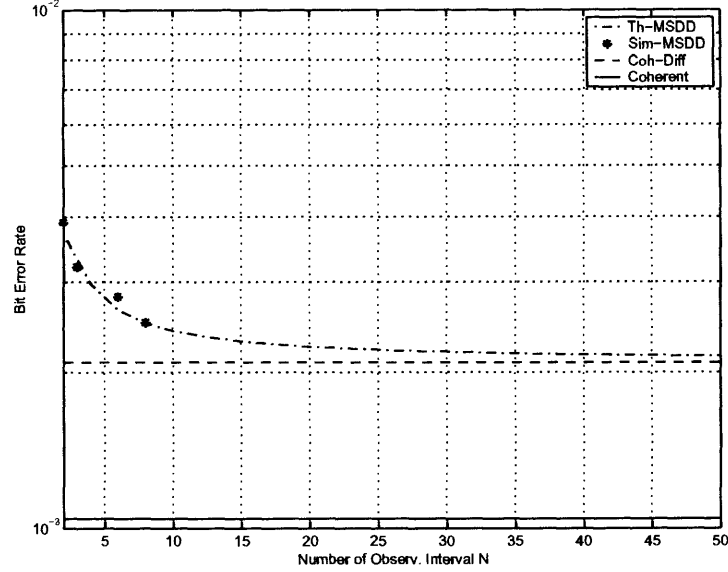


Figure 3.3 Asymptotic characteristics of MSDD for STBCs over two transmit antennas(14 dB SNR, BPSK, 1 bit/s/Hz).

By fixing the SNR at 14 dB, and the theoretical BER versus the length of observation interval N is shown in Figure 3.3. Since the computation complexity increases exponentially with the increase of N , only the simulation result for a moderate $N = 2, 3, 6, 8$ is provided. The simulation results for coherent detection are also illustrated. With increasing of N , the BER for MSDD of STBCs will converge to the blue dotted line, which is the approximate BER for differential STBC with coherent detection.

In Figure 3.4, the theoretical and simulated BERs versus the symbol SNR ($= E_s/N_0$) for $N = 2, 3, 6$ are plotted. The analysis and simulation results match well when the SNR is large enough. Moreover, with a growing of the number of observation interval blocks, the performance gets better and converges. When N goes to infinity, the BER of MSDD converges to the BER for differential STBC with coherent detection.

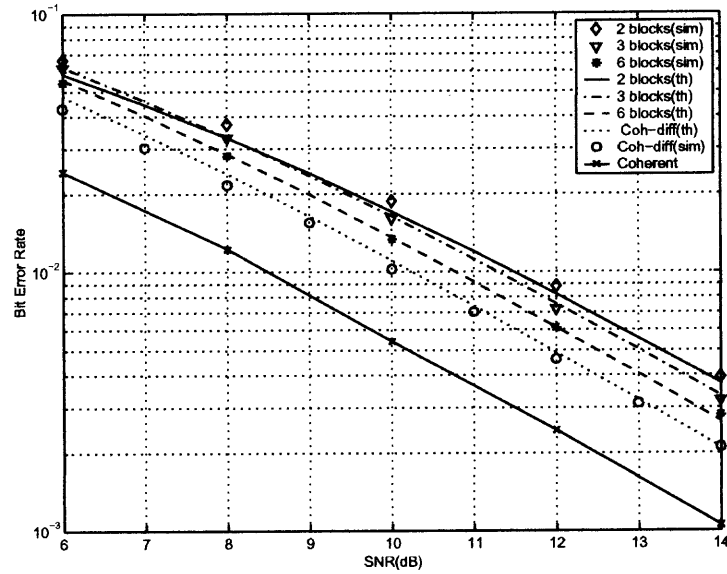


Figure 3.4 Theory and simulation result for MSDD of STBC.

3.6 Conclusions

A multiple-symbol differential detector was proposed for space-time block codes, in which neither the transmitters nor the receiver know the channel state information. A generalized decision metric for an observation interval of N blocks is derived. It was shown that previously published differential STBC schemes can be obtained as special cases of MSDD. Simulation results demonstrated that MSDD can greatly improve the performance of differential STBC. Previously proposed schemes utilizing a two and three block observation interval incur a SNR performance loss of 3 and 2.5 dB, respectively compared to related coherent detection for BPSK or QPSK modulations.

The performance analysis of multiple-symbol differential detection for MPSK space-time block code was presented. Based on the generalized decision metric for an observation interval of N blocks, a closed-form expression of pairwise error probability was derived, and the approximate bit error rate for this scheme is analyzed. Theoretical and simulation results showed that MSDD technique can greatly improve the performance of differential STBC, and is much better than the conventional

differential decoding approach, which has approximately 3 dB SNR loss compared to related coherent detection. However, when N goes to infinity, the performance for differential scheme with MSDD technique will converge to the BER for differential STBC with coherent detection.

CHAPTER 4

BER PERFORMANCE OF STBC OVER A SPATIO-TEMPORAL CORRELATED CHANNEL

4.1 Introduction

In Chapter 2, the BER performance of Alamouti's space-time block code over a $2 \times N$ flat Rayleigh fading channel with coherent and noncoherent detection have been analyzed, where no spatial and temporal correlations among channels are considered. Since the transmission matrix for two transmit antennas is unitary matrix which allows simple differential encoding with linear complexity, full spatial diversity is obtained with both detections.

When the transmission paths are correlated due to limited antenna spacing, there is some performance degradation due to loss in diversity. The idea of including spatial correlation at the receiver has been discussed in Hart's paper [31] for receive diversity. It is shown that exploiting spatial correlation at the receiver does not substantially improve the bit error rate (BER) compared to the receiver without it.

For a time-varying channel, a differential STBC using nonconstant quadrature amplitude modulation (QAM) constellations, which increases the minimum distance compared with that of the conventional differential STBC using PSK, was proposed in Hwang's paper [32]. The effect of temporal correlation on this scheme was illustrated according to different temporal correlation. It is obvious that the performance of this scheme is degraded over a fast fading channel with the change of Doppler frequency, however, no spatial correlation was discussed.

This chapter concentrates on performance analysis for transmit diversity employing Alamouti's STBC when there are both temporal and spatial correlations among the transmit antennas. Proposed by Abdi et al. [33], a general space-time

correlation model is utilized in this chapter, where it is given a closed-form, easy-to-use, and mathematically tractable expression for the space-time cross correlation between the links of a frequency nonselective MIMO Rayleigh wireless fading channel. Since this dissertation focuses primarily on performance analysis of communication systems with transmit diversity, only a simple space-time 2×1 channel as a special case of MIMO channel for simulation is considered.

4.2 The Spatial and Temporal Correlated MIMO Channel Model

For a wireless link between a base station (BS) and a user in macrocells, depicted in Figure 4.1, the BS, which is not surrounded by many local scatterers, receives the signal primarily from a particular direction through a narrow beamwidth. The local scatterers around the user may give rise to different models of signal propagation toward the user. In the general scenario of nonisotropic scattering, which corresponds to directional signal reception, the user receives the signal only from particular directions (See Figure 4.2). The special case of isotropic scattering is shown in Figure 4.3, where the user receives signals from all directions with equal probabilities. The isotropic scattering model, also known as the Clarke's model, corresponds to the uniform distribution for the angle of arrival (AOA). However, empirical measurements [34][35] have shown that the AOA distribution of waves impinging the user is more likely to be nonuniform. The nonuniform distribution of the AOA can significantly affect the performance of array based techniques, as the AOA statistics determine the cross correlation among the array elements.

It what follows, a closed-form, easy-to-use, and mathematically tractable expression for the space-time cross correlation between the links of a frequency nonselective MIMO Rayleigh wireless fading channel with multielement transmit and receive antennas is briefly derived, where nonisotropic scattering around the user is

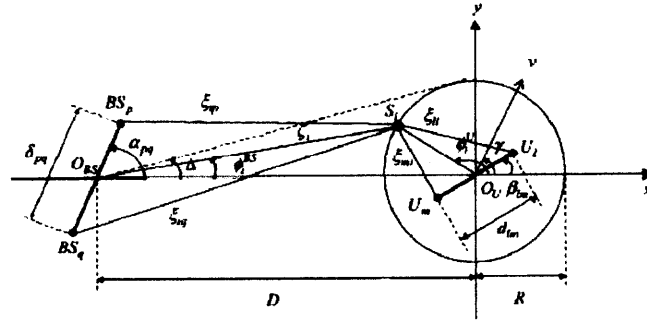


Figure 4.1 Geometrical configuration of a 2×2 channel with local scatterers around the mobile user (two-element arrays at the BS and the user).

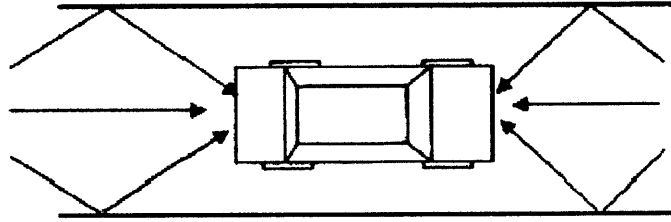


Figure 4.2 Non-isotropic scattering in a narrow street.

modeled by the von Mises distribution [36], a nonuniform distribution of the AOA. More details are shown in the paper [33].

Consider the multielement antenna system configuration shown in Figure 4.1, first proposed in Shiu's paper [37], where the BS and the user have n_{BS} and n_U omnidirectional antenna elements, respectively. There are uniform linear arrays with $n_{BS} = n_U = 2$ (a 2×2 MIMO channel), which constitutes the basic structure of multielement antenna systems with arbitrary array configurations. The convention for numbering the antenna is such that $1 \leq l \leq m < n_U$ and $1 \leq p \leq q < n_{BS}$. The BS receives the signal through the narrow beamwidth, while the user receives the signal from a large number of surrounding local scatterers, impinging the user from different directions. It is assumed that the waves are planar and only single scattering

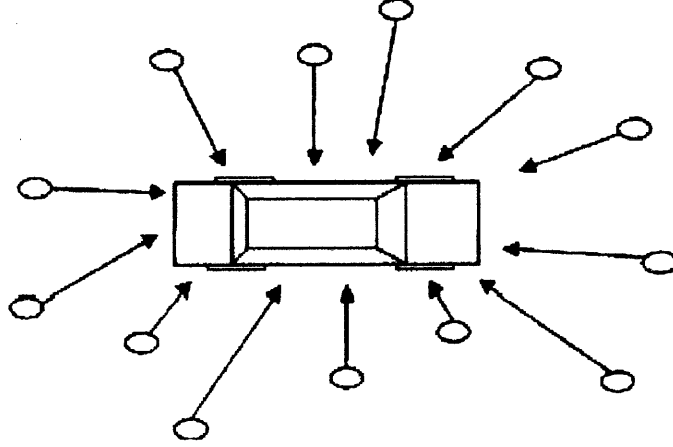


Figure 4.3 Isotropic scattering in an open area (circles are scatterers).

occurs. The i th scatterer is represented by S_i , D is the distance between the BS and the user, and R is the radius of the ring of scatterers. Clearly, Δ , R , and D are related through $\tan(\Delta) = R/D$.

For the frequency nonselective communication link between the element BS_p and the element U_l , note that such a link comprises of many paths $h_{lp}(t)$ that can be drawn from BS_p to U_l through the ring of local scatterers. Let $\mathbf{H}(t)$ represents a $n_U \times n_{BS}$ channel matrix complex envelope such that $[\mathbf{H}(t)]_{lp} = h_{lp}(t)$. The dependence of $\mathbf{H}(t)$ on time is a result of user mobility (Doppler effect). This implies that the effect of channel time selectivity has been taken into account. Needless to say, the space selectivity of the channel is also considered through the realistic assumption of nonisotropic scattering and nonuniform distribution of AOA [38].

In the channel model depicted in Figure 4.1, the ring of scatterers is assumed to be fixed (independent of time), and the motion of the user is characterized by its speed v and direction γ . The assumptions are necessary for obtaining a stationary space-time correlation model. Clearly, depending on the user's speed, the spatio-temporal correlation function obtained in the sequel will be accurate only over a time duration that is much smaller than R/v .

For a unit transmit power, suppose the power transferred through the $BS_p - U_t$ link is Ω_{lp} , i.e. $\Omega_{lp} = E [|h_{lp}(t)|^2] \leq 1$. The plane waves emitted from the array element BS_p travel over path with different length and after being scattered by the local scatterers around the mobile user, impinge the array element U_t from different directions. Mathematical representation of this propagation mechanism results in the following expressions

$$h_{lp}(t) = \sqrt{\Omega_{lp}} \lim_{N \rightarrow \infty} \frac{1}{\sqrt{N}} \sum_{i=1}^N g_i \times \exp \left\{ j\psi_i - \frac{j2\pi}{\lambda} [\zeta_{ip}(\phi_i^U) + \zeta_{ti}(\phi_i^U)] \right. \\ \left. + j2\pi f_D [\cos(\phi_i^U - \gamma)] t \right\} \quad (4.1)$$

where N is the number of independent scatterers S_i around the user, g_i represents the amplitude of the wave scattered by the i th scatterer toward the user such that $\frac{1}{N} \sum_{i=1}^N E[g_i^2] = 1$ as $N \rightarrow \infty$, ψ_i denotes the phase shift introduced by the i th scatterer, ζ_{ip} and ζ_{ti} are the distances shown in Figure 4.1 which are function of ϕ_i^U , the AOA of the wave traveling from the i th scatterer toward the user. λ is the wavelength, $j^2 = -1$, $f_D = \nu/\lambda$ is the maximum Doppler shift. The set $\{g_i\}_{i=1}^\infty$ consists of independent and identically distributed (iid) random variables with uniform distributions over $[0, 2\pi)$. The model represents a MIMO frequency nonselective Rayleigh fading channel, $h_{lp}(t)$ is a lowpass zero-mean complex Gaussian process.

Let us define the space-time cross correlation between the gains of the two arbitrary communication links $h_{lp}(t)$ and $h_{mq}(t)$ as

$$\rho_{lp,mq}(\tau, t) = E [h_{lp}(t) h_{mq}^*(t + \tau)] / \sqrt{\Omega_{lp}\Omega_{mq}} \quad (4.2)$$

where $*$ is the complex conjugate. The approximations generally hold when $D \gg R \gg v > \max(\delta_{lp}, d_{lm})$ which corresponds to the small values of Δ . According to the experiments conducted at different locations and frequencies, the angle spread Δ at the BS is generally small for macrocells in urban, suburban, and rural areas,

most often less than 15° , and in some cases very small less than 5° . There empirical observation justify the simple but useful approximate results for $\rho_{lp,mq}(\tau, t)$ derived in the sequel.

Based on the statistical properties of $\{g_i\}_{i=1}^\infty$ and $\{\psi_i\}_{i=1}^\infty$, the space-time cross correlation between h_{lp} and h_{mq} , according to Equation (4.1), can be written as

$$\begin{aligned}\rho_{lp,mq}(\tau, t) &= \rho_{lp,mq}(\tau) \\ &= \lim_{N \rightarrow \infty} \frac{1}{N} \sum_{i=1}^N E[g_i^2] \times \exp \left\{ -\frac{j2\pi}{\lambda} (\xi_{ip} - \xi_{iq} + \xi_{li} - \xi_{mi}) \right. \\ &\quad \left. - j2\pi f_D [\cos(\phi_i^U - \gamma)] \tau \right\}\end{aligned}\quad (4.3)$$

The total power of the link $BS_p - U_l$, scattered by all the scatterers toward the user's l th element is given by $E[|h_{lp}(t)|^2] = \Omega_{lp}$. For large N , the small contribution of the i th scatterer, out of the total Ω_{lp} , is proportional to $E[g_i^2]/N$. This is equal to the infinitesimal power coming from the differential angle $d\phi^U$ with probability $f(\phi_i^U)$, i.e. $E[g_i^2]/N = f(\phi_i^U) d\phi^U$, where $f(\phi_i^U)$ is the pdf of the AOA seen by the user. Therefore, Equation (4.3) can be written in the following integral form.

$$\begin{aligned}\rho_{lp,mq}(\tau) &= \int_{-\pi}^{\pi} \exp \left\{ -\frac{j2\pi}{\lambda} \times (\xi_{\phi_p^U} - \xi_{\phi_q^N} + \xi_{l\phi^U} - \xi_{m\phi^U}) \right. \\ &\quad \left. - j2\pi f_D [\cos(\phi^U - \gamma)] \tau \right\} \times f(\phi^U) d\phi^U\end{aligned}\quad (4.4)$$

where $\xi_{\phi_p^U}$ is the length of the path between the antenna element BS_p and the point on the ring of scatterers, determined by ϕ^U , and so on. For a given $f(\phi^U)$, PDF of which is given in the paper [36], finally the following key results after some algebraic manipulations are obtained

$$\begin{aligned}\rho_{lp,mq}(\tau) &\approx \frac{\exp[jc_{pq} \cos(\alpha_{pq})]}{I_0(\kappa)} \times I_0(\{\kappa^2 - a^2 - b_{lm}^2 - c_{pq}^2 \Delta^2 \sin^2(\alpha_{pq}) \\ &\quad + 2ab_{lm} \cos(\beta_{lm} - \gamma) + 2c_{pq} \Delta \sin^2(\alpha_{pq}) \\ &\quad \times [a \sin(\gamma) - b_{lm} \sin(\beta_{lm})] - j2\kappa [a \cos(\mu - \gamma) - b_{lm} \cos(\beta_{lm} - \gamma) \\ &\quad - c_{pq} \Delta \sin(\alpha_{pq}) \sin(\mu)]\}^{1/2}).\end{aligned}\quad (4.5)$$

where

$$a = 2\pi f_D \tau, \quad b_{lm} = 2\pi d_{lm}/\lambda, \quad c_{pq} = 2\pi \delta_{pq}/\lambda$$

and $I_0(\cdot)$ is the zero-order modified Bessel function, $\kappa \geq 0$ controls the angle spread at the MS.

The corresponding power spectrum can be shown to be [33]

$$\begin{aligned} S_{h_{lp}, h_{mq}}(f) &= \frac{\exp[jc_{pq} \cos(\alpha_{pq})]}{I_0(\kappa) \pi \sqrt{f_m^2 - f^2}} \exp\{-[\kappa \cos(\gamma - \mu) + j\vartheta_1](f/f_m)\} \\ &\quad \times \cosh\left\{[\kappa \sin(\gamma - \mu) + j\vartheta_2] \sqrt{1 - (f/f_m)^2}\right\}, \quad (4.6) \\ |f| &\leq f_m, \end{aligned}$$

where $\cosh(\cdot)$ in the hyperbolic cosine and

$$\begin{aligned} \vartheta_1 &= b_{lm} \cos(\beta_{lm}) \cos(\gamma) + [c_{pq} \Delta \sin(\alpha_{pq}) + b_{lm} \sin(\beta_{lm})] \sin(\gamma), \\ \vartheta_2 &= b_{lm} \cos(\beta_{lm}) \sin(\gamma) - [c_{pq} \Delta \sin(\alpha_{pq}) + b_{lm} \sin(\beta_{lm})] \cos(\gamma). \end{aligned}$$

To simulate a 2×2 MIMO correlated channel gain sequences, from Equation (4.5) and (4.6), a spectral representation method and a correlated channel simulator is provided in Acolatse's paper [39]. The Matlab files for the simulator are available at <http://web.njit.edu/~abdi>.

Based on this model, the level crossing rate (LCR) and average fade durations (AFD) for a mobile MIMO fading channel are studied in Appendix E.

4.3 A 2×1 Spatial and Temporal Correlated Rayleigh Fading Channel

Since this dissertation focuses primarily on performance analysis of communication systems with transmit diversity, only a simple 2×1 special case of MIMO channel for simulation is considered. The two channel gains $h_{1,k}$, $h_{2,k}$, $k = 1, 2, \dots$ can be generated by the simulator [39]. To obtain the performance of Alamouti's STBC over

the correlated channel, the system model of Alamouti's STBC, which was addressed in Chapter 1, is still used. Note that only one receive antenna is employed here, and channel gains are supposed not to be a constant during one frame anymore but change according to the codeword index k .

For the 2×1 Rayleigh channel, based on the definition of l , m , p and q in Section 4.2, $l = 1$, $p = 1$, $m = 1$ and $q = 2$ are obtained. Let $\gamma_0 = \gamma$, $\alpha = \alpha_{12}$ and $\delta = \delta_{12}$. Since $\alpha_{11} = 0$, $c_{11} = 0$ and $d_{11} = 0$, simplifying Equation (4.5) yields the correlations

$$\rho_{11,11}(\tau) = [I_0(\kappa)]^{-1} I_0\left(\left\{\kappa^2 - 4\pi^2 f_D^2 \tau^2 - j4\pi\kappa \cos(\gamma_0 - \mu) f_D \tau\right\}^{1/2}\right), \quad (4.7)$$

$$\begin{aligned} \rho_{11,12}(\tau) = & [I_0(\kappa)]^{-1} e^{j\cos(\alpha)2\pi\delta/\lambda} I_0\left(\left\{\kappa^2 - 4\pi^2 f_D^2 \tau^2 - j4\pi^2 (\delta/\lambda)^2 \Delta^2 \sin^2(\alpha) \right. \right. \\ & + 8\pi^2 (\delta/\lambda) f_D \tau \sin(\alpha) \sin(\gamma_0) \\ & \left. \left. - j2\kappa [2\pi f_D \tau \cos(\mu - \gamma_0) - 2\pi (\delta/\lambda) \Delta \sin(\alpha) \sin(\mu)]\right\}^{1/2}\right), \quad (4.8) \end{aligned}$$

where $\mu \in [-\pi, \pi)$ accounts for the mean direction of AOA at the MS, γ_0 is the direction of the motion of MS, f_D denotes the maximum Doppler shift, α represents the direction of the BS array, λ is the wavelength, δ stands for the element spacing at the BS, and finally 2Δ is the spread of the angle of departure from the BS.

Based on the paper [33], the spatial correlation ζ for $h_{1,k}$ and $h_{2,k}$ can be obtained from Equation (4.8) by $\zeta = |\rho_{11,12}(0)|$. Moreover, it is shown that temporal correlation for $h_{1,k}$ or $h_{2,k}$ is reversely and nonlinearly proportional to $T_b f_D$, where T_b is the symbol interval.

4.4 Simulation Results

Consider the transmit BS array, where the two elements are spaced by δ , is perpendicular to the horizontal x axis, $\alpha = 90^\circ$, and the receive single MS antenna is moving on the x axis, towards the transmit array, $\gamma_0 = 180^\circ$, with a constant speed.

The angle spread at the BS is $2\Delta = 4^\circ$, whereas at the MS is 66° , equivalent to $\kappa = 3$, around the mean AOA of $\mu = 36^\circ$ at the MS. The values κ of μ and are estimated from measured data [40].

Fast fading and slow fading are usually defined as $T_b f_D > 0.01$ and $T_b f_D \leq 0.01$ respectively. Since most wireless communication systems over a MIMO channel are applied on network links, the transmission rate is fairly high, more than 100 kbps will be available, and the symbol interval T_b is less than 10^{-5} . For a wireless system with a carrier frequency of 1.9 GHz, the Doppler shift is 10 Hz and 1000 Hz when the speed of a vehicle is 5.7 and 570 km/h respectively, so $T_b f_D$ will be 10^{-4} and 10^{-2} responsively. Hence, for a high data rate more than 10^5 kbs wireless system, fast fading does not occur due to the speed limit of a vehicle. To observe how the fast fading effects the BER performance, a transmission rate 1 kbps is also assumed to assign on this scheme during simulation. With the same assumption, $T_b f_D$ will be 10^{-2} and 10^0 respectively when $T_b = 10^{-3}$.

Simulations are performed to observe how the spatial and temporal correlation of a 2×1 Rayleigh fading channel effects the performance of Alamouti's STBC with coherent and non-coherent detection. The frame length is 260 symbol intervals, and BPSK modulation is employed. The simulation results are illustrated according to four different cases.

4.4.1 Spatial Correlation

Case 1 For this case, it is observed how the spatial correlation of channels effects the BER performance of Alamouti's STBC via symbol SNR when temporal correlation is fixed, for which BS element spacings of $\delta = \lambda$ and 5λ are considered, and the maximum Doppler shift f_D is assumed to be fixed at 100 Hz, where $T_b = 10^{-5}$ and $T_b f_D = 10^{-3}$; so it is a slow fading channel, and the spatial correlation $\zeta = |\rho_{11,12}(0)| = 0.995$ and 0.886, respectively. From Figure 4.4, due to the effect of spatial correlation, the BER

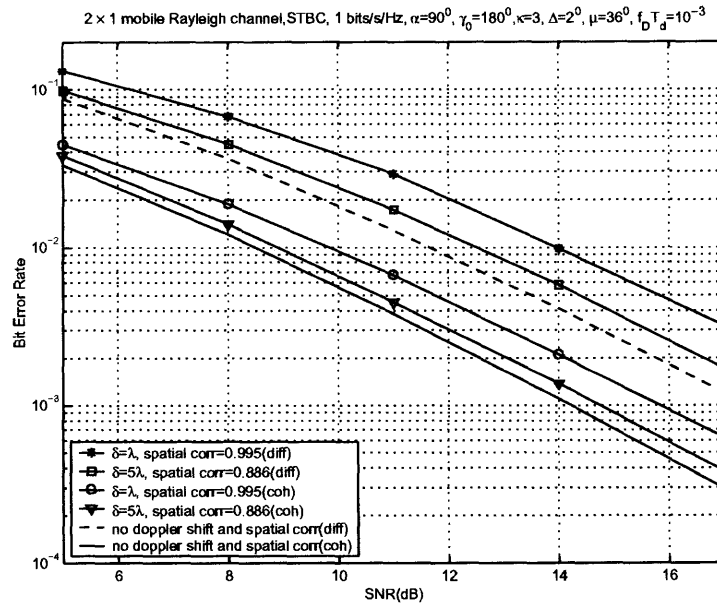


Figure 4.4 BER performance of Alamouti's STBCs for two channels with different spatial correlation but fixed temporal correlation.

performance of Alamouti's STBC with coherent and differential detection is obviously degraded if compared to that for no spatial correlation circumstance, and the more spatial correlation there is, the worse performance it is obtained. However, the BER gap for coherent and differential detection is still approximately 3 dB. Note that "diff" represents different detection and "coh" denotes coherent detection in the figure.

Case 2 In this case, it is observed how the spatial correlation effects the BER performance of Alamouti's STBC via the BS element spacings δ/λ at 15 dB SNR. BS element spacings δ/λ are set as 0.5, 1, 2, 3 and 5. Based on Equation (4.8), the spatial correlation ζ can be obtained as 0.995, 0.935, 0.885, 0.223 and 0.05 respectively. Figure 4.5 illustrates the BER of Alamouti's STBC with coherent and non-coherent detection over a fast fading channel ($T_b f_D = 10^{-1}$) and a slow fading channel ($T_b f_D = 10^{-3}$) respectively, where the symbol SNR is fixed at 15 dB. Obviously, during the simulation, the temporal correlation for the two different 2×1 channels still exists

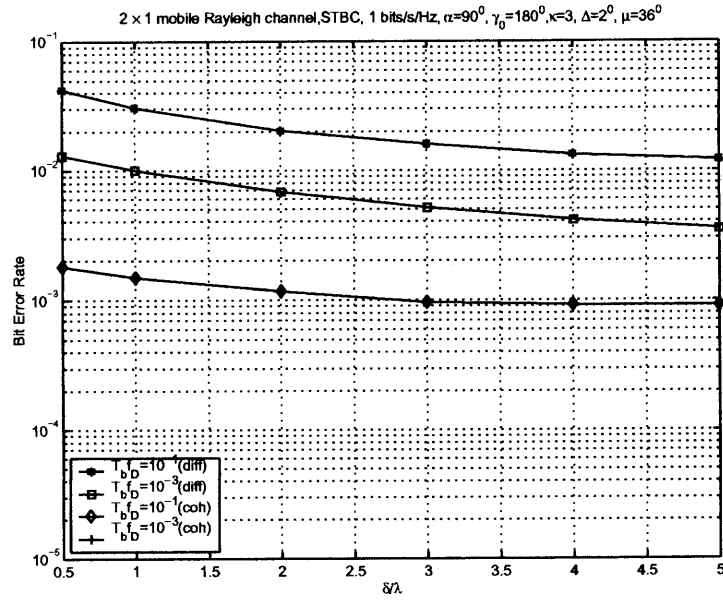


Figure 4.5 The effect of spatial correlation on BER performance of Alamouti's STBCs for a fast fading channel and a slow fading channel at 15 dB SNR.

but is a constant. With the increase of spatial correlation, the BER performance is obviously degraded for both coherent and non-coherent detection.

4.4.2 Temporal Correlation

Case 1 For this case, it is observed how the temporal correlation effects the BER performance of Alamouti's STBC via symbol SNR, for which the author sets BS element spacings of δ at 5λ , and it is over a fast fading channel ($T_b f_D = 10^{-1}$) and a slow fading channel ($T_b f_D = 10^{-3}$) respectively. Since the spatial correlation is fixed, the effect of temporal correlation is clearly illustrated. From Figure 4.6, the BER performance is greatly degraded with non-coherent detection, but it seems that temporal correlation doesn't effect performance of Alamouti's STBC scheme with coherent detection.

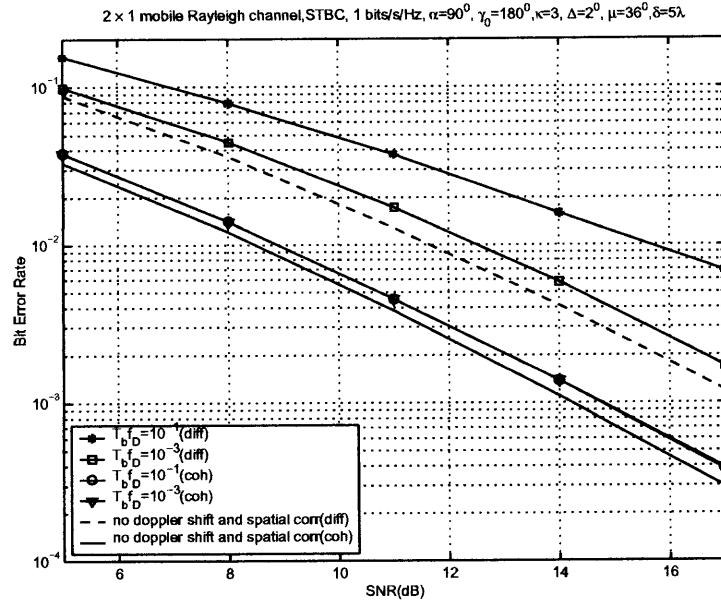


Figure 4.6 BER performance of Alamouti's STBCs for two channels with fixed spatial correlation but different temporal correlation.

Case 2 In this case, it is observed how the temporal correlation effects the BER performance of Alamouti's STBC via $T_b f_D$, the parameter to describe temporal correlation. Assume that the 2×1 channel is gradually changing from very slow fading ($T_b f_D = 10^{-4}$) to pretty fast fading ($T_b f_D = 10^0$), and BS element spacings of δ is supposed to be λ , and 5λ respectively. From Figure 4.7, with the decrease of the temporal correlation or the increase of $T_b f_D$, the BER performance of Alamouti's STBCs with differential detection will be degraded greatly for a fast fading channel ($T_b f_D > 10^{-2}$), but not for a slow fading channel ($T_b f_D \leq 10^{-2}$), and the degradation of BER performance from temporal correlation is not a linear function of $T_b f_D$, which is identical to the simulation results shown in Hwang's paper [32]. Moreover, the temporal correlation has no effect to Alamouti's STBC scheme with coherent detection, since it is assumed that receivers always know the channel state information perfectly when coherent detection is employed.

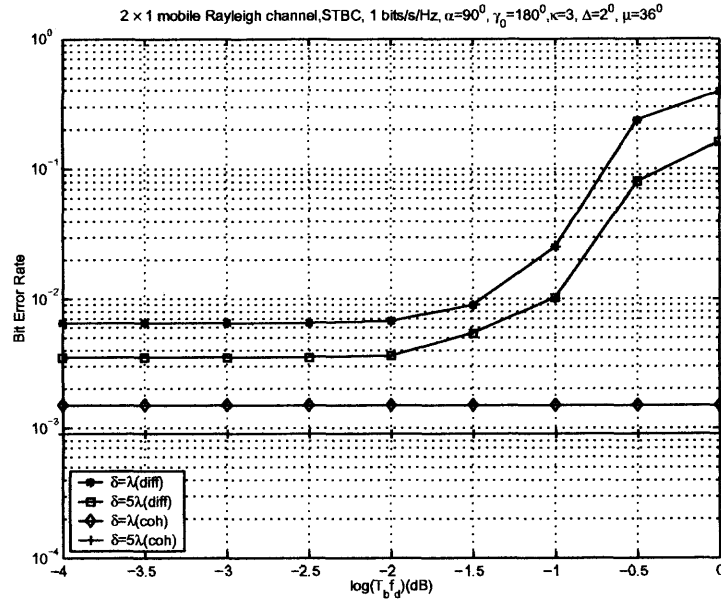


Figure 4.7 The effect of temporal correlation on BER performance of Alamouti's STBCs for two channels with a fixed spatial correlation at 15 dB SNR.

4.5 Conclusions

The BER performance of STBC over a spatio-temporal correlated channel with coherent and noncoherent detection have been illustrated, where a general space-time correlation model was utilized. The simulation results demonstrated that spatial correlation negatively effects the performance of the STBC scheme with differential detection but temporal correlation does positively; the less spatial correlation and more temporal correlation there are, the better performance is obtained. However, with coherent detection, spatial correlation still has negative effect on the performance but temporal correlation has no any impact on it.

CHAPTER 5

A DIFFERENTIAL SCHEME FOR DS/CDMA MIMO SYSTEM

5.1 Introduction

Multiple-input multiple-output (MIMO) links might play an important role in future wireless networks. It has been shown that capacity of MIMO systems grows linearly with the lower number of transmit or receive antennas. Hence, high transmission data rates can be obtained by such systems.

Several papers have been published, which study the MIMO link based on known channel parameters. Foschini proposed a layered space-time architecture, known as BLAST, which can achieve a tight lower bound on the capacity [41]. Tarokh explored an effective approach to increase data rate over wireless channels by combining array processing and space-time coding [42].

However, the assumption that the channel is perfectly known is questionable in a rapidly changing mobile environment, especially in MIMO systems. It might be impractical to accurately estimate all the channel gains. In order to reduce the cost and complexity of the system, it is of interest to search for methods, which do not require the CSI.

For a single transmit antenna, frequency-shift keying (FSK) and differential phase-shift keying (DPSK) can be demodulated without the use of channel information. It is natural to consider extensions of these schemes to MIMO systems.

As mentioned in Section 1.1, several space-time differential schemes were proposed recently. However, the scheme [13] can not be applied when the number of transmit antennas is more than two, unless the scheme is modified, thereby incurring a rate penalty [43]. Moreover, although the two schemes [15] and [16] can theoretically be applied to any number of transmit and receive antennas and any

signal constellation, the constellation cardinality for the group codes approach equals 2^{RM} , where R represents data rate and M is the number of transmit antennas. By their demodulation criterion, the computation complexity of the demodulation is exponential in R and M . If 3 bits per second is transmitted over 3 transmit antennas, group codes with a constellation of 512 should be found. Obviously, it is not trivial in practical use.

In this chapter, a new scheme, which is combines differential detection with orthogonal transmit diversity [44], is proposed. The proposed method can be used with any phase shift keying signal constellation, any number of transmit and receive antennas and without estimation of channel parameters. Full diversity gain is obtained. Most importantly, its implementation is simple.

5.2 Coherent Detection for Known CSI

5.2.1 Orthogonal Transmit Diversity

Before presenting the scheme, let us review the orthogonal transmit diversity scheme proposed in those papers [44] [45] [46] [47] for a known flat fading channel.

Two transmit antennas and one receive antenna for a K -user DS/CDMA system are considered. For simplicity, no intersymbol interference or multiple access interference are assumed to be present.

Assume that the channel is frequency non-selective and that the fading gain has a Rayleigh distribution for its amplitude and a uniform distribution for its phase. The point here is that the information bit is spread across the transmit antennas. The power per symbol is $E_s/2$, which means that the total transmit power per symbol interval is E_s . Two spreading codes are assigned to a single user. We restrict the constellation of transmitted symbols of the k th user s_k ($k = 1, 2, \dots, K$) to 2^b -PSK for some $b = 1, 2, 3, \dots$, but in reality only BPSK, QPSK and 8-PSK are of interest.

A matrix representation of the transmitted symbols for the k th user is

$$\begin{bmatrix} s_k(j)\underline{w}_{k,1} & s_k(j+1)\underline{w}_{k,1} \\ s_k(j)\underline{w}_{k,2} & s_k(j+1)\underline{w}_{k,2} \end{bmatrix}, \quad (5.1)$$

where the matrix rows represent different antennas, the columns represent different symbol intervals; $\underline{w}_{k,1}, \underline{w}_{k,2}$ are normalized spreading codes with a length L for the k th user at the first and second antenna, respectively; $s_k(j)$ and $s_k(j+1)$ are the j th and $(j+1)$ th symbols, respectively.

The signal at the receiver is

$$\underline{r}(j) = \sqrt{\frac{E_s}{2}} \sum_{k=1}^K (\underline{w}_{k,1}h_1 + \underline{w}_{k,2}h_2) s_k(j) + \underline{z}(j), \quad (5.2)$$

for $k = 1, 2, \dots, K$, where h_1 and h_2 are the fading gains from respectively, antenna 1 and antenna 2 to the receiver, $\underline{z}(j)$ is a noise vector with L elements, each of which has complex Gaussian distribution with a zero mean and variance σ^2 on each dimension, $\underline{r}(j)$ is the receive data vector with L elements.

Assuming orthogonality between users and between codes of the same user assigned to different transmit antenna, after despreading,

$$\begin{bmatrix} r_{k,1}(j) \\ r_{k,2}(j) \end{bmatrix} = \sqrt{\frac{E_s}{2}} s_k \begin{bmatrix} h_1 \\ h_2 \end{bmatrix} + \begin{bmatrix} z_{k,1}(j) \\ z_{k,2}(j) \end{bmatrix}. \quad (5.3)$$

Since fading gains are known and the signals from the different transmit antennas are separated at the receiver, maximum ratio combining (MRC) at the receiver can be used. Signals transmitted by antenna 1 and passing through the channel with gain h_1 are processed with gain h_1^* . Let $\mathbf{h}^\dagger = [h_1^* \ h_2^*]$, then

$$\begin{aligned} y_k(j) &= \sqrt{\frac{E_s}{2}} s_k \mathbf{h}^\dagger \begin{bmatrix} h_1 \\ h_2 \end{bmatrix} + \mathbf{h}^\dagger \begin{bmatrix} z_{k,1}(j) \\ z_{k,2}(j) \end{bmatrix} \\ &= \sqrt{\frac{E_s}{2}} \sum_{m=1}^2 |h_m|^2 s_k(j) + z'_k(j). \end{aligned} \quad (5.4)$$

Hard or soft detection of $s_k(j)$ may now be applied, and two-fold diversity gain is obtained.

5.2.2 MIMO OTD

Consider a K -user DS/CDMA wireless link with N transmit and M receive antennas.

Then the signal received at the m th receive antenna is:

$$\begin{aligned} r_m(j) &= \sqrt{\frac{E_s}{N}} \sum_{k=1}^K \sum_{n=1}^N \underline{w}_{k,n} h_{m,n} s_k(j) + z_m(j), \\ m &= 1, 2, \dots, M. \quad j = 1, 2, \dots \end{aligned} \quad (5.5)$$

Each user assigns N spreading codes $(\underline{w}_{k,1} \ \underline{w}_{k,2} \dots \underline{w}_{k,N})$. for spreading across the transmit antennas. After despreading,

$$\mathbf{r}_k(j) = \sqrt{\frac{E_s}{N}} s_k(j) \mathbf{h} + \mathbf{z}_k(j), \quad (5.6)$$

where

$$\begin{aligned} \mathbf{r}_k(j) &= [r_{k,1,1}(j), r_{k,2,1}(j), \dots, r_{k,M,N}(j)]^T, \\ \mathbf{h} &= [h_{1,1}, h_{2,1}, \dots, h_{M,N}]^T, \\ \mathbf{z}_k(j) &= [z_{k,1,1}(j), z_{k,2,1}(j), \dots, z_{k,M,N}(j)]^T. \end{aligned}$$

Using MRC \mathbf{h}^\dagger ,

$$y_k(j) = \mathbf{h}^\dagger \mathbf{r}_k(j) = \sqrt{\frac{E_s}{N}} s_k(j) \mathbf{h}^\dagger \mathbf{h} + \mathbf{h}^\dagger \mathbf{z}_k(j), \quad (5.7)$$

or equivalently,

$$y_k(j) = \sqrt{\frac{E_s}{N}} s_k(j) \sum_{n=1}^N \sum_{m=1}^M |h_{m,n}|^2 + z'_k(j), \quad (5.8)$$

where $z'_k(j) = \mathbf{h}^\dagger \mathbf{z}_k(j)$. Since $y_k(j)$ and $h_{m,n}$ are known, the j th symbol of the k th user can be detected and MN -fold spacial diversity gain is obtained.

5.3 Differential Detection

5.3.1 Single-Antenna System

Assume a single antenna system and a constellation S of transmitted symbols, which is 2^b -PSK for some $b = 1, 2, 3, \dots$. Also assume that the channel gain h from the transmitter to the receiver is unchanged during at least two symbol intervals. The transmitter sends the differentially encoded symbol streams $d_k(0)$, $d_k(1)$ and $d_k(2)$, where

$$d_k(j) = s_k(j)d_k(j-1), \quad (5.9)$$

for $j = 1, 2, \dots$ and $k = 1, 2, \dots, K$. The first symbol $d(0)$ is known.

Consider the desired k th user. Assuming orthogonality between users, after despreading,

$$r_k(j) = \sqrt{E_s} h d_k(j) + z_k(j).$$

At the receiver,

$$\begin{aligned} y_k(j) &= r_k^*(j-1)r_k(j) \\ &= E_s |d_k(j-1)|^2 |h|^2 s_k(j) + \Delta_k(j) \\ &\quad + \Psi_k(j) + Z_k(j), \end{aligned} \quad (5.10)$$

where $\Delta_k(j)$, $\Psi_k(j)$ and $Z_k(j)$ are noise terms as follows

$$\begin{aligned} \Delta_k(j) &= \sqrt{E_s} d_k^*(j-1) h^* z_k(j), \\ \Psi_k(j) &= \sqrt{E_s} z_k^*(j-1) h d_k(j), \\ Z_k(j) &= z_k^*(j-1) z_k(j). \end{aligned} \quad (5.11)$$

Obviously, $|d_k(j-1)|^2 = 1$, $j = 1, 2, \dots$, hence

$$y_k(j) = |h|^2 s_k(j) + \Delta_k(j) + \Psi_k(j) + Z_k(j). \quad (5.12)$$

Note that the last three terms of Expression (5.12) are noise terms. Even though the three noise terms $\Delta_k(j)$, $\Psi_k(j)$, $Z_k(j)$ and the channel gain h are unknown, they are constant. $s_k(j)$ can be detected by selecting $\tilde{s}_k(j)$ from the constellation A , the value closest to $y_k(j)$. This means

$$\hat{s}_k(j) = \arg \min_{\tilde{s}_k(j) \in A} |\tilde{s}_k(j) - y_k(j)|. \quad (5.13)$$

5.3.2 MIMO System

Now, it is desired to combine differential detection with a system of N transmit and M receive antennas.

Similar to Equation (5.5), for a K -user DS/CDMA system, the signal on the m th receive antenna is:

$$\begin{aligned} r_m(j) &= \sqrt{\frac{E_s}{M}} \sum_{k=1}^K \sum_{n=1}^N w_{k,n} h_{m,n} d_k(j) + z_m(j), \\ m &= 1, 2, \dots, M. \quad j = 1, 2, \dots \end{aligned} \quad (5.14)$$

here, $h_{m,n}$ ($m = 1, 2, \dots, M$, $n = 1, 2, \dots, N$) is unknown.

After despreading, the received signal can be expressed as:

$$\mathbf{r}_k(j) = \sqrt{\frac{E_s}{N}} d_k(j) \mathbf{h} + \mathbf{z}_k(j), \quad (5.15)$$

where

$$\begin{aligned} \mathbf{r}_k(j) &= [r_{k,1,1}(j) \ r_{k,2,1}(j) \dots r_{k,2,N}(j) \dots r_{k,M,N}(j)]^T, \\ \mathbf{h} &= [h_{1,1} \ h_{2,1} \dots h_{2,N} \dots h_{M,N}]^T, \\ \mathbf{z}_k(j) &= [z_{k,1,1}(j) \ z_{k,2,1}(j) \dots z_{k,2,N}(j) \dots z_{k,M,N}(j)]^T. \end{aligned} \quad (5.16)$$

The signal $d_k(j)$ is differentially encoded:

$$d_k(j) = s_k(j) d_k(j-1), \quad (5.17)$$

$$j = 1, 2, \dots, d(0) = 1, \quad k = 1, 2, \dots, K,$$

At the receiver,

$$\begin{aligned}
 y_k(j) &= \mathbf{r}_k(j-1)^\dagger \mathbf{r}(j) \\
 &= \frac{E_s}{N} \sum_{n=1}^N \sum_{m=1}^M |h_{m,n}|^2 d_k^\dagger(j-1) d_k(j) \\
 &\quad + \Delta_k(j) + \Psi_k(j) + Z_k(j),
 \end{aligned} \tag{5.18}$$

where $Z_k(j)$, $\Delta_k(j)$ and $\Psi_k(j)$ are noise terms defined:

$$\begin{aligned}
 \Delta_k(j) &= \sqrt{\frac{E_s}{M}} d_k^T(j-1) \mathbf{h}_k^\dagger \mathbf{z}_k(j), \\
 \Psi_k(j) &= \sqrt{\frac{E_s}{M}} \mathbf{z}_k^\dagger(j-1) d_k(j) \mathbf{h}, \\
 Z_k(j) &= \mathbf{z}_k^\dagger(j-1) \mathbf{z}_k(j).
 \end{aligned} \tag{5.19}$$

Using condition (5.17), Equation (5.18) can be simplified as

$$\begin{aligned}
 y_k(j) &= \left(\frac{E_s}{N} \sum_{n=1}^N \sum_{m=1}^M |h_{m,n}|^2 \right) s_k(j) \\
 &\quad + Z_k(j) + \Delta_k(j) + \Psi_k(j),
 \end{aligned} \tag{5.20}$$

The last three terms of Expression (5.20) are noise terms. Moreover, the coefficient $\frac{E_s}{N} \sum_{n=1}^N \sum_{m=1}^M |h_{m,n}|^2$ of $s_k(j)$ is unknown as well. However, all these terms are assumed constant. $s_k(j)$ can be detected by following criterion:

$$\hat{s}_k(j) = \arg \min_{\tilde{s}_k(j) \in A} |\tilde{s}_k(j) - y_k(j)|. \tag{5.21}$$

5.3.3 Capacity Analysis

Let's consider coherent detection first. From Equation (5.8), the variance for noise term $z'_k(j)$ can be expressed as [45]

$$\sigma_\xi^2 = \left(\sum_{n=1}^N \sum_{m=1}^M |h_{m,n}|^2 \right) \sigma^2. \tag{5.22}$$

Hence, the instantaneous SNR for $s_k(j)$ at the output should be

$$\text{SNR} = \frac{\rho}{N} \sum_{n=1}^N \sum_{m=1}^M |h_{m,n}|^2, \quad (5.23)$$

where $\rho = E_s/\sigma^2$ is the symbol SNR.

According to Shannon's capacity formula, the capacity for the k th user is

$$C_{M,N} = \log\left(1 + \frac{\rho}{N} \sum_{n=1}^N \sum_{m=1}^M |h_{m,n}|^2\right), \quad (5.24)$$

where the log is of base 2.

As to differential detection, from Equation (5.20), note that the noise term $Z_k(j)$ may be ignored since it is much smaller than the noise terms $\Delta_k(j)$ and $\Psi_k(j)$ when ρ is large enough. The variance for the terms $\Delta_k(j)$ and $\Psi_k(j)$ is

$$\sigma_\xi^2 = 2 \left(\sum_{n=1}^N \sum_{m=1}^M |h_{m,n}|^2 \right) \sigma^2. \quad (5.25)$$

Thus the capacity for the k th user is

$$C_{M,N} = \log\left(1 + \frac{\rho}{2N} \sum_{n=1}^N \sum_{m=1}^M |h_{m,n}|^2\right). \quad (5.26)$$

Comparing Expression (5.22) with Expression (5.25), it is found that the noise power for differential detection is two times that of coherent detection. This is the reason for the 3dB difference in the performance of coherent and non-coherent detection.

5.4 Numerical Results

In this section, the performance of the proposed scheme is assessed by simulation results. In Figure 5.1, a group of curves is presented, which compare the performance of the proposed scheme with that of coherent detection scheme in a multiple-input single-output scenario. Figure 5.2 shows numerical results for the single-input

multiple-output channel. Performance of a MIMO link with different number of transmit and receive antennas is illustrated in Figure 5.3. The curves in Figure 5.1 and Figure 5.2 demonstrate the 3 dB penalty for differential detection.

Moreover, from Figure 5.1 and Figure 5.2, it can be seen that those curves for differential detection are always parallel with those for coherent detection. Obviously, even though 3 dB SNR loss is paid for differential detection compared to coherent detection, the system provides the same spatial diversity both in differential detection case and in coherent detection case.

Figure 5.4 illustrates 10% outage capacity for different MIMO cases for coherent detection. Figure 5.5 shows the capacity in the differential detection case. Since the noise power for differential detection is two times that of coherent detection, the system has different capacity for the two cases. For instance, one user in a $4\text{Tr} \times 4\text{Re}$ system with coherent detection has capacity of 6.8 bits/sec/Hz at 16 dB (SNR) in Figure 5.4. Interestingly, in Figure 5.5, the user with differential detection has the capacity of 6.8 bits/sec/Hz at 19 dB, there is exactly 3 dB's difference.

Since the transmit power is fixed independent of the number of transmit antennas, while the total received power increases linearly with the number of receive antennas, the figures reflect an advantage for multiple receive antennas over multiple transmit antennas.

5.5 Conclusions

A differential detection scheme for a MIMO DS/CDMA link was proposed, which can provide full spatial diversity (both transmit diversity and receive diversity). The scheme is simple to implement, and can be applied to any phase shift keying signal constellation, and any number of transmit and receive antennas without estimation of channel parameters.

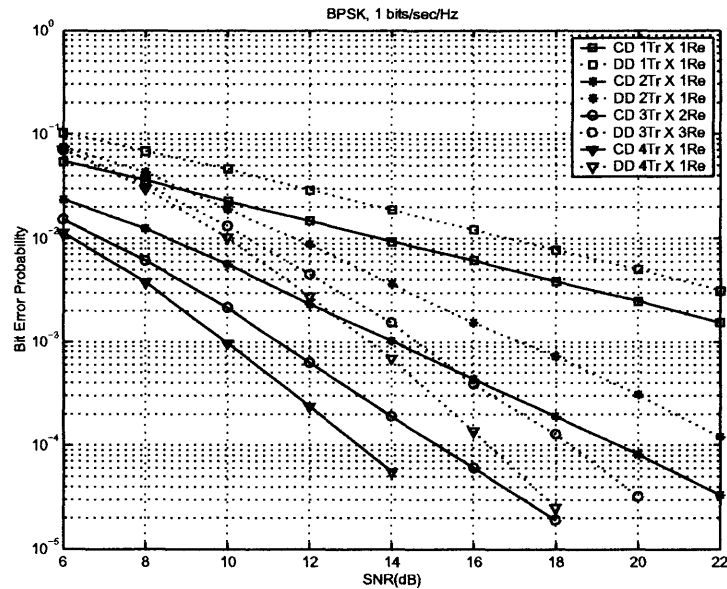


Figure 5.1 Performance of Differential Detection (DD) and Coherent Detection (CD) for one user in multiple-input and one-output case.

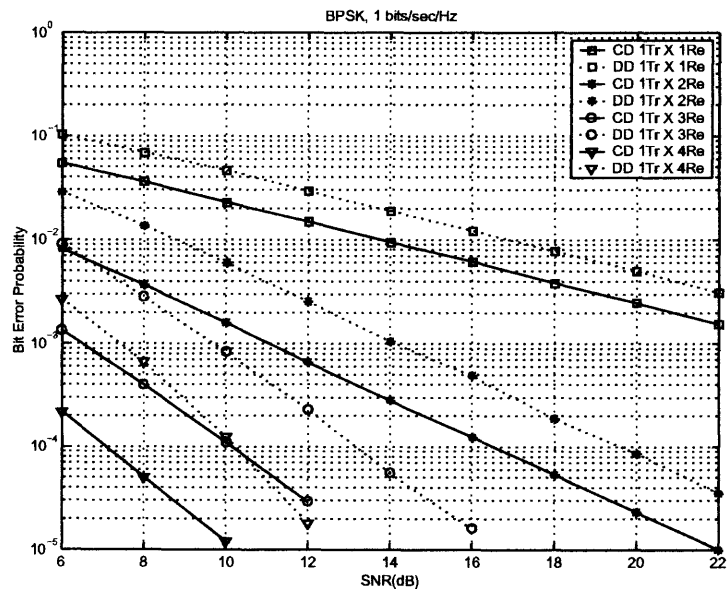


Figure 5.2 Performance of Differential Detection (DD) and Coherent Detection (CD) for one user in one-input and multiple-output case.

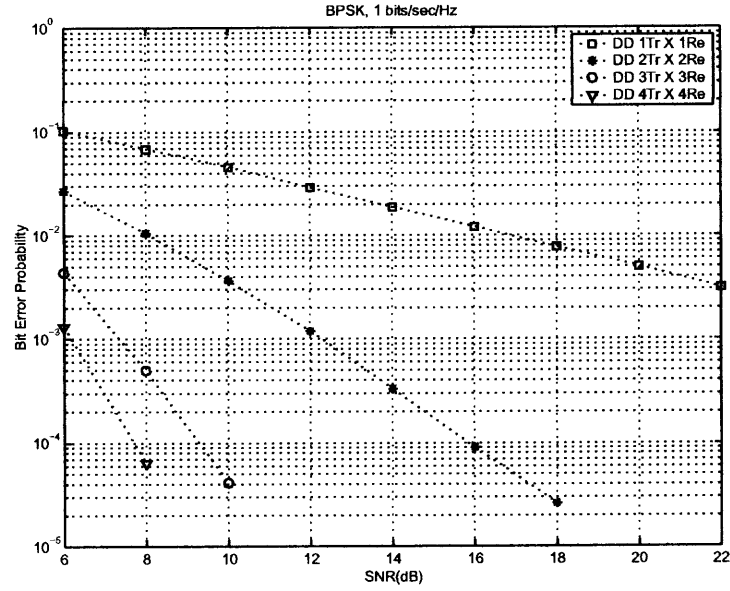


Figure 5.3 Performance of Differential Detection (DD) for one user in multiple-input and multiple-output case.

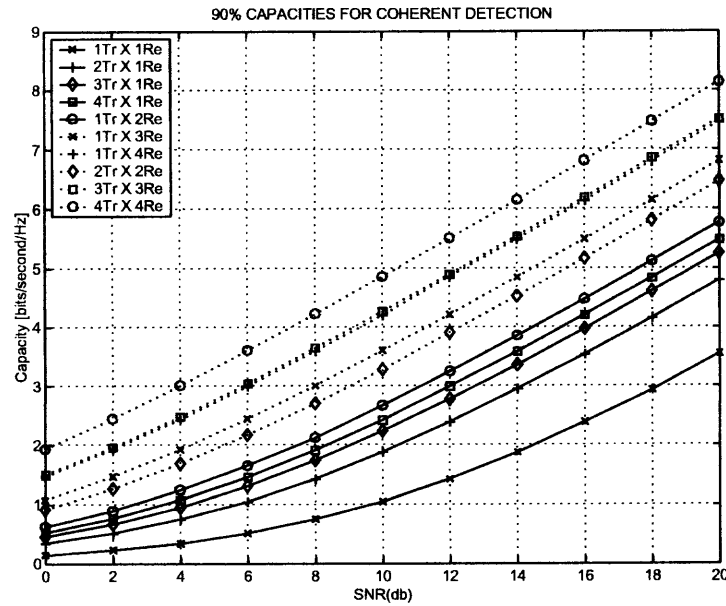


Figure 5.4 Capacity of one user for coherent detection.

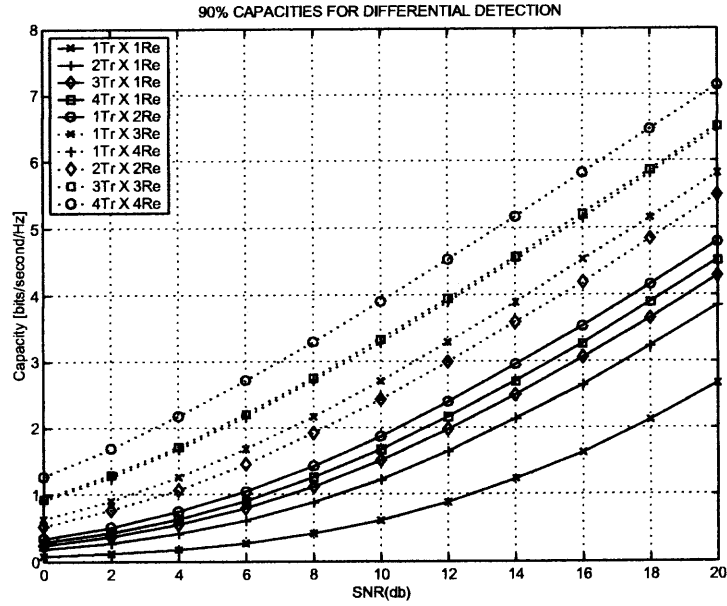


Figure 5.5 Capacity of one user for differential detection.

Even though 3 dB SNR loss is paid for differential detection compared to coherent detection, the noncoherent system has the same spatial diversity as the coherent system. The 3 dB penalty for non-coherent differential detection can be demonstrated from the capacity analysis. Provided that the total transmit power is fixed, a system with multiple antennas at the receiver site is advantageous over the system with multiple antennas at the transmitter site. For the former, fewer spreading codes for one user are needed.

CHAPTER 6

SUMMARY AND COMMENTS

In this dissertation, four aspects of transmit diversity have been studied:

1. Closed-form expressions of BER were derived for STBC based on Alamouti's scheme and utilizing M-ary phase shift keying (MPSK) modulation. The analysis was carried out for the slow, flat Rayleigh fading channel with coherent detection and with non-coherent differential encoding/decoding.

2. A MSDD technique was proposed for MPSK STBCs, which greatly reduces the performance loss by extending the observation interval for decoding. The technique uses maximum likelihood block sequence detection instead of the traditional block-by-block detection and was carried out on the slow, flat Rayleigh fading channel. A generalized decision metric for an observation interval of N blocks was derived. In addition, a closed-form pairwise error probability for differential BPSK STBC at N blocks of observation interval was derived, and an approximate BER was obtained to evaluate the performance.

3. The BER performance of Alamouti's STBCs over a spatio-temporal correlated channel with coherent and noncoherent detection was illustrated, where a general space-time correlation model was utilized. The simulation results demonstrated that spatial correlation negatively effects the performance of the STBC scheme with differential detection but temporal correlation positively impacts it. However, with coherent detection, spatial correlation still has negative effect on the performance but temporal correlation has no any impact on it.

4. A differential detection scheme for the DS/CDMA MIMO link was presented. The transmission provides for full transmit and receive diversity gain using a simple

detection scheme, which is a natural extension of differential detection combined with an Orthogonal Transmit Diversity approach.

For Item 1, even though the BER analysis in this dissertation is only for Alamouti's STBC scheme, the approach can also be utilized for a generalized STBC scheme with more than two transmit antennae. Moreover, comparing the BER expressions for $2T \times 1R$ Alamouti's STBC scheme with that for the $1T \times 2R$ receive diversity scheme in Proakis' book [18], it was found that the results are the same, although different analysis approaches were used.

In Item 2, it was assumed that the fading channels are flat and the path gains are modeled as quasi-static over some frame of arbitrary length. However, the statistic characteristic for fading channels are sometimes more complex. For example, Bhukania et al. [24] expanded the MSDD idea to Hochwald's STBC scheme [15] for 3 blocks and incorporated knowledge of the fading correlation, assuming that the channel changes once per block. Therefore, it would be interesting to use the MSDD technique for MPSK STBCs in the case that the channel fading is not flat but frequency selective with fast fading. However, it would be quite difficult to get the approximate BER expressions for this case.

In Item 3, some simulations for Alamouti's STBCs over a spatio-temporal correlated channel have been showed. Based those results, it will be an ideal choice for Alamouti's scheme to be employed on a high data rate wireless link over a MIMO channel if spatial correlation of the channel can be reduced to a very low level. Since fast fading never occurs because of the speed limit of a vehicle, temporal correlation has no impact on the performance of this scheme even with differential detection.

For Item 4, it is essential to consider MAI and ISI for a practical DS/CDMA system. Thus it would be of interest to explore the proposed scheme in a practical DS/CDMA system, and analyze how the performance is affected by MAI and ISI.

APPENDIX A

EVALUATION OF THE VARIANCE OF $\text{Re tr}(\Lambda)$

Let's first divide $\text{Re tr}(\Lambda)$ into two parts.

Define

$$\Lambda_1 = \sum_{i=1}^{N-1} \sum_{j=0}^{i-1} \left\{ \mathbf{C}_{k-j} \mathbf{H}_{k-j} \Psi_{k-i}^\dagger \mathbf{Q}_{k-i} \mathbf{Q}_{k-j}^\dagger + \Psi_{k-j} \mathbf{H}_{k-i}^\dagger \mathbf{C}_{k-i}^\dagger \mathbf{Q}_{k-i} \mathbf{Q}_{k-j}^\dagger \right\}, \quad (\text{A.1})$$

$$\Lambda_2 = \sum_{i=1}^{N-1} \sum_{j=0}^{i-1} \left\{ \mathbf{C}_{k-j} \mathbf{H}_{k-j} \Psi_{k-i}^\dagger \mathbf{C}_{k-i} \mathbf{C}_{k-j}^\dagger + \Psi_{k-j} \mathbf{H}_{k-i}^\dagger \mathbf{C}_{k-i}^\dagger \mathbf{C}_{k-i} \mathbf{C}_{k-j}^\dagger \right\}, \quad (\text{A.2})$$

then

$$\text{Re tr}(\Lambda) = \text{Re tr}(\Lambda_1) - \text{Re tr}(\Lambda_2). \quad (\text{A.3})$$

Now, the variance of $\text{Re tr}(\Lambda)$ consists of three parts: the variance of $\text{Re tr}(\Lambda_1)$, the variance of $\text{Re tr}(\Lambda_2)$, and the cross-correlation between $\text{Re tr}(\Lambda_1)$ and $\text{Re tr}(\Lambda_2)$. Namely

$$\begin{aligned} \text{Var}[\text{Re tr}(\Lambda)] = \\ \text{Var}[\text{Re tr}(\Lambda_1)] + \text{Var}[\text{Re tr}(\Lambda_2)] - 2\text{cov}(\text{Re tr}(\Lambda_1), \text{Re tr}(\Lambda_2)). \end{aligned} \quad (\text{A.4})$$

$\text{Var}[\text{Re tr}(\Lambda_1)]$, $\text{Var}[\text{Re tr}(\Lambda_2)]$ and the cross-correlation of $\text{Re tr}(\Lambda_1)$ and $\text{Re tr}(\Lambda_2)$ will be evaluated respectively in the following subsections.

A.1 Evaluation of $\text{Var}[\text{Re tr}(\Lambda_1)]$, $\text{Var}[\text{Re tr}(\Lambda_2)]$

Since $\text{Re tr}(\Lambda_1)$ and $\text{Re tr}(\Lambda_2)$ have similar structures. If the variance of $\text{Re tr}(\Lambda_1)$ is obtained, the variance of $\text{Re tr}(\Lambda_2)$ is straight forward.

Define

$$\Lambda_{i,j}^{(1)} = \mathbf{C}_{k-j} \mathbf{H}_{k-j} \Psi_{k-i}^\dagger \mathbf{Q}_{k-i} \mathbf{Q}_{k-j}^\dagger + \Psi_{k-j} \mathbf{H}_{k-i}^\dagger \mathbf{C}_{k-i}^\dagger \mathbf{Q}_{k-i} \mathbf{Q}_{k-j}^\dagger, \quad (\text{A.5})$$

$$\Lambda_{i,j}^{(2)} = \mathbf{C}_{k-j} \mathbf{H}_{k-j} \Psi_{k-i}^\dagger \mathbf{C}_{k-i} \mathbf{C}_{k-j}^\dagger + \Psi_{k-j} \mathbf{H}_{k-i}^\dagger \mathbf{C}_{k-i}^\dagger \mathbf{C}_{k-i} \mathbf{C}_{k-j}^\dagger. \quad (\text{A.6})$$

Then

$$\text{Var} [\text{Re tr} (\Lambda_1)] = V_1 + 2\Theta, \quad (\text{A.7})$$

where the auto-correlation of $\text{Var} [\text{Re tr} (\Lambda_1)]$ is expressed as

$$V_1 = \sum_{i=1}^{N-1} \sum_{j=0}^{i-1} \text{Var} \left[\text{Re tr} \left(\Lambda_{i,j}^{(1)} \right) \right], \quad (\text{A.8})$$

and the cross-correlation of $\text{Var} [\text{Re tr} (\Lambda_1)]$ is

$$\Theta = \text{cov} \left(\sum_{i=1}^{N-1} \sum_{j=0}^{i-1} \text{Re tr} \left(\Lambda_{i,j}^{(1)} \right), \sum_{i'=1}^{N-1} \sum_{j'=0}^{i'-1} \text{Re tr} \left(\Lambda_{i',j'}^{(1)} \right) \right) \Bigg|_{i' \neq i \text{ and } j' \neq j}. \quad (\text{A.9})$$

Similarly, the variance of $\text{Re tr} (\Lambda_2)$ can be divided into two parts:

$$\text{Var} [\text{Re tr} (\Lambda_2)] = V_2 + 2\Omega, \quad (\text{A.10})$$

where the auto-correlation of $\text{Re tr} (\Lambda_2)$ is

$$V_2 = \sum_{i=1}^{N-1} \sum_{j=0}^{i-1} \text{Var} \left[\text{Re tr} \left(\Lambda_{i,j}^{(2)} \right) \right], \quad (\text{A.11})$$

and the cross-correlation of $\text{Re tr} (\Lambda_2)$ can be expressed as

$$\Omega = \text{cov} \left(\sum_{i=1}^{N-1} \sum_{j=0}^{i-1} \text{Re tr} \left(\Lambda_{i,j}^{(2)} \right), \sum_{i'=1}^{N-1} \sum_{j'=0}^{i'-1} \text{Re tr} \left(\Lambda_{i',j'}^{(2)} \right) \right) \Bigg|_{i' \neq i \text{ and } j' \neq j}. \quad (\text{A.12})$$

Finally,

$$\begin{aligned} & \text{Var} [\text{Re tr} (\Lambda_1)] + \text{Var} [\text{Re tr} (\Lambda_2)] = \\ & V_1 + V_2 + 2(\Omega + \Theta). \end{aligned} \quad (\text{A.13})$$

In the following, V_1 , V_2 , Θ , and Ω will be evaluated respectively.

A.1.1 Evaluation of V_1 and V_2

V_1 and V_2 are auto-correlation terms. From Theorem 2 and 4 ,

$$\begin{aligned} V_1 &= \sum_{i=1}^{N-1} \sum_{j=0}^{i-1} \text{Var} \left[\text{Re tr} \left(\Lambda_{i,j}^{(1)} \right) \right] \\ &= \sum_{i=1}^{N-1} \sum_{j=0}^{i-1} \left\{ \text{Var} \left[\text{Re tr} \left(\mathbf{Q}_{k-i} \mathbf{Q}_{k-j}^\dagger \mathbf{C}_{k-j} \mathbf{H}_{k-j} \Psi_{k-i}^\dagger \right) \right] + \right. \\ &\quad \left. \text{Var} \left[\text{Re tr} \left(\mathbf{Q}_{k-j} \mathbf{Q}_{k-i}^\dagger \mathbf{C}_{k-i} \mathbf{H}_{k-i} \Psi_{k-j}^\dagger \right) \right] \right\}. \end{aligned} \quad (\text{A.14})$$

For BPSK messages, \mathbf{Q}_k and \mathbf{C}_k are orthogonal real matrices, so $\mathbf{Q}_{k-i} \mathbf{Q}_{k-j}^\dagger \mathbf{C}_{k-j}$, $\mathbf{Q}_{k-j} \mathbf{Q}_{k-i}^\dagger \mathbf{C}_{k-i}$ are orthogonal real matrices thus also (Theorem 3). From Theorem 5,

$$\begin{aligned} V_1 &= \sum_{i=1}^{N-1} \sum_{j=0}^{i-1} 4 \left(|h_{1,1}|^2 + |h_{2,1}|^2 \right) N_0 \\ &= 2N(N-1) \left(|h_{1,1}|^2 + |h_{2,1}|^2 \right) N_0. \end{aligned} \quad (\text{A.15})$$

Similarly,

$$\begin{aligned} V_2 &= \sum_{i=1}^{N-1} \sum_{j=0}^{i-1} \text{Var} \left[\text{Re tr} \left(\Lambda_{i,j}^{(2)} \right) \right] \\ &= 2N(N-1) \left(|h_{1,1}|^2 + |h_{2,1}|^2 \right) N_0. \end{aligned} \quad (\text{A.16})$$

A.1.2 Evaluation of cross-correlation Θ and Ω

The cross-correlation of $\text{Re tr}(\Lambda_1)$ can be expressed as

$$\begin{aligned} \Theta &= \text{Re tr}(\Lambda_1) = \text{cov}(\delta_1, \delta_2) \\ &= (N-2)N_0 \left(|h_{1,1}|^2 + |h_{2,1}|^2 \right) * \\ &\quad \text{Re tr} \left\{ \sum_{i=1}^{N-1} \sum_{j=0}^{i-1} (\mathbf{D}_{k-j} \mathbf{D}_{k-j-1} \dots \mathbf{D}_{k-i+1}) \right\}, \end{aligned} \quad (\text{A.17})$$

where

$$\begin{aligned} \delta_1 = & \sum_{i=1}^{N-1} \sum_{j=0}^{i-1} \text{Re tr} \left(\mathbf{C}_{k-j} \mathbf{H}_{k-j} \Psi_{k-i}^\dagger \mathbf{Q}_{k-i} \mathbf{Q}_{k-j}^\dagger + \right. \\ & \left. + \Psi_{k-j} \mathbf{H}_{k-i}^\dagger \mathbf{C}_{k-i}^\dagger \mathbf{Q}_{k-i} \mathbf{Q}_{k-j}^\dagger \right), \end{aligned} \quad (\text{A.18})$$

$$\begin{aligned} \delta_2 = & \sum_{i'=1}^{N-1} \sum_{j'=0}^{i'-1} \text{Re tr} \left(\mathbf{C}_{k-j'} \mathbf{H}_{k-j'} \Psi_{k-i'}^\dagger \mathbf{Q}_{k-i'} \mathbf{Q}_{k-j'}^\dagger + \right. \\ & \left. + \Psi_{k-j'} \mathbf{H}_{k-i'}^\dagger \mathbf{C}_{k-i'}^\dagger \mathbf{Q}_{k-i'} \mathbf{Q}_{k-j'}^\dagger \right) \Big|_{i' \neq i \text{ and } j' \neq j}. \end{aligned} \quad (\text{A.19})$$

Proof:

Since \mathbf{C}_k , \mathbf{H}_k , and \mathbf{Q}_k are constant matrices, the cross-correlation Θ is related to the N noise matrices $\Psi_k, \Psi_{k-1}, \dots, \Psi_{k-N+2}, \Psi_{k-N+1}$ only. Meanwhile, these noise matrices are mutually independent of each other. From Theorem 7, any cross-correlation between two terms with different noise matrices is zero. Hence Θ only consists of the cross-correlation between the terms with the same noise matrix.

For Ψ_k only, the cross-correlation terms can be obtained when $j = 0, i = 1, 2, \dots, N-1$ in Equation (A.18). There are a total of $N-1$ terms with noise matrix Ψ_k , so

$$\delta_1 = \sum_{i=0}^{N-1} \text{Re tr} \left(\Psi_k \mathbf{H}_{k-i}^\dagger \mathbf{C}_{k-i}^\dagger \mathbf{Q}_{k-i} \mathbf{Q}_k^\dagger \right) \Big|_{i \neq 0}, \quad (\text{A.20})$$

and

$$\delta_2 = \sum_{i'=0}^{N-1} \text{Re tr} \left(\Psi_k \mathbf{H}_{k-i'}^\dagger \mathbf{C}_{k-i'}^\dagger \mathbf{Q}_{k-i'} \mathbf{Q}_k^\dagger \right) \Big|_{i' \neq 0, i}, \quad (\text{A.21})$$

hence the cross-correlation for Ψ_k is

$$\begin{aligned} \Theta_0 &= E [\delta_1 \delta_2] \\ &= N_0 (|h_{1,1}|^2 + |h_{2,1}|^2) \sum_{i=1}^{N-1} \sum_{j=0}^{i-1} \text{Re tr} \left(\mathbf{C}_{k-i}^\dagger \mathbf{C}_{k-j} \mathbf{Q}_{k-i} \mathbf{Q}_{k-j}^\dagger \right) \Big|_{i,j \neq 0}. \end{aligned} \quad (\text{A.22})$$

For Ψ_{k-1} , the cross-correlation terms may be obtained from Equation (A.18) $j = 1$, $i = 2, 3 \dots N-1$ and $j = 0$, $i = 1$, and has a total of $N-1$ terms. Hence

$$\begin{aligned}
 \delta_1 &= \sum_{i=2}^{N-1} \text{Re tr} \left(\Psi_{k-1} \mathbf{H}_{k-i}^\dagger \mathbf{C}_{k-i}^\dagger \mathbf{Q}_{k-i} \mathbf{Q}_{k-1}^\dagger \right) + \text{Re tr} \left(\mathbf{C}_k \mathbf{H}_k \Psi_{k-1}^\dagger \mathbf{Q}_{k-1} \mathbf{Q}_k^\dagger \right) \\
 &= \sum_{i=2}^{N-1} \text{Re tr} \left(\Psi_{k-1} \mathbf{H}_{k-i}^\dagger \mathbf{C}_{k-i}^\dagger \mathbf{Q}_{k-i} \mathbf{Q}_{k-1}^\dagger \right) + \text{Re tr} \left(\Psi_{k-1} \mathbf{H}_k^\dagger \mathbf{C}_k^\dagger \mathbf{Q}_k \mathbf{Q}_{k-1}^\dagger \right) \\
 &= \sum_{i=0}^{N-1} \text{Re tr} \left(\Psi_{k-1} \mathbf{H}_{k-i}^\dagger \mathbf{C}_{k-i}^\dagger \mathbf{Q}_{k-i} \mathbf{Q}_{k-1}^\dagger \right) \Big|_{i \neq 1}. \quad (\text{A.23})
 \end{aligned}$$

Moreover

$$\delta_2 = \sum_{i'=0}^{N-1} \text{Re tr} \left(\Psi_{k-1} \mathbf{H}_{k-i'}^\dagger \mathbf{C}_{k-i'}^\dagger \mathbf{Q}_{k-i'} \mathbf{Q}_{k-1}^\dagger \right) \Big|_{i' \neq 1, i}. \quad (\text{A.24})$$

The cross-correlation for Ψ_{k-1} is

$$\begin{aligned}
 \Theta_1 &= E [\delta_1 \delta_2] \\
 &= N_0 (|h_{1,1}|^2 + |h_{2,1}|^2) \sum_{i=1}^{N-1} \sum_{j=0}^{i-1} \text{Re tr} \left(\mathbf{C}_{k-i}^\dagger \mathbf{C}_{k-j} \mathbf{Q}_{k-i} \mathbf{Q}_{k-j}^\dagger \right) \Big|_{i,j \neq 1}. \quad (\text{A.25})
 \end{aligned}$$

For Ψ_{k-2} , the cross-correlation terms can be obtained by $j = 2$, $i = 3, 4 \dots N-1$ and $i = 2$, $j = 0, 1$. Hence

$$\begin{aligned}
 \delta_1 &= \sum_{i=3}^{N-1} \text{Re tr} \left(\Psi_{k-2} \mathbf{H}_{k-i}^\dagger \mathbf{C}_{k-i}^\dagger \mathbf{Q}_{k-i} \mathbf{Q}_{k-2}^\dagger \right) \\
 &\quad + \sum_{j=0}^1 \text{Re tr} \left(\mathbf{C}_{k-j} \mathbf{H}_{k-j} \Psi_{k-2}^\dagger \mathbf{Q}_{k-2} \mathbf{Q}_{k-j}^\dagger \right) \\
 &= \sum_{i=3}^{N-1} \text{Re tr} \left(\Psi_{k-2} \mathbf{H}_{k-i}^\dagger \mathbf{C}_{k-i}^\dagger \mathbf{Q}_{k-i} \mathbf{Q}_{k-2}^\dagger \right) \\
 &\quad + \sum_{i=0}^1 \text{Re tr} \left(\Psi_{k-2} \mathbf{H}_{k-i}^\dagger \mathbf{C}_{k-i}^\dagger \mathbf{Q}_{k-i} \mathbf{Q}_{k-2}^\dagger \right) \\
 &= \sum_{i=0}^{N-1} \text{Re tr} \left(\Psi_{k-2} \mathbf{H}_{k-i}^\dagger \mathbf{C}_{k-i}^\dagger \mathbf{Q}_{k-i} \mathbf{Q}_{k-2}^\dagger \right) \Big|_{i \neq 2}, \quad (\text{A.26})
 \end{aligned}$$

and

$$\delta_2 = \sum_{i'=0}^{N-1} \text{Re tr} \left(\Psi_{k-2} \mathbf{H}_{k-i'}^\dagger \mathbf{C}_{k-i'}^\dagger \mathbf{Q}_{k-i'} \mathbf{Q}_{k-2}^\dagger \right) \Big|_{i' \neq 2, i}. \quad (\text{A.27})$$

The cross-correlation is

$$\begin{aligned} \Theta_2 &= E [\delta_1 \delta_2] \\ &= N_0 (|h_{1,1}|^2 + |h_{2,1}|^2) \sum_{i=1}^{N-1} \sum_{j=0}^{i-1} \text{Re tr} \left(\mathbf{C}_{k-i}^\dagger \mathbf{C}_{k-j} \mathbf{Q}_{k-i} \mathbf{Q}_{k-j}^\dagger \right) \Big|_{i,j \neq 2}. \end{aligned} \quad (\text{A.28})$$

For Ψ_{k-N+1} , there are two cases, $i = N - 1$, $j = 0, 1, N - 2$ which is equivalent to $j = 1$, $i = 0, 1, 3 \dots N - 1$. Hence

$$\delta_1 = \sum_{i=0}^{N-1} \text{Re tr} \left(\mathbf{C}_{k-i} \mathbf{H}_{k-i} \Psi_{k-N+1}^\dagger \mathbf{Q}_{k-N+1} \mathbf{Q}_{k-i}^\dagger \right) \Big|_{i \neq N-1}, \quad (\text{A.29})$$

and

$$\delta_2 = \sum_{i'=0}^{N-1} \text{Re tr} \left(\mathbf{C}_{k-i'} \mathbf{H}_{k-i'} \Psi_{k-N+1}^\dagger \mathbf{Q}_{k-N+1} \mathbf{Q}_{k-i'}^\dagger \right) \Big|_{i' \neq N-1, i}, \quad (\text{A.30})$$

so

$$\begin{aligned} \Theta_{N-1} &= E [\delta_1 \delta_2] \\ &= N_0 (|h_{1,1}|^2 + |h_{2,1}|^2) \sum_{i=1}^{N-1} \sum_{j=0}^{i-1} \text{Re tr} \left(\mathbf{C}_{k-i}^\dagger \mathbf{C}_{k-j} \mathbf{Q}_{k-i} \mathbf{Q}_{k-j}^\dagger \right) \Big|_{i,j \neq N-1} \end{aligned} \quad (\text{A.31})$$

Hence

$$\begin{aligned}
\Theta &= \Theta_0 + \Theta_1 + \dots \Theta_{N-1} \\
&= N_0 (|h_{1,1}|^2 + |h_{2,1}|^2) \left\{ \sum_{i=1}^{N-1} \sum_{j=0}^{i-1} \text{Re tr} \left(\mathbf{C}_{k-i}^\dagger \mathbf{C}_{k-j} \mathbf{Q}_{k-i} \mathbf{Q}_{k-j}^\dagger \right) \right\} \Big|_{i,j \neq 0} \\
&\quad + \sum_{i=1}^{N-1} \sum_{j=0}^{i-1} \text{Re tr} \left(\mathbf{C}_{k-i}^\dagger \mathbf{C}_{k-j} \mathbf{Q}_{k-i} \mathbf{Q}_{k-j}^\dagger \right) \Big|_{i,j \neq 1} \\
&\quad + \sum_{i=1}^{N-1} \sum_{j=0}^{i-1} \text{Re tr} \left(\mathbf{C}_{k-i}^\dagger \mathbf{C}_{k-j} \mathbf{Q}_{k-i} \mathbf{Q}_{k-j}^\dagger \right) \Big|_{i,j \neq 2} \\
&\quad + \dots + \sum_{i=1}^{N-1} \sum_{j=0}^{i-1} \text{Re tr} \left(\mathbf{C}_{k-i}^\dagger \mathbf{C}_{k-j} \mathbf{Q}_{k-i} \mathbf{Q}_{k-j}^\dagger \right) \Big|_{i,j \neq N-1} \Big\} \\
&= N_0 (|h_{1,1}|^2 + |h_{2,1}|^2) \{ (\mathbf{D}_{k-1} + \mathbf{D}_{k-2} + \dots + \mathbf{D}_{k-1} \mathbf{D}_{k-2} + \dots \\
&\quad + \mathbf{D}_{k-1} \mathbf{D}_{k-2} \dots \mathbf{D}_{k-N+1}) \\
&\quad + (\mathbf{D}_{k-2} + \mathbf{D}_{k-3} + \dots + \mathbf{D}_k \mathbf{D}_{k-1} + \dots + \mathbf{D}_{k-2} \mathbf{D}_{k-3} \dots \mathbf{D}_{k-N+1}) \\
&\quad + (\mathbf{D}_k + \mathbf{D}_{k-3} + \dots + \mathbf{D}_{k-1} \mathbf{D}_{k-2} + \dots + \mathbf{D}_{k-3} \mathbf{D}_{k-4} \dots \mathbf{D}_{k-N+1}) + \dots \\
&\quad + (\mathbf{D}_k + \mathbf{D}_{k-1} + \dots + \mathbf{D}_k \mathbf{D}_{k-1} + \mathbf{D}_{k-1} \mathbf{D}_{k-2} + \dots + \mathbf{D}_k \mathbf{D}_{k-2} \dots \mathbf{D}_{k-N+2}) \} \\
&= (N-2) N_0 (|h_{1,1}|^2 + |h_{2,1}|^2) * \\
&\quad \text{Re tr} \left\{ \sum_{i=1}^{N-1} \sum_{j=0}^{i-1} (\mathbf{D}_{k-j} \mathbf{D}_{k-j-1} \dots \mathbf{D}_{k-i+1}) \right\}. \tag{A.32}
\end{aligned}$$

Similarly, if all the \mathbf{Q}_k are replaced with \mathbf{C}_k in (A.32), the cross-correlation coefficient Ω can be easily obtained as

$$\Omega = (N-2) N_0 (|h_{1,1}|^2 + |h_{2,1}|^2) \text{Re tr} \left\{ \sum_{i=1}^{N-1} \sum_{j=0}^{i-1} (\mathbf{I}_2) \right\}, \tag{A.33}$$

where

$$\delta_1 = \sum_{i=1}^{N-1} \sum_{j=0}^{i-1} \text{Re tr} \left(\mathbf{C}_{k-j} \mathbf{H}_{k-j} \Psi_{k-i}^\dagger \mathbf{C}_{k-i} \mathbf{C}_{k-j}^\dagger + \Psi_{k-j} \mathbf{H}_{k-i}^\dagger \mathbf{C}_{k-i}^\dagger \mathbf{C}_{k-i} \mathbf{C}_{k-j}^\dagger \right), \quad (\text{A.34})$$

$$\delta_2 = \sum_{i'=1}^{N-1} \sum_{j'=0}^{i'-1} \text{Re tr} \left(\mathbf{C}_{k-j'} \mathbf{H}_{k-j} \Psi_{k-i'}^\dagger \mathbf{C}_{k-i'} \mathbf{C}_{k-j'}^\dagger + \Psi_{k-j'} \mathbf{H}_{k-i'}^\dagger \mathbf{C}_{k-i'}^\dagger \mathbf{C}_{k-i'} \mathbf{C}_{k-j'}^\dagger \right) \Big|_{i' \neq i \text{ and } j' \neq j}. \quad (\text{A.35})$$

Hence, substituting Expression (A.15) (A.16) (A.17) and (A.33) into Equation (A.13),

$$\begin{aligned} & \text{Var} [\text{Re tr} (\Lambda_1)] + \text{Var} [\text{Re tr} (\Lambda_2)] = 4N(N-1) (|h_1|^2 + |h_2|^2) E_s N_0 \\ & + 2(N-2) E_s N_0 (|h_1|^2 + |h_2|^2) * \\ & \text{Re tr} \left\{ \sum_{i=1}^{N-1} \sum_{j=0}^{i-1} (\mathbf{D}_{k-j} \mathbf{D}_{k-j-1} \dots \mathbf{D}_{k-i+1} + \mathbf{I}_2) \right\}. \end{aligned} \quad (\text{A.36})$$

A.2 Evaluation of $\text{cov} (\text{Re tr} (\Lambda_1), \text{Re tr} (\Lambda_2))$

The cross-correlation $\text{cov} (\text{Re tr} (\Lambda_1), \text{Re tr} (\Lambda_2))$ can be expressed as

$$\begin{aligned} \Phi &= \text{cov} (\text{Re tr} (\Lambda_1), \text{Re tr} (\Lambda_2)) \\ &= \text{cov} (\delta_1, \delta_2) \\ &= 2(N-1) N_0 (|h_{1,1}|^2 + |h_{2,1}|^2) * \\ & \text{Re tr} \left\{ \sum_{i=1}^{N-1} \sum_{j=0}^{i-1} (\mathbf{D}_{k-j} \mathbf{D}_{k-j-1} \dots \mathbf{D}_{k-i+1}) \right\}, \end{aligned} \quad (\text{A.37})$$

where

$$\delta_1 = \sum_{i=1}^{N-1} \sum_{j=0}^{i-1} \text{Re tr} \left(\mathbf{C}_{k-j} \mathbf{H}_{k-j} \Psi_{k-i}^H \mathbf{Q}_{k-i} \mathbf{Q}_{k-j}^H + \Psi_{k-j} \mathbf{H}_{k-i}^H \mathbf{C}_{k-i}^H \mathbf{Q}_{k-i} \mathbf{Q}_{k-j}^H \right), \quad (\text{A.38})$$

$$\delta_2 = \sum_{i'=1}^{N-1} \sum_{j'=0}^{i'-1} \text{Re tr} \left(\mathbf{C}_{k-j'} \mathbf{H}_{k-j} \Psi_{k-i'}^H \mathbf{C}_{k-i'} \mathbf{C}_{k-j'}^H + \Psi_{k-j'} \mathbf{H}_{k-i'}^H \mathbf{C}_{k-i'}^H \mathbf{C}_{k-j'} \mathbf{C}_{k-j'}^H \right) \quad (\text{A.39})$$

$$= \sum_{i'=1}^{N-1} \sum_{j'=0}^{i'-1} \text{Re tr} \left(\mathbf{H}_{k-j} \Psi_{k-i'}^H \mathbf{C}_{k-i'} + \Psi_{k-j'} \mathbf{H}_{k-i'}^H \mathbf{C}_{k-j'}^H \right). \quad (\text{A.40})$$

Proof:

Since \mathbf{C}_k , \mathbf{H}_k , and \mathbf{Q}_k are constant matrices, the cross-correlation Φ is related to the N noise matrices

$$\Psi_k, \Psi_{k-1}, \dots, \Psi_{k-N+2}, \Psi_{k-N+1} \quad (\text{A.41})$$

only. Moreover, these noise matrices are mutually independent of each other. From Theorem 7, any cross-correlation between two terms with different noise matrices is zero. Hence Φ only consists of the cross-correlation between the terms with the same noise matrix.

For Ψ_k only, the cross-correlation terms can be obtained when $j = 0$, $i = 1, 2, \dots, N-1$ in Expression (A.18), there are a total of $N-1$ terms with noise matrix Ψ_k , so

$$\delta_1 = \sum_{i=0}^{N-1} \text{Re tr} \left(\Psi_k \mathbf{H}_{k-i}^H \mathbf{C}_{k-i}^H \mathbf{Q}_{k-i} \mathbf{Q}_k^H \right) \Big|_{i \neq 0} \quad (\text{A.42})$$

$$\delta_2 = \sum_{i'=1}^{N-1} \text{Re tr} \left(\Psi_k \mathbf{H}_{k-i'}^H \mathbf{C}_k^H \right) = (N-1) \text{Re tr} \left(\Psi_k \mathbf{H}_k^H \mathbf{C}_k^H \right). \quad (\text{A.43})$$

Hence, the cross-correlation for Ψ_k is

$$\begin{aligned}
\Phi_0 &= E[\delta_1 \delta_2] \\
&= (N-1) N_0 (|h_{1,1}|^2 + |h_{2,1}|^2) \sum_{i=0}^{N-1} \text{Re tr} (\mathbf{C}_k \mathbf{C}_{k-i}^H \mathbf{Q}_{k-i} \mathbf{Q}_k^H) \Big|_{i \neq 0} \\
&= (N-1) N_0 (|h_{1,1}|^2 + |h_{2,1}|^2) \sum_{i=0}^{N-1} \text{Re tr} (\mathbf{D}_k \mathbf{D}_{k-1} \dots \mathbf{D}_{k-i+1}) \Big|_{i \neq 0} \quad (\text{A.44})
\end{aligned}$$

For Ψ_{k-1} , the cross-correlation terms may be obtained by $j = 1, i = 2, 3 \dots N-1$ and $j = 0, i = 1$, and has a total of $N-1$ terms. Hence

$$\begin{aligned}
\delta_1 &= \sum_{i=2}^{N-1} \text{Re tr} (\Psi_{k-1} \mathbf{H}_{k-i}^H \mathbf{C}_{k-i}^H \mathbf{Q}_{k-i} \mathbf{Q}_{k-1}^H) + \text{Re tr} (\mathbf{C}_k \mathbf{H}_k \Psi_{k-1}^H \mathbf{Q}_{k-1} \mathbf{Q}_k^H) \\
&= \sum_{i=2}^{N-1} \text{Re tr} (\Psi_{k-1} \mathbf{H}_{k-i}^H \mathbf{C}_{k-i}^H \mathbf{Q}_{k-i} \mathbf{Q}_{k-1}^H) + \text{Re tr} (\Psi_{k-1} \mathbf{H}_k^H \mathbf{C}_k^H \mathbf{Q}_k \mathbf{Q}_{k-1}^H) \\
&= \sum_{i=0}^{N-1} \text{Re tr} (\Psi_{k-1} \mathbf{H}_k^H \mathbf{C}_{k-i}^H \mathbf{Q}_{k-i} \mathbf{Q}_{k-1}^H) \Big|_{i \neq 1}, \quad (\text{A.45})
\end{aligned}$$

and

$$\begin{aligned}
\delta_2 &= \sum_{i'=1}^{N-1} \sum_{j'=0}^{i'-1} \text{Re tr} (\mathbf{H}_k \Psi_{k-i'}^H \mathbf{C}_{k-i'}^H + \Psi_{k-j} \mathbf{H}_k^H \mathbf{C}_{k-j'}^H) \\
&= \text{Re tr} (\mathbf{H}_k \Psi_{k-1}^H \mathbf{C}_{k-1}^H) + (N-2) \text{Re tr} (\Psi_{k-1} \mathbf{H}_k^H \mathbf{C}_{k-1}^H) \\
&= (N-1) \text{Re tr} (\Psi_{k-1} \mathbf{H}_k^H \mathbf{C}_{k-1}^H). \quad (\text{A.46})
\end{aligned}$$

The cross-correlation for Ψ_{k-1} is

$$\begin{aligned}
\Phi_1 &= E[\delta_1 \delta_2] \\
&= N_0 (N-1) (|h_{1,1}|^2 + |h_{2,1}|^2) \sum_{i=0}^{N-1} \text{Re tr} (\mathbf{C}_k \mathbf{C}_{k-i}^H \mathbf{Q}_{k-i} \mathbf{Q}_k^H) \Big|_{i \neq 1} \\
&= N_0 (N-1) (|h_{1,1}|^2 + |h_{2,1}|^2) * \\
&\quad \left(\text{Re tr} (\mathbf{D}_k) + \sum_{i=2}^{N-1} \text{Re tr} (\mathbf{D}_{k-1} \mathbf{D}_{k-2} \dots \mathbf{D}_{k-i+1}) \right) \Big|_{i \neq 1} \quad (\text{A.47})
\end{aligned}$$

For Ψ_{k-2} , the cross-correlation terms can be obtained by $j = 2, i = 3, 4 \dots N - 1$ and $i = 2, j = 0, 1$. Hence

$$\begin{aligned}
 \delta_1 &= \sum_{i=3}^{N-1} \text{Re tr} (\Psi_{k-2} \mathbf{H}_{k-i}^H \mathbf{C}_{k-i}^H \mathbf{Q}_{k-i} \mathbf{Q}_{k-2}^H) + \sum_{j=0}^1 \text{Re tr} (\mathbf{C}_{k-j} \mathbf{H}_{k-j} \Psi_{k-2}^H \mathbf{Q}_{k-2} \mathbf{Q}_{k-j}^H) \\
 &= \sum_{i=3}^{N-1} \text{Re tr} (\Psi_{k-2} \mathbf{H}_{k-i}^H \mathbf{C}_{k-i}^H \mathbf{Q}_{k-i} \mathbf{Q}_{k-2}^H) + \sum_{i=0}^1 \text{Re tr} (\Psi_{k-2} \mathbf{H}_{k-i}^H \mathbf{C}_{k-i}^H \mathbf{Q}_{k-i} \mathbf{Q}_{k-2}^H) \\
 &= \sum_{i=0}^{N-1} \text{Re tr} (\Psi_{k-2} \mathbf{H}_{k-i}^H \mathbf{C}_{k-i}^H \mathbf{Q}_{k-i} \mathbf{Q}_{k-2}^H) \Big|_{i \neq 2}, \tag{A.48}
 \end{aligned}$$

and

$$\begin{aligned}
 \delta_2 &= \sum_{i'=1}^{N-1} \sum_{j'=0}^{i'-1} \text{Re tr} (\mathbf{H}_k \Psi_{k-i'}^H \mathbf{C}_{k-i'} + \Psi_{k-j} \mathbf{H}_k^H \mathbf{C}_{k-j}^H) \\
 &= 2 \text{Re tr} (\mathbf{H}_k \Psi_{k-2}^H \mathbf{C}_{k-2}) + (N-3) \text{Re tr} (\Psi_{k-2} \mathbf{H}_k^H \mathbf{C}_{k-2}^H) \\
 &= (N-1) \text{Re tr} (\Psi_{k-2} \mathbf{H}_k^H \mathbf{C}_{k-2}^H).
 \end{aligned}$$

Thus, the cross-correlation is

$$\begin{aligned}
 \Phi_2 &= E [\delta_1 \delta_2] \\
 &= N_0 (|h_{1,1}|^2 + |h_{2,1}|^2) \sum_{i=0}^{N-1} \text{Re tr} (\mathbf{C}_{k-i}^H \mathbf{C}_{k-j} \mathbf{Q}_{k-i} \mathbf{Q}_{k-j}^H) \Big|_{i \neq 2} \\
 &= N_0 (N-1) (|h_{1,1}|^2 + |h_{2,1}|^2) \left(\sum_{i=0}^1 \text{Re tr} (\mathbf{D}_{k-i} \mathbf{D}_{k-i-1} \dots \mathbf{D}_{k-1}) + \right. \\
 &\quad \left. \sum_{i=3}^{N-1} \text{Re tr} (\mathbf{D}_{k-2} \mathbf{D}_{k-3} \dots \mathbf{D}_{k-i+1}) \right) \Big|_{i \neq 2}. \tag{A.49}
 \end{aligned}$$

For Ψ_{k-N+1} , there are two cases, $i = N-1, j = 0, 1, N-2$. Hence

$$\delta_1 = \sum_{j=0}^{N-1} \text{Re tr} (\mathbf{C}_{k-j} \mathbf{H}_{k-j} \Psi_{k-N+1}^H \mathbf{Q}_{k-N+1} \mathbf{Q}_{k-j}^H) \Big|_{i \neq N-1}, \tag{A.50}$$

$$\begin{aligned}
 \delta_2 &= \sum_{i'=1}^{N-1} \sum_{j'=0}^{i'-1} \text{Re tr} (\mathbf{H}_k \Psi_{k-i'}^H \mathbf{C}_{k-i'} + \Psi_{k-j} \mathbf{H}_k^H \mathbf{C}_{k-j}^H) \\
 &= \sum_{j'=0}^{N-2} \text{Re tr} (\mathbf{H}_k \Psi_{k-N+1}^H \mathbf{C}_{k-N+1}), \tag{A.51}
 \end{aligned}$$

and

$$\begin{aligned}
\Phi_{N-1} &= E[\delta_1 \delta_2] \\
&= N_0(N-1)(|h_{1,1}|^2 + |h_{2,1}|^2) \sum_{i=0}^{N-1} \text{Re tr}(\mathbf{C}_{k-i}^H \mathbf{C}_{k-j} \mathbf{Q}_{k-i} \mathbf{Q}_{k-j}^H) \Big|_{i \neq N-1} \\
&= N_0(N-1)(|h_{1,1}|^2 + |h_{2,1}|^2) * \\
&\quad \left(\sum_{i=0}^{N-2} \text{Re tr}(\mathbf{D}_{k-i} \mathbf{D}_{k-i-1} \dots \mathbf{D}_{k-N+2}) \right) \Big|_{i \neq N-1} \tag{A.52}
\end{aligned}$$

Therefore,

$$\begin{aligned}
\Phi &= \Phi_0 + \Phi_1 + \dots \Phi_{N-1} \\
&= N_0(N-1)(|h_{1,1}|^2 + |h_{2,1}|^2) \left\{ \sum_{i=0}^{N-1} \text{Re tr}(\mathbf{D}_k \mathbf{D}_{k-1} \dots \mathbf{D}_{k-i+1}) \Big|_{i \neq 0} \right. \\
&\quad + \left(\text{Re tr}(\mathbf{D}_k) + \sum_{i=2}^{N-1} \text{Re tr}(\mathbf{D}_{k-1} \mathbf{D}_{k-2} \dots \mathbf{D}_{k-i+1}) \right) \Big|_{i \neq 1} \\
&\quad + \left(\sum_{i=0}^1 \text{Re tr}(\mathbf{D}_{k-i} \mathbf{D}_{k-i-1} \dots \mathbf{D}_{k-1}) + \sum_{i=3}^{N-1} \text{Re tr}(\mathbf{D}_{k-2} \mathbf{D}_{k-3} \dots \mathbf{D}_{k-i+1}) \right) \Big|_{i \neq 2} \\
&\quad \left. + \dots + \left(\sum_{i=0}^{N-2} \text{Re tr}(\mathbf{D}_{k-i} \mathbf{D}_{k-i-1} \dots \mathbf{D}_{k-N+2}) \right) \Big|_{i \neq N-1} \right\} \\
&= 2(N-1)N_0(|h_{1,1}|^2 + |h_{2,1}|^2) * \\
&\quad \text{Re tr} \left\{ \sum_{i=1}^{N-1} \sum_{j=0}^{i-1} (\mathbf{D}_{k-j} \mathbf{D}_{k-j-1} \dots \mathbf{D}_{k-i+1}) \right\} \tag{A.53}
\end{aligned}$$

Finally, substituting Expression (A.36) and (A.37) into Equation (A.4), Expression (3.45) is obtained.

APPENDIX B

THE MINIMUM MSDD DISTANCE OF ρ FOR N BLOCKS

For BPSK messages, the constellation of S_k is

$$\left\{ \begin{bmatrix} 1/\sqrt{2} & 1/\sqrt{2} \\ -1/\sqrt{2} & 1/\sqrt{2} \end{bmatrix}, \begin{bmatrix} 1/\sqrt{2} & -1/\sqrt{2} \\ 1/\sqrt{2} & 1/\sqrt{2} \end{bmatrix}, \begin{bmatrix} -1/\sqrt{2} & 1/\sqrt{2} \\ -1/\sqrt{2} & -1/\sqrt{2} \end{bmatrix}, \begin{bmatrix} -1/\sqrt{2} & -1/\sqrt{2} \\ 1/\sqrt{2} & -1/\sqrt{2} \end{bmatrix} \right\}. \quad (\text{B.1})$$

If message matrix S_ζ is transmitted only, where

$$S_\zeta = \begin{bmatrix} 1/\sqrt{2} & 1/\sqrt{2} \\ -1/\sqrt{2} & 1/\sqrt{2} \end{bmatrix}, \quad (\text{B.2})$$

the constellation of D_k is

$$\left\{ \begin{bmatrix} 1 & 0 \\ 0 & 1 \end{bmatrix}, \begin{bmatrix} 0 & -1 \\ 1 & 0 \end{bmatrix}, \begin{bmatrix} 0 & 1 \\ -1 & 0 \end{bmatrix}, \begin{bmatrix} -1 & 0 \\ 0 & -1 \end{bmatrix} \right\}. \quad (\text{B.3})$$

Therefore, the constellation of $\text{Re tr}(\mathbf{I}_2 - \mathbf{D}_k)$ is $\{0, 2, 4\}$, which represents no-symbol error, one-symbol error and two-symbol error respectively. Note that the MSDD distance between message matrices $\mathbf{S}_k, \mathbf{S}_{k-1}, \dots, \mathbf{S}_{k-N+2}$ to error message matrices $\mathbf{E}_k, \mathbf{E}_{k-1}, \dots, \mathbf{E}_{k-N+2}$ is defined in Expression (3.42).

B.1 Two Blocks

For $N = 2$, there is only one transmitted message matrix \mathbf{S}_k , so

$$\rho = \text{Re tr} \{ \mathbf{I}_2 - \mathbf{D}_k \}. \quad (\text{B.4})$$

If error happens, for one-symbol error, $\rho = 2$, and for two-symbol error $\rho = 4$, hence

$$\rho_{\min} = 2(N - 1) = 2.$$

B.2 Three Blocks

For $N = 3$, there are two transmitted matrices $\mathbf{S}_k, \mathbf{S}_{k-1}$, therefore,

$$\rho = \text{Re tr} \{ \mathbf{I}_2 - \mathbf{D}_k + \mathbf{I}_2 - \mathbf{D}_{k-1} + \mathbf{I}_2 - \mathbf{D}_k \mathbf{D}_{k-1} \}. \quad (\text{B.5})$$

If error definitely happens, then

1-sym. error	$\text{Re tr} (\mathbf{D}_k) = 0$	$\text{Re tr} (\mathbf{D}_{k-1}) = 2$	$\rho_{\min} = 4$
1-sym. error	$\text{Re tr} (\mathbf{D}_k) = 2$	$\text{Re tr} (\mathbf{D}_{k-1}) = 0$	$\rho_{\min} = 4$
2-sym., $D_k \neq D_{k-1}$	$\text{Re tr} (\mathbf{D}_k) = 0$	$\text{Re tr} (\mathbf{D}_{k-1}) = 0$	$\rho_{\min} = 4$
2-sym., $D_k = D_{k-1}$	$\text{Re tr} (\mathbf{D}_k) = 0$	$\text{Re tr} (\mathbf{D}_{k-1}) = 0$	$\rho = 8$
3-sym. error	$\text{Re tr} (\mathbf{D}_k) = 0$	$\text{Re tr} (\mathbf{D}_{k-1}) = -2$	$\rho = 8$
3-sym. error	$\text{Re tr} (\mathbf{D}_k) = -2$	$\text{Re tr} (\mathbf{D}_{k-1}) = 0$	$\rho = 8$
4-sym. error	$\text{Re tr} (\mathbf{D}_k) = -2$	$\text{Re tr} (\mathbf{D}_{k-1}) = -2$	$\rho = 8$

Obviously, for this case

$$\rho_{\min} = 2(N - 1) = 4 \quad (\text{B.6})$$

B.3 N Blocks

For an observation interval of N blocks, there are $N - 1$ message matrices $S_k, S_{k-1}, \dots, S_{k-N+2}$, so there are $N - 1$ code distance matrices $D_k, D_{k-1}, \dots, D_{k-N+2}$.

B.3.1 One-symbol error

For one-symbol error, only one message matrix has one-symbol error and all other message matrices are correct. If the error matrix is $S_{k-\xi}$, ($0 \leq \xi \leq N - 2$), then $\text{Re tr} (\mathbf{D}_{k-\xi}) = 0$, and $\mathbf{D}_{k-i} = \mathbf{I}_2$, $0 \leq i \leq N - 2$ but $i \neq \xi$.

If S_k or S_{k-N+2} is in error, then

$$\begin{aligned}\rho &= \text{Re tr} \left\{ \sum_{i=1}^{N-1} \sum_{j=0}^{i-1} (\mathbf{I}_2 - \mathbf{D}_{k-j} \mathbf{D}_{k-j-1} \dots \mathbf{D}_{k-i+1}) \right\} \\ &= \text{Re tr} \left\{ \sum_{i=1}^{N-1} (\mathbf{I}_2 - \mathbf{D}_k) \right\} = 2(N-1).\end{aligned}\tag{B.7}$$

If S_{k-1} or S_{k-N+3} is in error, then

$$\begin{aligned}\rho &= \text{Re tr} \left\{ \sum_{i=1}^{N-1} \sum_{j=0}^{i-1} (\mathbf{I}_2 - \mathbf{D}_{k-j} \mathbf{D}_{k-j-1} \dots \mathbf{D}_{k-i+1}) \right\} \\ &= \text{Re tr} (\mathbf{I}_2 - \mathbf{D}_k) + 2 \text{Re tr} \left\{ \sum_{i=2}^{N-2} (\mathbf{I}_2 - \mathbf{D}_k) \right\} + \text{Re tr} (\mathbf{I}_2 - \mathbf{D}_k) \\ &= 4(N-2) > 2(N-1).\end{aligned}\tag{B.8}$$

If S_{k-2} or S_{k-N+4} is in error, then

$$\begin{aligned}\rho &= \text{Re tr} \left\{ \sum_{i=1}^{N-1} \sum_{j=0}^{i-1} (\mathbf{I}_2 - \mathbf{D}_{k-j} \mathbf{D}_{k-j-1} \dots \mathbf{D}_{k-i+1}) \right\} \\ &= \text{Re tr} (\mathbf{I}_2 - \mathbf{D}_{k-2}) + 2 \text{Re tr} (\mathbf{I}_2 - \mathbf{D}_{k-2}) + 3 \text{Re tr} \left\{ \sum_{i=3}^{N-3} (\mathbf{I}_2 - \mathbf{D}_{k-2}) \right\} \\ &\quad + 2 \text{Re tr} (\mathbf{I}_2 - \mathbf{D}_{k-2}) + \text{Re tr} (\mathbf{I}_2 - \mathbf{D}_{k-2}) \\ &= 6(N-3) > 4(N-2).\end{aligned}\tag{B.9}$$

If S_{k-i} or $S_{k-N+2+i}$ ($i \geq 3$) is in error,

$$\rho > \dots > 6(N-3) > 4(N-2) > 2(N-1).\tag{B.10}$$

Obviously, for one-symbol error

$$\rho_{\min} = 2(N-1).\tag{B.11}$$

B.3.2 Two-symbol error

For two-symbol error, there are two cases: two-symbol error in one matrix or two-symbol error in two different matrices.

Two-symbol error in one block For this case, two-symbol error happens in one matrix and there is no error in other matrices. If the error matrix is $S_{k-\xi}$, ($0 \leq \xi \leq N-2$), then $\text{Re tr}(\mathbf{D}_{k-\xi}) = -2$, and $\mathbf{D}_{k-i} = \mathbf{I}_2$, $0 \leq i \leq N-2$ but $i \neq \xi$.

If S_k or S_{k-N+2} is in error, then

$$\begin{aligned} \rho &= \text{Re tr} \left\{ \sum_{i=1}^{N-1} \sum_{j=0}^{i-1} (\mathbf{I}_2 - \mathbf{D}_{k-j} \mathbf{D}_{k-j-1} \dots \mathbf{D}_{k-i+1}) \right\} \\ &= \text{Re tr} \left\{ \sum_{i=1}^{N-1} (\mathbf{I}_2 - \mathbf{D}_k) \right\} = 4(N-1). \end{aligned} \quad (\text{B.12})$$

If S_{k-1} or S_{k-N+3} is wrong, then

$$\begin{aligned} \rho &= \text{Re tr} \left\{ \sum_{i=1}^{N-1} \sum_{j=0}^{i-1} (\mathbf{I}_2 - \mathbf{D}_{k-j} \mathbf{D}_{k-j-1} \dots \mathbf{D}_{k-i+1}) \right\} \\ &= \text{Re tr}(\mathbf{I}_2 - \mathbf{D}_k) + 2 \text{Re tr} \left\{ \sum_{i=2}^{N-2} (\mathbf{I}_2 - \mathbf{D}_k) \right\} + \text{Re tr}(\mathbf{I}_2 - \mathbf{D}_k) \\ &= 8(N-2) > 4(N-1). \end{aligned} \quad (\text{B.13})$$

If S_{k-i} or $S_{k-N+2+i}$ ($i \geq 2$) is in error,

$$\rho > \dots > 8(N-2) > 4(N-1). \quad (\text{B.14})$$

Obviously, for this case

$$\rho_{\min} = 4(N-1). \quad (\text{B.15})$$

Two-symbol error in two different blocks For this case, two-symbol error happens in two different matrices and there is no error in other matrices. If the two error matrices are $S_{k-\xi}$, $S_{k-\eta}$ ($0 \leq \xi \leq \eta \leq N-2$), then $\text{Re tr}(\mathbf{D}_{k-\xi}) = 0$, $\text{Re tr}(\mathbf{D}_{k-\eta}) = 0$, and $\mathbf{D}_{k-i} = \mathbf{I}_2$, $0 \leq i \leq N-2$ but $i \neq \xi, \eta$.

If S_k and S_{k-1} are in error, and E_k and E_{k-1} are different, then

$$\begin{aligned}\rho &= \text{Re tr} \left\{ \sum_{i=1}^{N-1} \sum_{j=0}^{i-1} (\mathbf{I}_2 - \mathbf{D}_{k-j} \mathbf{D}_{k-j-1} \dots \mathbf{D}_{k-i+1}) \right\} \\ &= \text{Re tr} \left\{ \sum_{i=1}^{N-1} (\mathbf{I}_2 - \mathbf{D}_k) \right\} = 2(N-1).\end{aligned}\tag{B.16}$$

If S_k and S_{k-1} are in error, and E_k and E_{k-1} are the same, then

$$\begin{aligned}\rho &= \text{Re tr} \left\{ \sum_{i=1}^{N-1} \sum_{j=0}^{i-1} (\mathbf{I}_2 - \mathbf{D}_{k-j} \mathbf{D}_{k-j-1} \dots \mathbf{D}_{k-i+1}) \right\} \\ &= 4(N-1).\end{aligned}\tag{B.17}$$

For other cases,

$$\rho > \dots > 4(N-1) > 2(N-1).\tag{B.18}$$

Obviously, for this case

$$\rho_{\min} = 2(N-1).\tag{B.19}$$

B.3.3 Three-symbol error or more errors

For three-symbol error or more errors, it can be shown that $\rho > 2(N-1)$. Finally,

$$\rho_{\min} = 2(N-1).\tag{B.20}$$

APPENDIX C

PROPERTIES OF THE MSDD DISTANCE ρ

The pairwise error probability is

$$\begin{aligned} P_{\text{pw}} &= \frac{1}{2} \left[1 - \mu - \frac{1}{2} \mu (1 - \mu^2) \right] \\ &= \frac{1}{2} - \frac{3}{4} \mu + \frac{1}{4} \mu^3, \end{aligned} \tag{C.1}$$

where

$$\mu = \sqrt{\frac{(\rho/2N)\gamma}{(\rho/2N)\gamma + 2}}. \tag{C.2}$$

Let $a = \rho\gamma/2N$, then

$$\begin{aligned} \mu &= \sqrt{\frac{a}{a+2}} \\ &= \sqrt{\frac{1}{1+2/a}} \\ &= \left(1 + \frac{2}{a}\right)^{-\frac{1}{2}} \\ &\simeq 1 - \frac{1}{a} \text{ for } a \gg 1. \end{aligned} \tag{C.3}$$

Hence

$$\begin{aligned} P_{\text{pw}} &= \frac{1}{2} - \frac{3}{4} \mu + \frac{1}{4} \mu^3 \\ &= \frac{1}{2} - \frac{1}{4} \mu (3 - \mu^2) \\ &= \frac{1}{2} - \frac{1}{4} \mu \left(3 - \frac{a}{a+2}\right) \\ &= \frac{1}{2} - \frac{1}{4} \mu \left(3 - \frac{1}{1+2/a}\right) \\ &\simeq \frac{1}{2} - \frac{1}{4} \mu [3 - (1 - 2/a)]. \end{aligned} \tag{C.4}$$

If $a \gg 1$, then

$$\begin{aligned}
 P_{\text{pw}} &\simeq \frac{1}{2} - \frac{1}{4} \left(1 - \frac{1}{a} \right) (2 + 2/a) \\
 &\simeq \frac{1}{2a^2} \\
 &\simeq \frac{1}{2 \left(\frac{\gamma}{2N} \right)^2} \frac{1}{\rho^2}.
 \end{aligned} \tag{C.5}$$

Since $\rho_{\min} = 2(N-1)$ [Appendix B], when N and γ are large enough and fixed,

$$a_{\min} = \frac{\rho_{\min} \gamma}{2N} = \frac{2(N-1)\gamma}{2N} \gg 1. \tag{C.6}$$

Hence,

$$P_{\text{pw}} \sim \frac{1}{\rho^2}. \tag{C.7}$$

APPENDIX D

APPROXIMATE BER FOR DIFFERENTIAL STBC WITH COHERENT DETECTION

Based on decision metric (3.9), the decision value for a correct decision can be expressed as

$$\zeta_c = \text{Re tr} \{ \mathbf{H}_k^H \mathbf{C}_{k-1}^H \mathbf{S}_k \mathbf{R}_k + \mathbf{H}_{k-1}^H \mathbf{C}_{k-1}^H \mathbf{R}_{k-1} \}, \quad (\text{D.1})$$

and the decision value for an erroneous decision can be obtained from

$$\zeta_e = \text{Re tr} \{ \mathbf{H}_k^H \mathbf{Q}_{k-1}^H \mathbf{E}_k \mathbf{R}_k + \mathbf{H}_{k-1}^H \mathbf{Q}_{k-1}^H \mathbf{R}_{k-1} \}. \quad (\text{D.2})$$

where

$$\mathbf{R}_{k-1} = \mathbf{C}_{k-1} \mathbf{H}_{k-1} + \mathbf{N}_{k-1}, \quad (\text{D.3})$$

$$\mathbf{R}_k = \mathbf{C}_{k-1} \mathbf{S}_k \mathbf{H}_k + \mathbf{N}_k. \quad (\text{D.4})$$

Moreover, \mathbf{Q}_{k-1} and \mathbf{E}_k are the erroneous matrices of \mathbf{C}_{k-1} and \mathbf{S}_k respectively.

Let $\Delta_2 = \zeta_e - \zeta_c$. Since Δ_2 can be simplified as an approximately Gaussian variable, similar to Δ in Equation (3.41), its mean and variance are

$$E[\Delta_2] = -E_s (|h_1|^2 + |h_2|^2) \rho_2, \quad (\text{D.5})$$

$$\text{Var}[\Delta_2] = 2E_s \rho_2 (|h_1|^2 + |h_2|^2) N_0, \quad (\text{D.6})$$

where

$$\rho_2 = \text{Re tr} \{ 2\mathbf{I}_2 - \mathbf{D}_{k-1} \mathbf{D}_k - \mathbf{D}_{k-1} \}, \quad (\text{D.7})$$

and $\mathbf{D}_k = \mathbf{E}_k \mathbf{S}_k^\dagger$, $\mathbf{D}_{k-1} = \mathbf{Q}_{k-1} \mathbf{C}_{k-1}^\dagger$. Note that it is assumed that \mathbf{C}_{k-1} and \mathbf{S}_k have the same constellation here, so \mathbf{D}_{k-1} and \mathbf{D}_k must also have the same constellation.

Using Equation (3.39),

$$\begin{aligned}
 P(\mathbf{S} \longrightarrow \mathbf{E}|\mathbf{S}) &= P(\eta_e - \eta_c > 0|\mathbf{S}) \\
 &= P(\Delta_2 > 0) \\
 &= Q\left(\sqrt{\gamma\rho_2(|h_1|^2 + |h_2|^2)/2}\right).
 \end{aligned} \tag{D.8}$$

Using the same approach in Section 3.4, the closed-form pairwise probability for differential STBC with coherent detection can be obtained as

$$P_r(\mathbf{S} \longrightarrow \mathbf{E}|\mathbf{S})_{coh} = \frac{1}{2} \left[1 - \mu_{coh} - \frac{1}{2} \mu_{coh} (1 - \mu_{coh}^2) \right], \tag{D.9}$$

where

$$\mu_{coh} = \sqrt{\frac{(\rho_2/2)\gamma}{(\rho_2/2)\gamma + 2}}. \tag{D.10}$$

Assuming that BSPK message is employed, there are then a total of 4 information bits for an observation interval of two blocks with coherent detection. Since an approximate BER is dominated by the minimum value of ρ_2 , which is 2 here, and there are two options for one-symbol error and two options for three-symbol error, based on Equation (3.54), the approximate BER can be expressed as

$$\begin{aligned}
 P_b &\simeq \frac{1*2}{4}P_b^{(1)} + \frac{3*2}{4}P_b^{(3)} \\
 &= \frac{1}{2} * \frac{1}{2} \left[1 - \mu_{coh} - \frac{1}{2} \mu_{coh} (1 - \mu_{coh}^2) \right] \\
 &\quad + \frac{3}{2} * \frac{1}{2} \left[1 - \mu_{coh} - \frac{1}{2} \mu_{coh} (1 - \mu_{coh}^2) \right] \\
 &= 2 * \frac{1}{2} \left[1 - \mu_{coh} - \frac{1}{2} \mu_{coh} (1 - \mu_{coh}^2) \right],
 \end{aligned} \tag{D.11}$$

where

$$\mu_{coh} = \sqrt{\frac{\gamma}{\gamma + 2}}. \tag{D.12}$$

APPENDIX E

LCR AND AFD IN MIMO MOBILE FADING CHANNELS

E.1 Introduction

The concepts of level crossing rate (LCR) and average fade durations (AFD) for MIMO fading channels have not yet been defined and analyzed, and most of the LCR- and AFD-related research has been carried out in the context of SISO systems. The recent works on LCR and AFD for receive diversity combiners [48] [49] [50], which eventually boil down to the crossing theory of a scalar process, appear in MIMO channels, as what will see in the sequel. However, in general, for an M -transmit N -receive multiantenna system, the joint dynamic behavior of MN correlated random signals is of interest (which has not been addressed in the literature). This requires a multidimensional approach to LCR and AFD problems.

To show the utility of the theoretical results derived in this chapter, adaptive modulation, Markov modeling, the block fading model, and the concept of vector AFD in MIMO systems are briefly discussed. In the first two cases, there is a scalar crossing problem, whereas the last two require a vector crossing approach.

E.2 Scalar Crossing in MIMO Systems

In this section, first the mathematical formulation of the problem and its solution is presented, followed by a numerical example. Then the applications are highlighted.

E.2.1 Mathematical Formulation

Consider a time-selective narrowband $M \times N$ channel, with MN complex Gaussian processes, correlated in both space and time, and corrupted by a spatio-temporal white Gaussian noise. Obviously, depending on the presence or absence of line-of-sight (LOS), the envelope of subchannels could be Rice or Rayleigh, respectively. The

instantaneous received signal-to-noise ratio (SNR) per symbol over the subchannel from the p -th transmitter to the l -th receiver is proportional to $|h_{lp}(t)|^2$, assuming perfect channel estimation at the receiver. The total instantaneous received SNR per symbol, $\gamma(t)$, is therefore proportional to $\sum_{l,p} |h_{lp}(t)|^2$, and is a useful measure for Markov modeling of diversity systems [51], MIMO channel characterization [52] [53], and design of MIMO systems [54] [55].

Now it is desired to determine the average stay duration (ASD) of $\gamma(t)$ within the region $[\gamma_1, \gamma_2]$, $ASD\{\gamma(t), [\gamma_1, \gamma_2]\}$, defined as the average time over which $\gamma_1 \leq \gamma(t) \leq \gamma_2$. The concept of ASD is applicable to both scalar processes such as $\gamma(t)$, as well as vector processes, discussed later, and includes AFD as the special case where $\gamma_1 = -\infty$. Similar to AFD, the ASD of $\gamma(t)$ within the region $[\gamma_1, \gamma_2]$ can be calculated by

$$ASD\{\gamma(t), [\gamma_1, \gamma_2]\} = \frac{\Pr[\gamma_1 \leq \gamma(t) \leq \gamma_2]}{ICR\{\gamma(t), [\gamma_1, \gamma_2]\}} \quad (E.1)$$

where $\Pr[\cdot]$ is the probability and the denominator is the incrossing rate (ICR), i.e., the average number of times that crosses one of the two borders and enters the region $[\gamma_1, \gamma_2]$. The numerator can be calculated via the Euler method [56]. For the denominator the result of Hasofer's paper [57] is used.

Specifically, let $x(t) = \sum_{i=1}^J u_i^2(t)$, where $u_i(t)$ s are correlated nonzero mean real Gaussian processes. Also let $\mathbf{u} = [u_1 \ u_2 \ \dots \ u_J]^T$ and $\mathbf{u}' = [u'_1 \ u'_2 \ \dots \ u'_J]^T$, where prime denotes differentiation with respect to time t and $'^T$ is the transpose operator. The mean vector and the covariance matrix of $[\mathbf{u}^T \ \mathbf{u}'^T]$ are respectively given by

$$\Gamma = [\eta^T \ \mathbf{0}^T]^T, \quad (E.2)$$

$$\Sigma = \begin{bmatrix} \Sigma_{11} & \Sigma_{12} \\ \Sigma_{21} & \Sigma_{22} \end{bmatrix}, \quad (E.3)$$

where η is a $J \times 1$ vector, $\mathbf{0}$ is a $J \times 1$ zero vector, and $\Sigma_{21} = \Sigma_{12}^T$. The following transformations are also needed:

$$u_1 = \sqrt{x} \cos(\theta_1) \dots \cos(\theta_J), \quad (\text{E.4})$$

$$u_2 = \sqrt{x} \cos(\theta_1) \dots \cos(\theta_{J-2}) \cos(\theta_{J-1}), \quad (\text{E.5})$$

$$\vdots$$

$$u_i = \sqrt{x} \cos(\theta_1) \dots \cos(\theta_{J-1}) \cos(\theta_{J-i+1}), \quad (\text{E.6})$$

$$\vdots$$

$$u_J = \sqrt{x} \cos(\theta_1), \quad (\text{E.7})$$

where $\theta_1 \in [-\pi/2, \pi/2)$, $i = 1, 2, \dots, J-2$, and $\theta_{J-1} \in [0, 2\pi)$. Then the upcrossing rate (UCR) of $x(t)$ with respect to the threshold x_0 can be written as [57]

$$\begin{aligned} UCR\{x(t), x_0\} &= (2\pi)^{-(J+1)/2} [\det(\Sigma_{11})]^{-1/2} x_0^{(J-2)/2} \\ &\times \int_{-\pi/2}^{\pi/2} \dots \int_{-\pi/2}^{\pi/2} \int_0^{2\pi} \left\{ \sigma \exp\left(\frac{-\theta^2}{2\sigma^2}\right) + (2\pi)^{1/2} \vartheta \left[1 - \Phi\left(\frac{-\vartheta}{\sigma}\right) \right] \right\} \\ &\times \exp\left[-\frac{1}{2} A(x_0, \theta_1, \dots, \theta_{J-1})\right] B(\theta_1, \dots, \theta_{J-2}) d\theta_1 \dots d\theta_{J-1}, \quad (\text{E.8}) \end{aligned}$$

where $\det(\cdot)$ is the determinant and

$$\sigma^2 = 4\mathbf{u}^T (\Sigma_{22} - \Sigma_{21}\Sigma_{11}^{-1}\Sigma_{12}) \mathbf{u}, \quad (\text{E.9})$$

$$\vartheta = 2\mathbf{u}^T \Sigma_{21}\Sigma_{11}^{-1} (\mathbf{u} - \eta), \quad (\text{E.10})$$

$$\Phi(y) = (2\pi)^{-1/2} \int_{-\infty}^y \exp(-z^2/2) dz, \quad (\text{E.11})$$

$$A(x_0, \theta_1, \dots, \theta_{J-1}) = (\mathbf{u} - \eta)^T \Sigma_{11}^{-1} (\mathbf{u} - \eta), \quad (\text{E.12})$$

$$B(\theta_1, \dots, \theta_{J-2}) = \frac{1}{2} \cos^{J-2}(\theta_1) \cos^{J-3}(\theta_2) \dots \cos(\theta_{J-2}). \quad (\text{E.13})$$

When $u_i(t)$ s are identically-distributed and correlated zero-mean real Gaussian processes, a compact form is given in Lindgren's paper [58] for $UCR\{x(t), x_0\}$. Note that $DCR\{x(t), x_0\} = UCR\{x(t), x_0\}$, where DCR stands for the downcrossing rate.

Obviously, $ICR\{\gamma(t), [\gamma_1, \gamma_2]\} = UCR\{\gamma(t), \gamma_1\} + DCR\{\gamma(t), \gamma_2\}$. In an $M \times N$ MIMO system, $J = 2MN$. Therefore, to calculate $ICR\{\gamma(t), [\gamma_1, \gamma_2]\}$, two $(2MN - 1)$ -fold finite-range integrals need to be calculated. This could be very cumbersome even for a simple 2×2 system, which entails two seven-fold integrals. A technique, which has much less computational complexity, will be dissertationed in another paper.

E.2.2 Numerical Example

Consider a 2×1 Rayleigh channel, i.e., $M = 2$ and $N = 1$. Then total instantaneous received SNR per symbol is given by

$$\gamma(t) = (E_{av}/N_0) (|h_{11}|^2 + |h_{12}|^2), \quad (\text{E.14})$$

where E_{av}/N_0 is the average SNR per symbol. Let $E[|h_{11}|^2] = E[|h_{12}|^2] = 1$. Therefore the average received SNR per symbol over each subchannel is given by $\bar{\gamma}_{11} = E_s/N_0$. Now the total instantaneous received SNR per symbol is rewritten as

$$\gamma(t) = \bar{\gamma}_{11} (|h_{11}|^2 + |h_{12}|^2). \quad (\text{E.15})$$

The temporal autocorrelation is also defined

$$\rho_{11,11}(\tau) = E[h_{11}(t) h_{11}^*(t + \tau)] = \rho_{12,12}(\tau), \quad (\text{E.16})$$

and spatio-temporal crosscorrelation

$$\rho_{11,12}(\tau) = E[h_{11}(t) h_{12}^*(t + \tau)]. \quad (\text{E.17})$$

To calculate the AFD of $\gamma(t)$ below the threshold γ_{th} , $AFD\{\gamma(t), \gamma_{th}\}$, it is needed to calculate $\Pr[\gamma \leq \gamma_{th}]$ and $DCR\{\gamma(t), \gamma_{th}\}$. For the former the result given in Lee's

paper [59] is used, p. 368

$$\begin{aligned} Pr[\gamma \leq \gamma_{th}] &= 1 - (2|\zeta|)^{-1} [(1 + |\zeta|) \exp \{-\gamma_{th} [\bar{\gamma}_{11} (1 + |\zeta|)]^{-1}\} \\ &\quad - (1 - |\zeta|) \exp \{-\gamma_{th} [\bar{\gamma}_{11} (1 - |\zeta|)]^{-1}\}] \end{aligned} \quad (\text{E.18})$$

where $\zeta = \rho_{11,12}(0)$, and for the latter expression (E.8) is computed, numerically.

To compute Expression (E.8), $u_i(t)$ s are defined such that $h_{11}(t) = u_1(t) + ju_2(t)$ and $h_{12}(t) = u_3(t) + ju_4(t)$, in which $j^2 = -1$. For mathematical convenience, the vector \mathbf{u} is defined as $\mathbf{u} = [u_1 \ u_2 \ u_3 \ u_4]^T$. Such a definition makes Σ_{11} , Σ_{12} and Σ_{22} in Equation (E.3), block matrices. Due to Rayleigh fading $\eta = E[\mathbf{u}] = \mathbf{0}$. To build the covariance matrix in Equation (E.3), it is necessary to express $E[u_i(t)u_k(t+\tau)]$, $i, k = 1, \dots, 4$, in terms of $\rho_{11,11}(\tau)$ and $\rho_{11,12}(\tau)$. It is easy to verify that

$$E[u_i(t)u_i(t+\tau)] = \frac{1}{2} \text{Re}[\rho_{11,11}(\tau)], \quad i = 1, 2, \dots, 4, \quad (\text{E.19})$$

$$E[u_1(t)u_2(t+\tau)] = E[u_3(t)u_4(t+\tau)] = -\frac{1}{2} \text{Im}[\rho_{11,11}(\tau)], \quad (\text{E.20})$$

$$E[u_1(t)u_3(t+\tau)] = E[u_2(t)u_4(t+\tau)] = \frac{1}{2} \text{Re}[\rho_{11,12}(\tau)], \quad (\text{E.21})$$

$$E[u_1(t)u_4(t+\tau)] = -E[u_2(t)u_3(t+\tau)] = -\frac{1}{2} \text{Im}[\rho_{11,12}(\tau)], \quad (\text{E.22})$$

where $\text{Re}[\cdot]$ and $\text{Im}[\cdot]$ give the real and imaginary parts, respectively. In deriving the equations in (E.19)~(E.22), the class of widely-used rotation invariant [60] (also called proper [61]) complex random vectors and processes have been considered. This translates into

$$E[h_{11}^2(t)] = E[h_{12}^2(t)] = E[h_{11}(t)h_{12}(t)] = 0. \quad (\text{E.23})$$

Based on Equation (E.19)~(E.22), it is easy to construct Σ_{11} , which is a symmetric matrix. To calculate the elements of the other two covariance matrices in Equation

(E.3), define

$$R_{yz}(\tau) = E[y(t)z(t+\tau)], \quad (\text{E.24})$$

where $y(t)$ and $z(t)$ are two real processes. Then it is easy to verify [62]

$$E[y(t)z'(t+\tau)] = \dot{R}_{yz}(\tau) \quad (\text{E.25})$$

$$E[z(t)y'(t+\tau)] = \dot{R}_{zy}(\tau) = \dot{R}_{yz}(-\tau) \quad (\text{E.26})$$

$$E[y'(t)z'(t+\tau)] = -\ddot{R}_{yz}(\tau) \quad (\text{E.27})$$

where dot denotes differentiation with respect to τ . Based on Equation (E.25)~(E.27), Σ_{12} and Σ_{22} , antisymmetric and symmetric matrices are built, respectively, as follows

$$\Sigma_{12} = \frac{1}{2} \begin{bmatrix} \text{Re}[\dot{\xi}] & \text{Re}[\dot{\zeta}] & -\text{Im}[\dot{\xi}] & -\text{Im}[\dot{\zeta}] \\ -\text{Re}[\dot{\zeta}] & \text{Re}[\dot{\xi}] & -\text{Im}[\dot{\zeta}] & -\text{Im}[\dot{\xi}] \\ \text{Im}[\dot{\xi}] & \text{Im}[\dot{\zeta}] & \text{Re}[\dot{\xi}] & \text{Re}[\dot{\zeta}] \\ \text{Im}[\dot{\zeta}] & \text{Im}[\dot{\xi}] & -\text{Re}[\dot{\zeta}] & \text{Re}[\dot{\xi}] \end{bmatrix} \quad (\text{E.28})$$

$$\Sigma_{22} = \frac{1}{2} \begin{bmatrix} -\text{Re}[\ddot{\xi}] & -\text{Re}[\ddot{\zeta}] & \text{Im}[\ddot{\xi}] & \text{Im}[\ddot{\zeta}] \\ -\text{Re}[\ddot{\zeta}] & -\text{Re}[\ddot{\xi}] & -\text{Im}[\ddot{\zeta}] & \text{Im}[\ddot{\xi}] \\ \text{Im}[\ddot{\xi}] & -\text{Im}[\ddot{\zeta}] & -\text{Re}[\ddot{\xi}] & -\text{Re}[\ddot{\zeta}] \\ \text{Im}[\ddot{\zeta}] & \text{Im}[\ddot{\xi}] & -\text{Re}[\ddot{\zeta}] & -\text{Re}[\ddot{\xi}] \end{bmatrix} \quad (\text{E.29})$$

in which the shorthand notations $\dot{\xi} = \dot{\rho}_{11,11}(0)$, $\dot{\zeta} = \dot{\rho}_{11,12}(0)$, $\ddot{\xi} = \ddot{\rho}_{11,11}(0)$, $\ddot{\zeta} = \ddot{\rho}_{11,12}(0)$ have been used.

In the numerical example, the macrocell space-time correlation model of [9] is used. Macrocells are chosen because the correlation among subchannels is particularly high within macrocells, where the angle spread at the elevated base station (BS) is normally small, say, less than 10 degrees (see references in [33]), and the distribution

of angle of arrival (AOA) at the mobile station (MS) could be far from uniform [36] [63]. Both of these induce high nonnegligible correlations. For a 2×1 Rayleigh channel, Equation (12) of [33] yields these correlations

$$\rho_{11,11}(\tau) = [I_0(\kappa)]^{-1} I_0\left(\left\{\kappa^2 - 4\pi^2 f_D^2 \tau^2 - j4\pi\kappa \cos(\gamma_0 - \mu) f_D \tau\right\}^{1/2}\right) \quad (\text{E.30})$$

$$\begin{aligned} \rho_{11,12}(\tau) = & [I_0(\kappa)]^{-1} e^{j\cos(\alpha)2\pi\delta/\lambda} I_0\left(\left\{\kappa^2 - 4\pi^2 f_D^2 \tau^2 - j4\pi^2 (\delta/\lambda)^2 \Delta^2 \sin^2(\alpha) \right. \right. \\ & + 8\pi^2 (\delta/\lambda) f_D \tau \sin(\alpha) \sin(\gamma_0) \\ & \left. \left. - j2\kappa [2\pi f_D \tau \cos(\mu - \gamma_0) - 2\pi (\delta/\lambda) \Delta \sin(\alpha) \sin(\mu)]\right\}^{1/2}\right) \quad (\text{E.31}) \end{aligned}$$

where $I_0(\cdot)$ is the zero-order modified Bessel function, $\kappa \geq 0$ controls the angle spread at the MS, $\mu \in [-\pi, \pi)$ accounts for the mean direction of AOA at the MS, γ_0 is the direction of the motion of MS (not to be confused with SNR in this chapter), f_D denotes the maximum Doppler shift, α represents the direction of the BS array, λ is the wavelength, δ stands for the element spacing at the BS, and finally 2Δ is the spread of the angle of departure from the BS.

Consider the transmit BS array, where the two elements are spaced by δ , is perpendicular to the horizontal x axis, $\alpha = 90^\circ$, and the receive single MS antenna is moving on the x axis, towards the transmit array, $\gamma_0 = 180^\circ$, with a constant speed such $f_D = 20\text{Hz}$. The angle spread at the BS is $2\Delta = 4^\circ$, whereas at the MS is 66° , equivalent to $\kappa = 3$, around the mean AOA of $\mu = 36^\circ$ at the MS. The values κ of μ and are estimated from measured data [40]. In Figure E.1 and Figure E.2 the author has plotted the DCR and AFD of $\gamma(t)$ with respect to the threshold γ_{th} , obtained via Expression (E.8) and (E.18) divided by Expression (E.8), respectively, as a function of the normalized power threshold $\gamma_{th}/\bar{\gamma}_{11}$. In both figures, two BS element spacings of $\delta = \lambda$ and 5λ are considered, which correspond, respectively, to these spatial correlations: $|\zeta| = |\rho_{11,12}(0)| = 0.995$ and 0.886 . Close agreement between the simulation results, given in both figures for $\delta = 5\lambda$, and the theoretical curves

verifies the accuracy of the analytic calculations. The spatio-temporally correlated MIMO channel is simulated using the spectral representation method [64].

Also in Figure E.1 and Figure E.2 the DCR and AFD have been plotted if the spatial correlation is ignored, i.e., incorrect assumption of independent subchannels $h_{11}(t)$ and $h_{12}(t)$. To do this, Equation (15) and (17) of the paper [56] have been used, which after minor corrections result in

$$DCR\{\gamma(t), \gamma_{th}\} = \frac{1}{\sqrt{\pi}} \left(\frac{\gamma_{th}}{\bar{\gamma}_{11}} \right)^{3/2} \exp \left(\frac{-\gamma_{th}}{\bar{\gamma}_{11}} \right) \left(\frac{b_2}{b_0} - \frac{b_1^2}{b_0^2} \right)^{1/2}, \quad (\text{E.32})$$

$$AFD\{\gamma(t), \gamma_{th}\} = \frac{\sqrt{\pi} [\exp(\gamma_{th}/\bar{\gamma}_{11}) - 1 - (\gamma_{th}/\bar{\gamma}_{11})]}{(\gamma_{th}/\bar{\gamma}_{11})^{3/2}} \left(\frac{b_2}{b_0} - \frac{b_1^2}{b_0^2} \right)^{-1/2}, \quad (\text{E.33})$$

$$b_1/b_0 = 2\pi f_D \tau \cos(\mu) I_1(\kappa) [I_0(\kappa)]^{-1}, \quad (\text{E.34})$$

$$b_2/b_0 = 2\pi^2 f_D^2 [I_0(\kappa) + I_2(\kappa) \cos(2\mu)] [I_0(\kappa)]^{-1}, \quad (\text{E.35})$$

Note that b_1/b_0 and b_2/b_0 in Equation (E.34) and (E.35) have been calculated according to $\rho_{11,11}(\tau)$ in Equation (E.30) and (E.31), whereas $\rho_{11,12}(\tau) \equiv 0$ due to neglecting the existing spatial correlation. As Figure E.1 shows, high spatial correlations introduce large deviations from the case where there is no correlation between the two subchannels. On the other hand, according to Figure E.2, AFD increases as the spatial correlation increases. This was expected since the correlation reduces the amount of diversity. As a numerical example, to have an AFD of 10 msec. below a fixed threshold, one needs a 2.6 dB increase in $\bar{\gamma}_{11} = E_s/N_0$, the average received SNR per symbol over each subchannel, for a spatial correlation of 0.995. This increase for the 0.886 spatial correlation is 2 dB.

E.2.3 Applications of Scalar ASD

In adaptive modulation schemes for MIMO channels, the total received (post-processing) SNR is a good measure of channel quality as it captures the impacts of

many parameters involved such as the space-time coding/decoding used, constellation size/shape, antenna correlations and polarizations, etc. [53]. The entire range of total received SNR, $[0, \infty]$, needs to be discretized into $k + 1$ regions $[0, \gamma_1]$, $[\gamma_1, \gamma_2]$, \dots , $[\gamma_{k-1}, \gamma_k]$, and $[\gamma_k, \infty]$. The ASD of each individual region can be used to determine, for example, the tradeoff between power/rate adaptation policies and the number of regions, as well as the thresholds $\{\gamma_1, \gamma_2, \dots, \gamma_k\}$.

There is a growing interest in representing fading channels with finite state Markov models [65] [66]-[67] as they significantly facilitate the performance analysis of complex communication protocols over channels with memory. Development of a Markov model for MIMO fading channels can be done using the approach taken for receive diversity combiners [51], i.e., partitioning the entire range of total received SNR, and treating each subregion as a state. The transition probability $\gamma(t)$ of from one state to another can be determined using the ICR of $\gamma(t)$. The ASD of $\gamma(t)$ can be employed for choosing the thresholds in order to obtain, for example, an equal-duration partitioning, or other types of partitioning.

E.3 Vector Crossing in MIMO Systems

Here first the problem is formulated and the solution is discussed. Since the solution in the most general case is rather complicated, the author considers a special situation and then apply it to two cases of interest.

E.3.1 Mathematical Formulation

Consider a time-selective narrowband $M \times N$ matrix channel, composed of MN complex zero-mean Gaussian processes, correlated in both space and time. Obviously the envelope of subchannels are Rayleigh distributed. As before, $h_{lp}(t)$ denotes the complex gain of the subchannel connecting the p -th transmitter to the l -th receiver. Suppose at $t = t_0$, all the subchannel gains are observed. Now it is needed to

determine for how long, in average, the maximum absolute deviation of all the MN processes from their observed values at $t = t_0$, simultaneously, does not exceed a certain bound ε . In other words, starting at $t = t_0$, this is the average time over which $|\text{Re}[h_{lp}(t)] - \text{Re}[h_{lp}(t_0)]| < \varepsilon$ and $|\text{Im}[h_{lp}(t)] - \text{Im}[h_{lp}(t_0)]| < \varepsilon$, for all l 's and p 's. Mathematically speaking, this is equivalent to the average stay time of a vector Gaussian process consisting of $2MN$ real correlated processes, within a hypercube with equal sides of length 2ε . For $M = N = 1$, a SISO channel, the idea is depicted in Figure E.3, where T_{stay} is the stay time of the real and imaginary parts of $h_{11}(t)$ within the 2ε -square, centered on the process at $t = t_0$. Obviously it is interesting to calculate $E[T_{stay}]$, the ASD.

To compute this vector ASD, similar to the scalar ASD of the previous section, it is needed to divide the probability of falling this Gaussian vector into the 2ε -hypercube, by the associated outcrossing rate (OCR) of the vector process. For the numerator, many techniques are available [68], whereas the OCR can be derived from Equation (3.1) of [69], in the form of a multidimensional surface integral (one can also derive (3) from Equation (3.1) of [69]). More specifically, let $\mathbf{H}(t)$ represents the $M \times N$ matrix channel. Also let $\mathbf{h}_{\text{Re}}(t) = \text{vec}(\text{Re}[\mathbf{H}(t)])$ and $\mathbf{h}_{\text{Im}}(t) = \text{vec}(\text{Im}[\mathbf{H}(t)])$, two $MN \times 1$ real vectors, where $\text{vec}(\cdot)$ gives a column vector, constructed by stacking the columns of its matrix argument. The ASD of the $2MN \times 1$ real vector process $\mathbf{h}(t) = [\mathbf{h}_{\text{Re}}(t)^T, \mathbf{h}_{\text{Im}}(t)^T]^T$ within the hypercube of side 2ε , centered at $\mathbf{h}(t_0)$, $HC[\mathbf{h}(t_0), 2\varepsilon]$, is given by

$$ASD\{\mathbf{h}(t), HC[\mathbf{h}(t_0), 2\varepsilon]\} = \frac{\Pr[\mathbf{h}(t) \in HC[\mathbf{h}(t_0), 2\varepsilon]]}{OCR\{\mathbf{h}(t), HC[\mathbf{h}(t_0), 2\varepsilon]\}}. \quad (\text{E.36})$$

E.3.2 Special Case of Isotropic Scattering and No Spatial Correlation

To come up with a simple solution for Equation (E.36) to obtain some intuition, assume that there is no spatial correlation between the MN subchannels. Isotropic scattering is further assumed, i.e., uniform distribution of AOA at the receiver,

which entails Clarke's correlation $2J_0(2\pi f_D\tau)$ for each individual complex subchannel, where $J_0(\cdot)$ is the zero-order Bessel function. Under these conditions it is easy to verify that all the elements of $\mathbf{h}(t)$ are independent processes, with zero mean and unit variance. Let $\mathbf{h}(t_0) = \theta \mathbf{1}$, where θ is a real number and $\mathbf{1}$ is an all one vector. Obviously it is interesting to observe the case where at time t_0 , the real and imaginary parts of all the subchannels have taken the same value θ . It is easy to show that the numerator of Equation (E.36) is given by $[\Phi(\theta + \varepsilon) - \Phi(\theta - \varepsilon)]^{2MN}$. The denominator from Equation (19) of the paper [70] is derived as

$$2\sqrt{2}MNf_D \exp[-(\theta^2 + \varepsilon^2)/2] \cosh(\theta\varepsilon) [\Phi(\theta + \varepsilon) - \Phi(\theta - \varepsilon)]^{2MN},$$

where $\cosh(\cdot)$ is the hyperbolic cosine. This gives us

$$ASD\{\mathbf{h}(t), HC[\theta\mathbf{1}, 2\varepsilon]\} = \frac{[\Phi(\theta + \varepsilon) - \Phi(\theta - \varepsilon)] \exp[(\theta^2 + \varepsilon^2)/2]}{2\sqrt{2}MNf_D \cosh(\theta\varepsilon)}. \quad (\text{E.37})$$

E.3.3 Application: Analysis of the Block Fading Model

In many wireless communication scenarios, due to the low mobility of the users and also the quasi-stationarity of the environment, it is common to assume that the channel remains constant over a long block of symbols, and then jumps to another random constant for the next block. This gives rise to the so-called block fading model [71], which has been used extensively for coding/information-theoretic studies in fading channels [72]. Besides the physical motivation just described, this piecewise-constant approximation of the continuously time-varying random fading facilitates the theoretical analysis [73]. The block fading model also appears in the context of differential detection schemes, which are devised to bypass the channel estimation at the receiver [14] [16]. However, error floors appear at high SNR when the time-varying nature of the channel dominates, i.e., the piecewise-constant approximation of block fading model becomes less accurate [74] [24], which in turn degrades the performance of the associated designs. So, in general, it is important

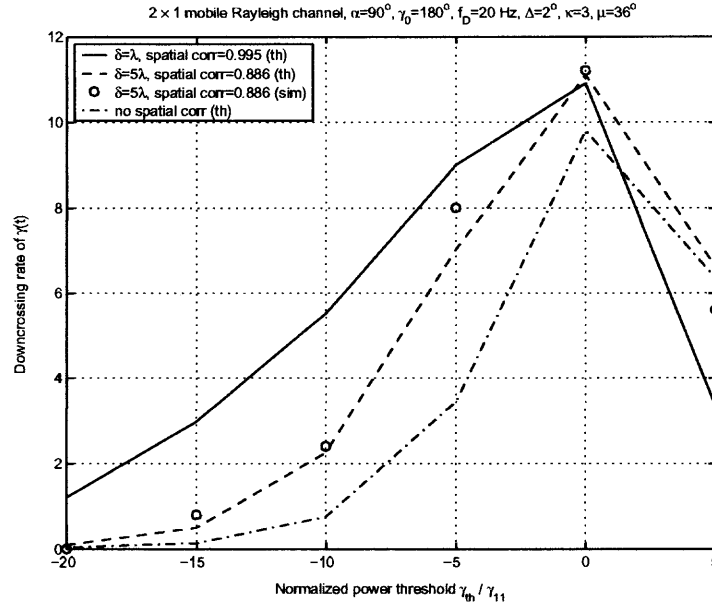


Figure E.1 Downcrossing rate of total instantaneous SNR in a 2×1 channel, with and without spatial correlation (th: theory, sim: simulation).

to quantify the conditions under which the block fading model is a reasonable approximation to the continuously varying MIMO fading channel.

For $M = N$, the normalized ASD, $f_D ASD\{\mathbf{h}(t), HC[\theta \mathbf{1}, 2\varepsilon]\}$, is plotted in Figure E.4 with respect to θ , with ε as a parameter. Some simulation results are also included, to verify the theory. Interestingly, for any fixed ε , ASD decreases as M increases. This means that the block fading model remains accurate for a shorter period, as the number of transmitters and/or receivers increases. On the other hand, when M is fixed, ASD decreases as ε decreases. This was expected as it should take less time for a vector process to exit a small region than a large one. Finally note that for any M and ε , ASD decreases when θ increases. This implies that the zero-mean vector Gaussian process tends to stay more often around small values, rather than large values.

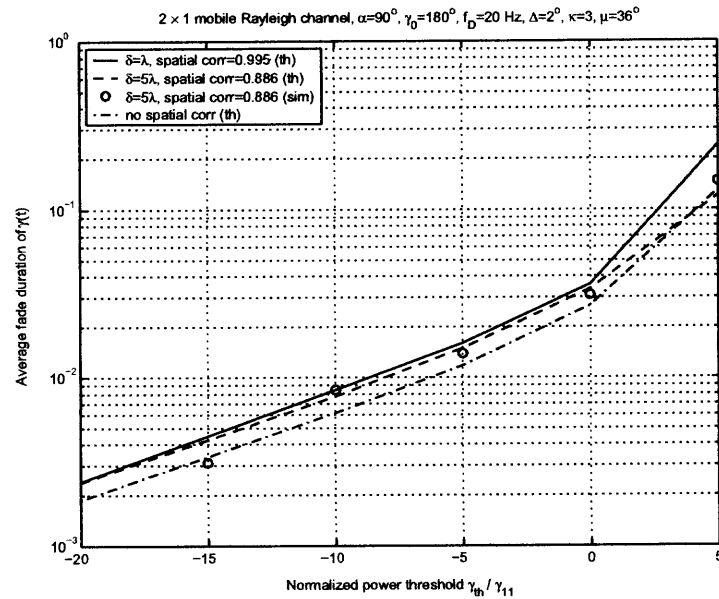


Figure E.2 Average fade duration of total instantaneous SNR in a 2×1 channel, with and without spatial correlation (th: theory, sim: simulation).

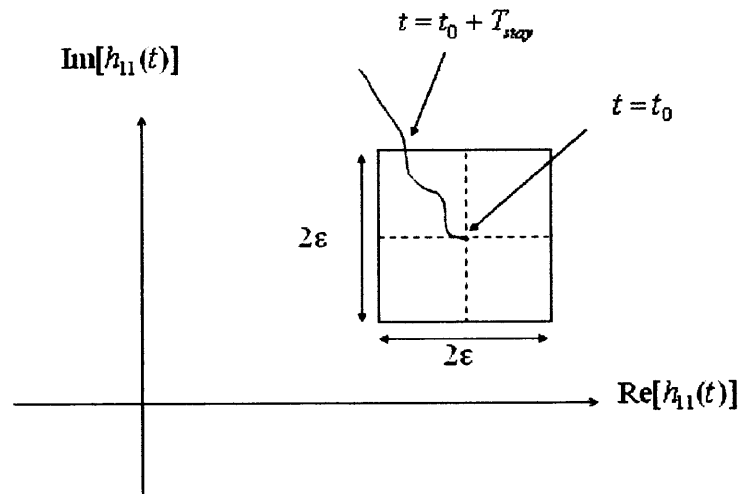


Figure E.3 Graphical representation of the concept of the stay duration of a single complex process, a SISO channel, within a square region.

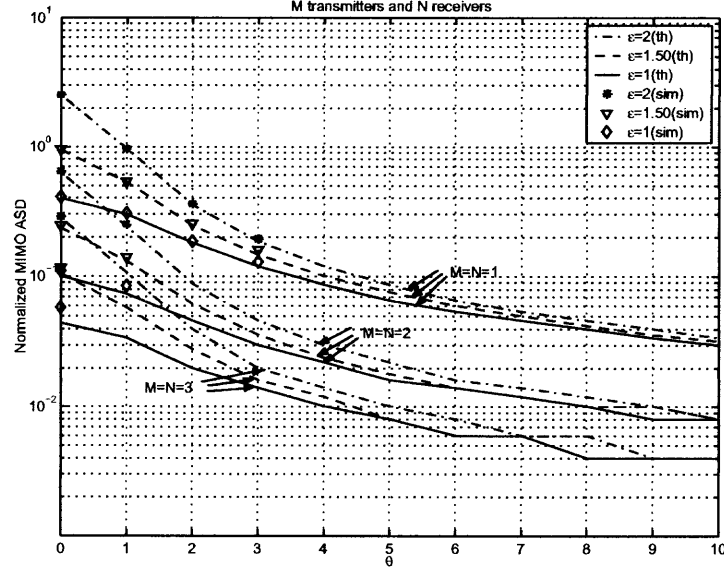


Figure E.4 Normalized average stay duration in a MIMO channel with the same number of transmit and receive antennas (th: theory, sim: simulation).

E.3.4 Application: Vector AFD in MIMO Channels

In the numerical example of Section 5.2.2, the scalar AFD in MIMO channels is focused on, where the AFD was defined for the total instantaneous received SNR per symbol, $\gamma(t) \propto \sum_{l,p} |h_{lp}(t)|^2$, a scalar process. Now the vector AFD is defined as the average stay duration inside a hypercube with equal sides of size 2ε , centered at the origin, i.e., $\theta = 0$. Then Equation (E.37) gives the vector AFD as

$$\left(2\sqrt{2}MNf_D\right)^{-1} [1 - 2\Phi(-\varepsilon)] \exp[\varepsilon^2/2].$$

Obviously the vector AFD tends to zero and infinity as $\varepsilon \rightarrow 0$ and ∞ , respectively.

E.4 Conclusion

The concepts of level crossing rate (LCR) and average fade duration (AFD) are well understood for single-input single-output fading channels. However, apparently they have not been studied so far, in the context of multiple-input multiple-output (MIMO)

channels. In this chapter it has been addressed at a variety of possible approaches and definitions for MIMO LCR and AFD. When feasible, closed-form solutions are provided, and illustrated by numerical examples and simulations. Applications of MIMO LCR and AFD to adaptive modulation in MIMO channels, Markov modeling, and block fading approximation of MIMO channels are discussed as well.

REFERENCES

- [1] E. Telatar, "Capacity of multi-antenna gaussian channels," *Bell Labs Internal Tech. Memo*, Autumn 1995.
- [2] A. Narula, M. Lopez, M. Trott, and G. Wornell, "Efficient use of side information in multiple-antenna data transmission over fading channels," *IEEE Transactions on Information Theory*, vol. 16, pp. 1423–1436, Nov. 1999.
- [3] A. Narula, M. Trott, and G. Wornell, "Performance limits of coded diversity methods for transmitter antenna arrays," *IEEE Transactions on Information Theory*, vol. 45, pp. 2418–2433, Nov. 1999.
- [4] A. Wittneben, "Base station modulation diversity for digital SIMULCAST," *Proc. IEEE'VTC Spring*, pp. 505–511, 1993.
- [5] N. Seshadri and J. Winters, "Two signaling schemes for improving the error performance of frequency-division-duplex (FDD) transmission systems using transmitter antenna diversity," *Int. J. Wireless Inform. Networks*, vol. 1, 1994.
- [6] V. Tarokh and A. Seshadri, "Space-time codes for high data rate wireless communication: performance criterion and code construction," *IEEE Transactions on Information Theory*, vol. 44, pp. 744–765, March 1998.
- [7] S. Alamouti, "A simple transmit diversity technique for wireless communications," *IEEE Journal on Selected Areas in Communications*, vol. 16, pp. 1451–1458, Oct. 1998.
- [8] V. Tarokh and H. Jafarkhani, "Space-time block coding for wireless communications: performance results," *IEEE Journal on Selected Areas in Communications*, vol. 17, pp. 451–460, Mar. 1999.
- [9] X. Li, T. Luo, G. Yue, and C. Yin, "A squaring method to simplify the decoding of orthogonal space-time block codes," *IEEE Transactions on Communications*, vol. 49, pp. 1700–1703, Oct. 2001.
- [10] G. Bauch and J. Hagenauer, "Analytical evaluation of space-time transmit diversity with FEC-coding," *GLOBECOM*, vol. 1, pp. 435–439, 2001.
- [11] A. Hiroike, F. Adachi, and N. Nakajima, "Combined effects of phase sweeping transmitter diversity and channel coding," *IEEE Transactions on Vehicular Technology*, vol. 41, pp. 170–176, May 1992.
- [12] T. Hattori and K. Hirade, "Multi-transmitter simulcast digital signal transmission by using frequency offset strategy in land mobile radio-telephone system," *IEEE Transactions on Vehicular Technology*, vol. 27, pp. 231–238, 1978.

- [13] V. Tarokh and H. Jafarkhani, "A differential detection scheme for transmit diversity," *IEEE Journal on Selected Areas in Communications*, vol. 18, pp. 1169–1174, Jul. 2000.
- [14] H. Jafarkhani and V. Tarokh, "Multiple transmit antenna differential detection from generalized orthogonal designs," *IEEE Transactions on Information Theory*, vol. 47, pp. 2625–2631, Sept. 2001.
- [15] B. Hochwald and W. Sweldens, "Differential unitary space-time modulation," *IEEE Transactions on Communications*, vol. 48, pp. 2041–2052, Dec. 2000.
- [16] B. Hughes, "Differential space-time modulation," *IEEE Transactions on Information Theory*, vol. 46, pp. 2567–2578, Nov. 2000.
- [17] M. Simon and M. S. Alouini, "Some new results for integrals involving the generalized Marcum Q function and their application to performance evaluation over fading channels," *IEEE Transactions on Wireless Communications*, vol. 2, pp. 611–615, July 2003.
- [18] J. G. Proakis, "Digital communications, 3th edition," *McGraw-Hill*, 1998.
- [19] T. Lo, "Maximum ratio transmission," *IEEE Transactions on Communications*, vol. 47, pp. 1458–1461, Oct. 1999.
- [20] D. Divsalar and M. Simon, "Multiple-symbol differential detection of MPSK," *IEEE Transactions on Communications*, vol. 38, pp. 300–308, March 1990.
- [21] D. Divsalar and M. Simon, "Maximum-likelihood differential detection of uncoded and trellis coded amplitude phase modulation over AWGN and fading channels—metrics and performance," *IEEE Transactions on Communications*, vol. 38, pp. 300–308, March 1990.
- [22] P. Ho and D. Fung, "Error performance of multiple-symbol differential detection of PSK signals transmitted over correlated Rayleigh fading channels," *IEEE Transactions on Communications*, vol. 40, pp. 25–29, Oct. 1992.
- [23] P. Fan, "Multiple-symbol detection for transmit diversity with differential encoding scheme," *IEEE Transaction on Consumer Electronics*, vol. 47, pp. 96–100, Feb. 2001.
- [24] B. Bhukania and P. Schniter, "Multiple-symbol detection of differential unitary space-time modulation in fast-fading channels with known correlation," *Proc. Conf. Inform. Sci. Syst., Princeton University, Princeton, NJ*, pp. 248–253, 2002.
- [25] H. Poor, "An introduction to signal detection and estimation," *New York: Springer-Verlag*, 1988.
- [26] W. E. Lewis, "The application of matrix theory to electrical engineering," *London, Spon Inc.*, 1965.

- [27] M. Win and J. Winters, "Exact error probability expressions for H-S/MRC in Rayleigh fading: a virtual branch technique," *Globecom*, pp. 537–542, 1999.
- [28] Z. Liu, G. Giannakis, and B. Hughes, "Double differential space-time block coding for time-selective fading channels," *IEEE Transactions on Communications*, vol. 49, pp. 1529–1536, Sept. 2001.
- [29] D. Lao and A. M. Haimovich, "Multiple-symbol differential detection with interference suppression," *IEEE Transactions on Communications*, vol. 51, pp. 208–217, Feb. 2003.
- [30] C. Gao, A. M. Haimovich, and D. Lao, "Bit error probability for space-time block code with coherent and differential detection," *VTC-FALL'2002 IEEE 56th, Vancouver, Canada*, vol. 1, pp. 410–414, Sept. 2002.
- [31] B. D. Hart and D. P. Taylor, "Maximum-likelihood synchronization, equalization, and sequence estimation for unknown time-varying frequency-selective rician channels," *IEEE Transactions on Communications*, vol. 46, pp. 211–221, 1998.
- [32] C.-S. Hwang, S.-H. Nam, J. Chung, and V. Tarokh, "Differential space time block codes using noncoherent modulus constellations," *IEEE Transactions on Signal Processing*, vol. 51, pp. 2955–2957, 2003.
- [33] A. Abdi and M. Kaveh, "A space-time correlation model for multielement antenna systems in mobile fading channels," *IEEE Journal on Selected Areas in Communications*, vol. 20, pp. 550–560, 2002.
- [34] J. Fuhl, J. P. Rossi, and E. Bonek, "High-resolution 2-d direction-of-arrival determination for urban mobile radio," *IEEE Trans. Inform. Theory*, vol. 45, pp. 672–682, 1997.
- [35] A. Abdi and M. Kaveh, "A versatile spatio-temporal correlation function for mobile fading channels with nonisotropic scattering," *Proc. IEEE Workshop Statistical Signal Array Processing*, vol. 51, pp. 58–62, 2000.
- [36] A. Abdi, J. A. Barger, and M. Kaveh, "A parametric model for the distribution of the angle of arrival and the associated correlation function and power spectrum at the mobile station," *IEEE Transactions on Vehicular Technology*, vol. 51, pp. 425–434, 2002.
- [37] D. S. Shiu, G. J. Foschini, M. J. Gans, and J. M. Kahn, "Fading correlation and its effect on the capacity of multielement antenna systems," *IEEE Transactions on Communications*, vol. 48, pp. 502–513, 2000.
- [38] B. H. Fleury, "First- and second-order characterization of direction dispersion and space selectivity in the radio channel," *IEEE Trans. Inform. Theory*, vol. 46, pp. 2027–2044, 2000.

- [39] K. Acolatse and A. Abdi, "Efficient simulation of space-time correlated MIMO mobile fading channels," *Proc. IEEE Vehic. Technol. Conf.*, vol. 51, pp. 32–36, 2003.
- [40] A. Abdi, W. C. Lau, M. S. Alouini, and M. Kaveh, "A new simple model for land mobile satellite channels: First- and second-order statistics," *IEEE Transactions on Wireless Communications*, vol. 2, pp. 519–528, 2003.
- [41] G. Foschini, "Layered space-time architecture for wireless communication in a fading environment when using multi-element antennas," *Bell Labs Tech. J.*, pp. 41–59, Autumn 1996.
- [42] V. Tarokh and A. Naguib, "Combined array processing and space-time coding," *IEEE Transactions on Information Theory*, vol. 45, pp. 1121–1128, May 1999.
- [43] V. Tarokh, H. Jafarkhani, and A. R. Calderbank, "Space-time block codes from orthogonal designs," *IEEE Transactions on Information Theory*, vol. 45, pp. 1456–1476, July 1999.
- [44] L. Jalloul and K. Rohani, "Performance analysis of CDMA transmit diversity methods," *Vehicular Technology Conference, VTC 1999 - Fall, IEEE VTS 50th*, vol. 3, pp. 1326–1330, 1999.
- [45] B. Hochwald and T. Marzetta, "A transmitter diversity scheme for wideband CDMA systems based on space-time spreading," *IEEE Journal on Selected Areas in Communications*, vol. 19, pp. 48–60, Jan. 2001.
- [46] V. Weerackody, "Diversity for the direct-sequence spread spectrum system using multiple transmit antennas," *AT&T Tech. Memo.*, 1993.
- [47] H. Huang, "Increasing IS-95 downlink capacity with transmit and receive diversity," *Bell Labs Tech. Memo.*, 1997.
- [48] A. Abdi and M. Kaveh, "Level crossing rate in terms of the characteristic function: A new approach for calculating the fading rate in diversity systems," *IEEE Transactions on Communications*, vol. 50, pp. 1397–1400, 2002.
- [49] M. D. Yacoub, C. R. C. M. da Silva, and J. E. V. Bautista, "Second-order statistics for diversity-combining techniques in nakagami-fading channels," *IEEE Transactions on Vehicular Technology*, vol. 50, pp. 1464–1470, 2001.
- [50] C. D. Iskander and P. T. Mathiopoulos, "Analytical level crossing rates and average fade durations for diversity techniques in nakagami fading channels," *IEEE Transactions on Communications*, vol. 50, pp. 1301–1309, 2002.
- [51] W. Tang and S. A. Kassam, "Finite-state Markov models for correlated Rayleigh fading channel," *Proc. Conf. Infor. Sci. Syst., Princeton University, Princeton, NJ*, pp. 404–409, 2002.

- [52] R. W. Heath and A. J. Paulraj, "Characterization of mimo channels for special multiplexing systems," *Proc. IEEE Int. Conf. Commun., Helsinki, Finland*, pp. 591–595, 2001.
- [53] S. Catreux, V. Erceg, D. Gesbert, and R. W. Heath, "Adaptive modulation and mimo coding for broadband wireless data networks," *IEEE Communications Magazine*, vol. 40, pp. 108–115, 2002.
- [54] P. Stoica and G. Ganesan, "Maximum-snr space-time design for MIMO channels," *Proc. IEEE Int. Conf. Acoust. Speech, signal processing, Salt Lake City, UT*, pp. 2425–2428, 2001.
- [55] G. Ganesan and P. Stoica, "Space-time block codes: a maximum snr approach," *IEEE Transactions on Information Theory*, vol. 47, pp. 1650–1656, 2001.
- [56] Y. C. Ko, A. Abdi, M. S. Alouini, and M. Kaveh, "A general framework for the calculation of the average outage duration of diversity systems over generalized fading channels," *IEEE Transactions on Vehicular Technology*, vol. 51, pp. 1672–1680, 2002.
- [57] A. M. Hasofer, "The upcrossing rate of a class of stochastic processes," *New York: North-Holland*, 1974.
- [58] G. Lindgren, "Slepian models for a process with dependent components with application to envelope upcrossings," *J. Appl. Prob.*, vol. 26, pp. 36–49, 1989.
- [59] W. C. Y. Lee, "A study of the antenna array configuration of an m-branch diversity combining mobile radio receiver," *IEEE Transactions on Vehicular Technology*, vol. 20, pp. 93–104, 1971.
- [60] B. Picinbono, "On circularity," *IEEE Transactions on Signal Processing*, vol. 42, pp. 3473–3482, 1994.
- [61] F. D. Neeser and J. L. Massey, "Proper complex random processes with applications to information theory," *IEEE Transactions on Information Theory*, vol. 39, pp. 1293–1302, 1999.
- [62] A. Papoulis, "Probability, Random Variables, and Stochastic processes, 3rd ed.," *Singapore: McGraw-Hill*, 1991.
- [63] H. Xu, M. Gans, D. Chizhik, J. Ling, P. Wolniansky, and R. Valenzuela, "Spatial and temporal variations of mimo channels and impacts on capacity," *Proc. IEEE Conf. Commun., New York*, pp. 262–266, 2002.
- [64] K. Acolatse and A. Abdi, "Efficient simulation of space-time correlated mimo mobile fading channel," *To be published in Proc. IEEE Vehic. Technol. Conf., Orlando, FL*, 2003.

- [65] H. S. Wang and N. Moayeri, "Finite-state markov channel-a useful model for radio communication channels," *IEEE Transactions on Vehicular Technology*, vol. 40, pp. 163–171, 1995.
- [66] W. Turin and R. V. Nobelen, "Hidden markov modeling of flat fading channels," *IEEE Journal on Selected Areas in Communications*, vol. 40, pp. 1809–1817, 1998.
- [67] M. J. Chu, D. L. Goeckel, and W. E. Stark, "On the design of markov models for fading channels," *Proc. IEEE Vehic. Technol. Conf., Amsterdam, the Netherlands*, pp. 2372–2376, 1999.
- [68] S. S. Gupta, "Bibliography on the multivariate normal integrals and related topics," *Ann. Math. Statist.*, vol. 34, 1963.
- [69] R. Illsley, "The excursions of a stationary gaussian process outside a large two-dimensional region," *Adv. Appl. Prob.*, vol. 33, pp. 141–159, 2001.
- [70] D. Veneziano, M. Grigoriu, and C. A. Cornell, "Vector-process models for system reliability," *Journal of the engineering mechanics division*, vol. 20, pp. 441–460, 1977.
- [71] E. Biglieri, G. Caire, and G. Taricco, "Coding and modulation under power constraints," *IEEE Pers. Commun. Mag.*, vol. 5, pp. 32–39, 1998.
- [72] E. Biglieri, J. Prokis, and S. Shamai, "Fading channels: Information-theoretic and communication aspects," *IEEE Transactions on Information Theory*, vol. 44, pp. 2619–2692, 1998.
- [73] G. Kaplan and S. Shamai, "Achievable performance over the correlated rician channel," *IEEE Transactions on Communications*, vol. 42, pp. 2967–2978, 1994.
- [74] C. B. Peel and A. L. Swindlehurst, "Performance of unitary space-time modulation in a continuously changing channel," *Proc. IEEE Int. Conf. Commun., Helsinki, Finland*, pp. 2805–2808, 2001.